UNIVERSITY OF CALIFORNIA SAN DIEGO

Quantifying the rates and drivers of coral and coral reef calcification in the Anthropocene

A dissertation submitted in partial satisfaction of the
requirements for the degree Doctor of Philosophy

in

Oceanography

by

Travis A. Courtney

Committee in charge:

Professor Andreas Andersson, Chair
Professor James Leichter
Professor Richard Norris
Professor Jonathan Shurin
Professor Jennifer Smith

2019

The Dissertation of Travis A. Courtney is approved, and it is acceptable in quality and form for publication on microfilm and electronically:

_____

_____

_____

_____

_____
Chair

University of California San Diego

2019

TABLE OF CONTENTS

LIST OF TABLES

LIST OF FIGURES

ACKNOWLEDGMENTS

I would first like to acknowledge to the chair of my dissertation, Andreas Andersson, for further training me as a scientist through conversations about coral reefs, manuscript edits, field training, and networking opportunities. I have grown so much throughout my dissertation and am incredibly grateful to have been able to learn from such a fantastic advisor and mentor. I would also like to thank my committee members James Leichter, Richard Norris, Jonathan Shurin, and Jennifer Smith for expanding my research with analytical methods and to more holistically view the geology, physics, functional traits, and benthic communities of coral reef ecosystems as part of this interdisciplinary dissertation on coral reef growth.

I would like to further extend my gratitude for the Scripps Institution of Oceanography, Bermuda Institute of Ocean Science, and the University of Hawai'i communities in general and will highlight just a few individuals here. I'd first like to acknowledge the support of my fellow lab members of the Scripps Coastal and Open Ocean Biogeochemistry Lab and in particular to Tyler Cyronak for reminding me to collect Smartfin data and to Alyssa Griffin, Sam Kekuewa, Theo Kindeberg, Heather Page, and Ariel Pezner for countless shared experiences in both the office and the field. I am incredibly grateful also to Becky Garley, Fernando Pacheco, Matt Hayden, Tim Noyes, and Kaitlin Noyes in Bermuda and Eric De Carlo, Noah Howins, Ku'ulei Rodgers, and Keisha Bahr in Hawai'i for facilitating field research and making my time spent in the field feel more like home.

I'd like to further acknowledge that the groundwork for my PhD started long before my time at Scripps Institution of Oceanography with support from friends, family, and teachers along the way. In particular, my undergraduate research advisor, Justin Ries, provided me opportunities and training to study the impacts of carbonate chemistry and environmental change

on coral reef organisms. Thank you also to Karl Castillo for training me in the study of coral coring on the reefs of Belize and allowing me to share in the first year of the Castillo Lab. Outside of research, thank you to my parents, Mark and Barb Courtney, and sister, Alyson Courtney, for fostering a lifetime of exploration, curiosity, and learning. I would like to further acknowledge the overwhelming support and endless adventures with Lark Starkey and to Justin Baumann, Frederick Dowell, David Koweek, Carlos Minces, Daniel Portner, and Daniel Yee for their constant friendship and support throughout my dissertation.

This research would not have been possible without financial support from the National Science Foundation, Australian Research Council, French Ministry of Ecology, NOAA Office of Oceanic and Atmospheric Research, NOAA Office of Sea Grant, Hawai'i Sea Grant, USGS John Wesley Powell Center, Shepard Foundation, Scripps Fellowship, Cody Fellowship, Engel Student Prize, and Kastner Student Prize. I would like to further thank Scripps Institution of Oceanography (SIO), Bermuda Institute of Ocean Sciences (BIOS), University of Hawai'i, Hawai'i Institute of Marine Biology, USGS John Wesley Powell Center, NOAA PMEL, and the Government of Bermuda for institutional support and to the volunteers and staff at those institutions who facilitated this research. In particular, I would like to also thank Sharyn Kilpatrick (SIO) for processing countless travel and research reimbursements, the graduate office (SIO) for administrative support, support from the *R* users group (SIO), and Christian McDonald (SIO), Richard Walsh (SIO), and Alex Hunter (BIOS) for facilitating SCUBA diving.

It is with the utmost gratitude that I acknowledge and thank Peter Edmunds, Ruth Gates, Jeff Miller, and the co-authors of my dissertation: Andreas Andersson, Brian Barnes, Keisha Bahr, Anthony Barro, Nicholas Bates, Iliana Chollett, Andrew Collins, Tyler Cyronak, Eric De Carlo, Samantha de Putron, Robin Elahi, Bradley Eyre, Rebecca Garley, Kevin Gross, James

Guest, Eric Hochberg, Noah Howins, Rod Johnson, Ilsa Kuffner, Mario Lebrato, Elizabeth Lenz, Juan Carlos Molinero, Sylvia Musielewicz, Hannah Nelson, Tim Noyes, Heather Page, Ku'ulei Rodgers, Caroline Rogers, Christopher Sabine, Adrienne Sutton, Ryan Tabata, Gerianne Terlouw, Jessy Toncin, Lauren Toth, and Aline Tribollet. Thank you all so much for your time spent in the field, lab, workshops, meetings, emails, and edits to help make these research projects possible. I have learned so much from your expertise and the completion of this dissertation would not have been possible without your contributions and support.

Chapter 2, in full, is a reprint of the material as it appears in Courtney TA & Andersson AJ. Evaluating measurements of coral reef net ecosystem calcification rates. *Coral Reefs* 2019. The dissertation author was the primary investigator and author of this paper.

Chapter 3, in full, is a reprint of the material as it appears in Courtney TA, Andersson AJ, Bates NB, Collins A, Cyronak T, de Putron SJ, Eyre BD, Garley R, Hochberg EJ, Johnson R, Musielewicz S, Noyes T, Sabine CL, Sutton AJ, Toncin J, Tribollet A. Comparing Chemistry and Census-based Estimates of Net Ecosystem Calcification on a Rim Reef in Bermuda. *Frontiers in Marine Science* 2016, 3:181. The dissertation author was the primary investigator and author of this paper.

Chapter 4, in full, is a reprint of the material as it appears in Courtney TA, Lebrato M, Bates NR, Collins A, de Putron SJ, Garley R, Johnson, R, Molinero JC, Noyes TJ, Sabine CL, Andersson AJ. Environmental controls on modern scleractinian coral and reef-scale calcification. *Science Advances*, 2017, 3(11), p.e1701356. The dissertation author was the primary investigator and author of this paper.

Chapter 5, in full, is a reprint of the material as it appears in Courtney TA, De Carlo EH, Page HN, Bahr KD, Barro A, Howins N, Tabata R, Terlouw G, Rodgers KS, Andersson AJ.

Recovery of reef-scale calcification following a bleaching event in Kāne'ohe Bay, Hawai'i. *Limnology & Oceanography Letters* 2018, 3:1–9. The dissertation author was the primary investigator and author of this paper.

Chapter 6, in full, is currently in review as Courtney TA, Barnes BB, Chollett I, Elahi R, Gross K, Guest JR, Kuffner IB, Lenz EA, Nelson HR, Rogers CS, Toth LT, Andersson AJ. Disturbances drive changes in coral community assemblages and coral calcification capacity. The dissertation author was the primary investigator and author of this paper.

VITA

2013 Bachelor of Science, University of North Carolina at Chapel Hill

2018 Master of Science, University of California, San Diego

2019 Doctor of Philosophy, University of California, San Diego

PUBLICATIONS

Baumann JH, Ries JB, Rippe JP, Courtney TA, Aichelman HE, Westfield I, Castillo KD. Nearshore coral growth declining on the Mesoamerican Barrier Reef System. Global Change Biology 2019.

Courtney TA & Andersson AJ. Evaluating measurements of coral reef net ecosystem calcification rates. Coral Reefs 2019.

Page HN, Courtney TA, De Carlo EH, Howins NM, Koester I, Andersson AJ. Spatiotemporal variability in seawater carbon chemistry for a coral reef flat in Kāne'ohe Bay, Hawai'i. Limnology and Oceanography 2019, 63:913–934.

Guest JR, Edmunds PJ, Gates RD, Kuffner IB, Andersson AJ, Barnes BB, Chollett I, Courtney TA, Elahi R, Gross K, Lenz EA, Mitarai S, Mumby PJ, Nelson HR, Parker BA, Putnam HM, Rogers CS, Toth LT. A framework for identifying and characterising coral reef "oases" against a backdrop of degradation. Journal of Applied Ecology 2018, 00:1-11.

Courtney TA, De Carlo EH, Page HN, Bahr KD, Barro A, Howins N, Tabata R, Terlouw G, Rodgers KS, Andersson AJ. Recovery of reef-scale calcification following a bleaching event in Kāne'ohe Bay, Hawai'i. Limnology & Oceanography Letters 2018, 3:1–9.

Courtney TA, Lebrato M, Bates NR, Collins A, de Putron SJ, Garley R, Johnson, R, Molinero JC, Noyes TJ, Sabine CL, Andersson AJ. Environmental controls on modern scleractinian coral and reef-scale calcification. Science Advances, 2017, 3(11), p.e1701356.

Page HN, Courtney TA, Collins A, De Carlo EH, Andersson AJ. Net community metabolism and seawater carbonate chemistry scale non-intuitively with coral cover. Frontiers in Marine Science 2017, 4:161.

Courtney TA, Andersson AJ, Bates NB, Collins A, Cyronak T, de Putron SJ, Eyre BD, Garley R, Hochberg EJ, Johnson R, Musielewicz S, Noyes T, Sabine CL, Sutton AJ, Toncin J, Tribollet A. Comparing Chemistry and Census-based Estimates of Net Ecosystem Calcification on a Rim Reef in Bermuda. Frontiers in Marine Science 2016, 3:181

Baumann JH, Townsend JE, Courtney TA, Aichelman HE, Davies SW, Lima FP, Castillo KD. Temperature Regimes Impact Coral Assemblages along Environmental Gradients on Lagoonal Reefs in Belize. PLoS ONE 2016, 11(9): e0162098.

Aichelman HE, Townsend JE, Courtney TA, Baumann JH, Davies SW, Castillo KD. Heterotrophy mitigates the response of the temperate coral *Oculina arbuscula* to temperature stress. Ecology and Evolution 2016, 6(18): 6758-6769.

Horvath KM, Castillo KD, Armstrong P, Westfield IT, Courtney T, Ries JB. Next-century ocean acidification and warming both reduce calcification rate, but only acidification alters skeletal morphology of reef-building coral *Siderastrea siderea*. Scientific Reports 2016, 6:29613.

Courtney T, Ries JB. Impact of atmospheric pCO_2, seawater temperature, and calcification rate on the $\delta^{18}O$ and $\delta^{13}C$ composition of echinoid calcite (*Echinometra viridis*). Chemical Geology 2015, 411: 228-239.

Courtney T, Ries JB, Westfield I. Predicted end of 21st century CO_2-induced ocean acidification decreases calcification rates in the tropical urchin *Echinometra viridis*. Journal of Experimental Marine Biology and Ecology 2013, 440: 169-175.

ABSTRACT OF THE DISSERTATION

Quantifying the rates and drivers of coral and coral reef calcification in the Anthropocene

by

Travis Alexander Courtney

Doctor of Philosophy in Oceanography

University of California San Diego, 2019

Professor Andreas J. Andersson, Chair

Anthropogenic environmental change threatens the ability for many coral reefs to maintain the calcium carbonate structures that provide shoreline protection, fisheries provision, and tourism revenue to human populations worldwide. Rigorous quantification of the rates and drivers of coral and coral reef net ecosystem calcification (NEC) represents a significant challenge but is tantamount for understanding how these services to humanity may be affected by environmental change. This challenge is addressed here by leveraging a combination of field

observations, numerical models, and statistical analyses. The major findings showed that extremely large NEC errors of –91% to +1000% can be driven by interacting ±83% uncertainties in the difficult to measure seawater depth and residence time parameters used to calculate NEC. Confidence in NEC rates can nonetheless be improved by leveraging multiple NEC methods as evidenced by the agreement between chemistry and census-based NEC calculated for Hog Reef, Bermuda. Analysis of the environmental drivers of coral and reef-scale calcification at Hog Reef and Crescent Reef, Bermuda showed that temperature was the strongest driver of coral and reef-scale calcification rates with little influence by the other environmental parameters studied. This suggests that reduced warming rates driven by lower global carbon dioxide emissions pathways could maintain Bermudan coral calcification through the twenty-first century. However, more rapid warming can cause coral bleaching that reduces NEC as evidenced by the observation of zero NEC during the fall 2015 coral bleaching event in Kāne'ohe Bay, Hawai'i. The subsequent recovery to pre-bleaching NEC rates by the following summer highlights the capacity of coral reef NEC to rapidly recover in the absence of continued stressors. Conversely, the cumulative effects of 20 years of disturbances on coral calcification capacity (CCC) across the main Hawaiian Islands, Mo'orea, Florida Keys reef tract, and St. John revealed disturbance-driven reductions in CCC and community-level shifts in contributions to CCC from competitive to weedy corals that may increase CCC resilience to future disturbances. This dissertation collectively improves projections for how the Anthropocene may change reef structures and the services they provide humanity by advancing our understanding of the rates and drivers of coral and coral reef calcification.

CHAPTER 1

Introduction: The growth of coral reef ecosystems in the Anthropocene

Travis A. Courtney

1.1 Background Information

Early descriptions by some Western scientists referred to coral reefs as navigational hazards occupied by corals with more inclusive definitions now spanning the scientific literature that encompass a range of biological, geological, social, and cultural characteristics (Kleypas et al. 2001; Williams et al. 2019). The coral reefs of today are incredibly important to humanity and despite covering just 0.2% of the global ocean surface area, contain an estimated 35% of all ocean species (Reaka-Kudla 1997; Knowlton et al. 2010) and partially sustain approximately 10% of the global human population (Donner and Potere 2007). Services such as shoreline protection, provision of food and materials, and tourism revenue generation are among the major socioeconomic benefits that coral reefs provide to humanity with global economic valuations of all coral reef ecosystem services ranging up to 9.9 trillion USD/yr (Moberg and Folke 1999; de Groot et al. 2012; Costanza et al. 2014; Woodhead et al. 2019).

These disproportionately large economic and societal benefits for the relatively limited geographic coverage of reef systems are intimately tied to the maintenance of coral reef calcium carbonate ($CaCO_3$) structures (Moberg and Folke 1999; Kleypas et al. 2001; Donner and Potere 2007; Knowlton et al. 2010; de Groot et al. 2012; Costanza et al. 2014; Edmunds et al. 2016; Cyronak et al. 2018; Perry et al. 2018; Woodhead et al. 2019). Calcifying scleractinian corals are the primary coral reef calcium carbonate producers (Pratchett et al. 2015) with further contributions by red coralline algae, molluscs, *Halimeda* calcifying algae, and benthic foraminifera (Montaggioni and Braithwaite 2009). Conversely, coral reef $CaCO_3$ structures can also be reduced through both biologically mediated and inorganic calcium carbonate ($CaCO_3$) dissolution processes (Andersson and Gledhill 2013). Biological (e.g., parrotfishes, sea urchins, molluscs, crustaceans, worms, sponges, and microborers) and nonbiological (e.g., waves, storm

events) mechanical erosion processes can also physically break apart $CaCO_3$ materials into smaller sizes that can enhance $CaCO_3$ dissolution rates and facilitate transport either on to or away from a coral reef (Stearn et al. 1977; Perry et al. 2017; Schönberg et al. 2017; Tuck et al. 2019). Collectively these $CaCO_3$ formation, breakdown, and transport processes result in a simplified coral reef growth equation (Chave et al. 1972; Stearn et al. 1977; Kleypas et al. 2001):

Reef Growth = $CaCO_3$ production – $CaCO_3$ dissolution + $CaCO_3$ import – $CaCO_3$ export (1)

where positive reef growth is a basic requirement for maintaining coral reef structures on interannual timescales (Kleypas et al. 2001).

One key point of confusion in the field of coral reef growth however is that the census-based and chemistry-based methods capture differing aspects of the reef growth equation. For example, census-based studies typically include $CaCO_3$ production by the major calcifiers, physical/chemical $CaCO_3$ bioerosion rates, and omit sediment $CaCO_3$ dissolution rates (Chave et al. 1972; Stearn et al. 1977; Hubbard et al. 1990; Perry et al. 2012, 2018). Alternatively, chemistry-based studies utilize changes in reef seawater total alkalinity (TA), which is reduced by two moles for each mole of $CaCO_3$ formed, to quantify NEC rates using the following equation (Smith and Key 1975; Chisholm and Gattuso 1991; Langdon et al. 2010):

$$\mathrm{NEC} = \frac{\rho z(\mathrm{TA_{offshore}} - \mathrm{TA_{reef}})}{2\tau} \quad (2)$$

where ρ is seawater density, z is the seawater density, $TA_{offshore}$–TA_{reef} is the alkalinity anomaly, and τ is seawater residence time. Importantly, both census and chemistry-based approaches often do not account for net import/export of $CaCO_3$ and therefore lack the complete information to account for the total $CaCO_3$ accumulated on a coral reef via Eqn. 1 (Chave et al. 1972; Smith 1973; Stearn et al. 1977; Hubbard et al. 1990; Chisholm and Gattuso 1991; Kleypas et al. 2001; Langdon et al. 2010; Perry et al. 2012, 2018). Nonetheless, these methods provide relatively

rapid assessments of the net $CaCO_3$ production of coral reef systems that can be coupled with environmental data to quantify the environmental and ecological drivers of reef-scale calcification on timescales that are short enough to match the ecosystem dynamics of present-day reef systems.

The environmental conditions that govern coral reef systems are constantly in a state of change resulting in non-equilibrium ecological communities (Connell 1978). However, human-induced changes in ocean temperatures, aqueous CO_2 chemistry, nutrient loading, land use, and fishing pressures are further modifying coral reef communities into novel ecosystems and threaten the maintenance of positive reef growth globally (e.g., Kleypas et al. 2001; Gardner et al. 2003; Bruno and Selig 2007; Hoegh-Guldberg et al. 2007; Andersson and Gledhill 2013; Graham et al. 2014; Jackson et al. 2014; Hughes et al. 2017; Perry et al. 2018; Eyre et al. 2018; Perry and Filip 2018; Toth et al. 2019; Williams et al. 2019). Most notably, increasing ocean temperatures have driven three global coral bleaching events in recent decades (Donner et al. 2017; Hughes et al. 2018a), which is the widespread breakdown of symbiosis between coral host and zooxanthellae symbiont that can result in coral mortality if temperature stress is severe enough (Jokiel and Coles 1977; Glynn 1993). Coral bleaching events are further expected to increase in both frequency and magnitude to continue to reshape 21st century coral reef ecosystems (Donner et al. 2005; van Hooidonk et al. 2016). Collectively, environmental change has the capacity to modify reef growth primarily via the following: (1) reduced calcification capacity via decreasing calcifier cover and benthic community shifts (e.g., Loya et al. 2001; Gardner et al. 2003; Bruno and Selig 2007; Darling et al. 2013; Perry et al. 2013, 2015, 2018; Hughes et al. 2017); (2) altered rates of calcification, $CaCO_3$ dissolution, and bioerosion via shifts in the environmental conditions that drive these processes (e.g., Jokiel and Coles 1977;

Andersson and Gledhill 2013; McMahon et al. 2013; Pratchett et al. 2015; Schönberg et al. 2017; Eyre et al. 2018); and (3) shifts in net $CaCO_3$ import/export through feedbacks between changing rates of sea level rise, wave climates, and island geomorphologies (e.g., Perry et al. 2011; Hemer et al. 2013; Tuck et al. 2019).

The rates and environmental drivers of coral and reef-scale calcification and how these relationships may be affected by local and global environmental change is limited by the difficulties in accurately measuring and untangling the complex interactions between rates of coral and reef-scale calcification and the relevant environmental drivers (e.g., seawater temperature, seawater carbonate chemistry, light and depth, food availability, nutrients, water flow rates, sedimentation, and competition [Pratchett et al. 2015]) of calcification for extended periods of time in the field (Jokiel and Coles 1977; McMahon et al. 2013). However, these difficulties are currently being overcome by the advancement of *in situ* autonomous instruments, satellite products, and computational tools to work towards an improved understanding of the controls on coral reef growth. Understanding these complex and interconnected processes is essential to improve our projections for how the maintenance of coral reef structures and the ecosystem services they provide may continue to be shaped by local and global environmental change.

1.2 Outline of the Dissertation

This dissertation represents an interdisciplinary perspective on the rates and drivers of coral and coral reef calcification in the Anthropocene. The primary goal was to leverage the advantages of ecological, geological, and biogeochemical perspectives on coral reef growth to improve confidence in rates of reef-scale calcification and the environmental and ecological processes that drive this important function of coral reefs. In doing so, this dissertation provides

critical knowledge for how the environmental change of the Anthropocene may impact the maintenance of pantropical coral reef structures and the ecosystem services they provide to human populations around the world. Chapters 2–6 therefore contain elements of these interdisciplinary perspectives and were written as stand-alone research publications with partially overlapping individual introductory and methodological sections (Courtney et al., 2016, 2017, 2018, in review; Courtney and Andersson 2019). Chapter 7 concludes this dissertation with a summary of its key findings.

Previous work has intuitively shown coral calcification to scale linearly with coral cover in mesocosms (Page et al. 2017), but no significant linear relationship exists between *in situ* NEC and coral reef calcifier cover in the field (Decarlo et al. 2017). Chapter 2 addresses this apparent contradiction by leveraging census-based methodology in a biogeochemical box model to test whether uncertainties in seawater depth and residence time may generate large enough errors that interact with the effects of reef structural complexity to mask a potential linear scaling of NEC with calcifier cover in the field. Chapter 2, in full, is a reprint of the material as it appears in Courtney TA & Andersson AJ. Evaluating measurements of coral reef net ecosystem calcification rates. *Coral Reefs* 2019.

Historically, measurements of reef-scale calcification have utilized either census/accretion based methods (e.g., Chave et al. 1972; Stearn et al. 1977; Hubbard et al. 1990; Eakin 1996; Harney and Fletcher 2003; Perry et al. 2012, 2013) or chemistry-based NEC methods (e.g., Broecker and Takahashi 1966; Smith and Key 1975; Smith and Kinsey 1976; Gattuso et al. 1996; Atkinson 2011; Andersson and Gledhill 2013), but there has been no formal comparison of these methods to date. In Chapter 3, the primary objective was to directly compare rates using published methods for chemistry-based NEC calculations and census-based

budgets and evaluate the dominant calcifiers across a two-year time series for a rim reef site in Bermuda. We hypothesized that chemistry-based NEC and census-based $CaCO_3$ production budgets would agree within uncertainties and that the dominant corals by benthic coverage at Hog Reef would be the primary reef calcifiers. Chapter 3, in full, is a reprint of the material as it appears in Courtney TA, Andersson AJ, Bates NB, Collins A, Cyronak T, de Putron SJ, Eyre BD, Garley R, Hochberg EJ, Johnson R, Musielewicz S, Noyes T, Sabine CL, Sutton AJ, Toncin J, Tribollet A. Comparing Chemistry and Census-based Estimates of Net Ecosystem Calcification on a Rim Reef in Bermuda. *Frontiers in Marine Science* 2016, 3:181.

Previous understanding of the environmental drivers of coral calcification in the field has been limited by our ability to both measure and untangle environmental and coral growth parameters for extended periods of time. The goal of Chapter 4 was to address these previous limitations with a two-year observational study in Bermuda designed to evaluate the interconnected environmental drivers of coral and reef-scale calcification. We hypothesized that coral calcification would increase up to the taxon-specific thermal growth optimum as seawater temperatures warmed in the summertime. Further, we hypothesized that because seawater temperatures vary greatly over seasonal timescales, temperature would be the dominant control on coral and reef-scale calcification. Chapter 4 builds upon the *in situ* coral and reef-scale calcification rates in Chapter 3 by adding coral calcification rates for a second lagoonal patch reef site in Bermuda and environmental parameters for both sites to evaluate the drivers of coral and reef-scale calcification. Chapter 4, in full, is a reprint of the material as it appears in Courtney TA, Lebrato M, Bates NR, Collins A, de Putron SJ, Garley R, Johnson, R, Molinero JC, Noyes TJ, Sabine CL, Andersson AJ. Environmental controls on modern scleractinian coral and reef-scale calcification. *Science Advances*, 2017, 3(11), p.e1701356.

Coral bleaching events are increasing in frequency and intensity (Donner et al. 2017; Hughes et al. 2018a), but relatively few studies have investigated the effects of coral bleaching on NEC (Kayanne et al. 2005; Watanabe et al. 2006; DeCarlo et al. 2017). The goal of Chapter 5 was to utilize changes in seawater alkalinity across the Kāne'ohe Bay reef flat to assess the impacts of coral bleaching and subsequent coral recovery on coral reef NEC following the fall 2015 coral bleaching event. We hypothesized that Kāne'ohe Bay reef flat NEC would be suppressed during the 2015 coral bleaching event owing to coral stress and/or mortality. Furthermore, we hypothesized that NEC would either remain suppressed in the absence of coral recovery or return to pre-bleaching levels if corals fully recovered following the bleaching event. Chapter 5, in full, is a reprint of the material as it appears in Courtney TA, De Carlo EH, Page HN, Bahr KD, Barro A, Howins N, Tabata R, Terlouw G, Rodgers KS, Andersson AJ. Recovery of reef-scale calcification following a bleaching event in Kāne'ohe Bay, Hawai'i. *Limnology & Oceanography Letters* 2018, 3:1–9.

Increasing frequencies and intensities of coral reef disturbances can reduce overall coral cover and shift coral communities from fast-growing, architecturally complex competitive reef-building corals to slower-growing stress-tolerant and/or fast-growing weedy corals (e.g., Loya et al. 2001; Gardner et al. 2003; Bruno and Selig 2007; Fabricius et al. 2011; Van Woesik et al. 2011; Darling et al. 2013; Grottoli et al. 2014; Jackson et al. 2014; Hughes et al. 2018b). These changes in coral communities have the capacity to reduce reef-scale calcification (e.g., Alvarez-Filip et al. 2013; Perry et al. 2015; Kuffner and Toth 2016; Lange and Perry 2019; Toth et al. 2019), but remains to be rigorously characterized through time and across broad geographic spatial scales with respect to coral life history strategies. The goal of Chapter 6 was to evaluate changes in coral community calcification and the relative contributions by the respective coral

taxa across 121 reef sites at four focal regions in the Pacific (i.e., main Hawaiian Islands and Mo'orea) and Western Atlantic (i.e., Florida Keys Reef Tract and St. John). We hypothesized that the contribution to CCC by competitive corals would decrease throughout the time series and, in contrast, the contribution to CCC by stress-tolerant and weedy corals would increase owing to alterations of coral communities by disturbances throughout the time series of this study. Chapter 6, in full, is currently in review as Courtney TA, Barnes BB, Chollett I, Elahi R, Gross K, Guest JR, Kuffner IB, Lenz EA, Nelson HR, Rogers CS, Toth LT, Andersson AJ. Disturbances drive changes in coral community assemblages and coral calcification capacity.

Final thoughts and concluding statements based on the collective findings of this dissertation are presented in Chapter 7.

1.3 Research Significance

Coral reefs are currently experiencing rapid rates of environmental change resulting in shifts to the geo-ecological function of present day coral reefs with future change likely to threaten the form and function of near-future coral reef systems around the world (e.g., Kleypas et al. 2001; Gardner et al. 2003; Bruno and Selig 2007; Hoegh-Guldberg et al. 2007; Andersson and Gledhill 2013; Graham et al. 2014; Jackson et al. 2014; Hughes et al. 2017; Perry et al. 2018; Eyre et al. 2018; Perry and Filip 2018; Toth et al. 2019; Williams et al. 2019). This dissertation synthesizes census and chemistry-based net reef calcification methods to critically evaluate rates of reef-scale calcification and make recommendations to improve the precision of future net reef calcification studies in Chapters 2 and 3. These methods were further applied to better understand the primary environmental drivers of coral and reef-scale calcification in Chapter 4 and how coral bleaching and other disturbance events affect reef-scale calcification and the relative contribution of coral taxa to reef-scale calcification in Chapters 5 and 6. Most notably,

these chapters highlight the benefits of reduced rates of ocean warming for maintaining reef-scale calcification, the capacity for reef-scale calcification to recover following elevated thermal stress, and the ability for shifting coral community compositions to maintain reef-scale calcification under repeated disturbances. The collective result of this dissertation is therefore a more nuanced, mechanistic understanding of how pantropical coral reef growth adapts and responds to environmental change that advances evidence-based management and conservation of coral reef structures and the services these structures provide to humanity.

1.4 References Cited

Alvarez-Filip L, Carricart-Ganivet JP, Horta-Puga G, Iglesias-Prieto R (2013) Shifts in coral-assemblage composition do not ensure persistence of reef functionality. Sci Rep 3:3486

Andersson AJ, Gledhill D (2013) Ocean Acidification and Coral Reefs: Effects on Breakdown, Dissolution, and Net Ecosystem Calcification. Ann Rev Mar Sci 5:321–348

Atkinson MJ (2011) Biogeochemistry of nutrients. Coral Reefs: An Ecosystem in Transition. pp 199–206

Broecker WS, Takahashi T (1966) Calcium carbonate precipitation on the Bahama Banks. J Geophys Res 71:1575

Bruno JF, Selig ER (2007) Regional decline of coral cover in the Indo-Pacific: Timing, extent, and subregional comparisons. PLoS One 2:e711

Chave KE, Smith S V., Roy KJ (1972) Carbonate production by coral reefs. Mar Geol 12:123–140

Chisholm JRM, Gattuso J-P (1991) Validation of the alkalinity anomaly technique for investigating calcification of photosynthesis in coral reef communities. Limnol Oceanogr 36:1232–1239

Connell JH (1978) Diversity in Tropical Rain Forests and Coral Reefs. Science 199:1302–1310

Costanza R, de Groot R, Sutton P, van der Ploeg S, Anderson SJ, Kubiszewski I, Farber S, Turner RK (2014) Changes in the global value of ecosystem services. Glob Environ Chang 26:152–158

Courtney TA, Andersson AJ (2019) Evaluating measurements of coral reef net ecosystem calcification rates. Coral Reefs

Courtney TA, Andersson AJ, Bates NR, Collins A, Cyronak T, de Putron SJ, Eyre BD, Garley R,

Hochberg EJ, Johnson R, Musielewicz S, Noyes TJ, Sabine CL, Sutton AJ, Toncin J, Tribollet A (2016) Comparing Chemistry and Census-Based Estimates of Net Ecosystem Calcification on a Rim Reef in Bermuda. Front Mar Sci 3:181

Courtney TA, Barnes B, Chollett I, Elahi R, Gross K, Guest J, Kuffner I, Lenz E, Nelson H, Rogers C, Toth L, Andersson A Disturbances drive changes in coral community assemblages and coral calcification capacity. in review.

Courtney TA, De Carlo EH, Page HN, Bahr KD, Barro A, Howins N, Tabata R, Terlouw G, Rodgers KS, Andersson AJ (2018) Recovery of reef-scale calcification following a bleaching event in Kāne'ohe Bay, Hawai'i. Limnol Oceanogr Lett 3:1–9

Courtney TA, Lebrato M, Bates NR, Collins A, de Putron SJ, Garley R, Johnson R, Molinero J-CC, Noyes TJ, Sabine CL, Andersson AJ (2017) Environmental controls on modern scleractinian coral and reef-scale calcification. Sci Adv 3:e1701356

Cyronak T, Andersson AJ, Langdon C, Albright R, Bates NR, Caldeira K, Carlton R, Corredor JE, Dunbar RB, Enochs I, Erez J, Eyre BD, Gattuso JP, Gledhill D, Kayanne H, Kline DI, Koweek DA, Lantz C, Lazar B, Manzello D, McMahon A, Meléndez M, Page HN, Santos IR, Schulz KG, Shaw E, Silverman J, Suzuki A, Teneva L, Watanabe A, Yamamoto S (2018) Taking the metabolic pulse of the world's coral reefs. PLoS One 13:1–17

Darling ES, McClanahan TR, Côté IM (2013) Life histories predict coral community disassembly under multiple stressors. Glob Chang Biol 19:1930–1940

DeCarlo TM, Cohen AL, Wong GTF, Shiah F, Lentz SJ, Davis KA, Shamberger KEF, Lohmann P (2017) Community production modulates coral reef pH and the sensitivity of ecosystem calcification to ocean acidification. J Geophys Res Ocean 122:745–761

Donner SD, Potere D (2007) The Inequity of the Global Threat to Coral Reefs. Bioscience 57:214–215

Donner SD, Rickbeil GJM, Heron SF (2017) A new, high-resolution global mass coral bleaching database. PLoS One 12:e0175490

Donner SD, Skirving WJ, Little CM, Oppenheimer M, Hoegh-Gulberg O (2005) Global assessment of coral bleaching and required rates of adaptation under climate change. Glob Chang Biol 11:2251–2265

Eakin CM (1996) Where have all the carbonates gone? A model comparison of calcium carbonate budgets before and after the 1982-1983 El Niño at Uva Island in the eastern Pacific. Coral Reefs 15:109–119

Edmunds PJ, Comeau S, Lantz C, Andersson A, Briggs C, Cohen A, Gattuso JP, Grady JM, Gross K, Johnson M, Muller EB, Ries JB, Tambutté S, Tambutté E, Venn A, Carpenter RC (2016) Integrating the Effects of Ocean Acidification across Functional Scales on Tropical Coral Reefs. Bioscience 66:350–362

Eyre BD, Cyronak T, Drupp P, Carlo EH De, Sachs JP, Andersson AJ (2018) Coral reefs will transition to net dissolving before end of century. Science 911:908–911

Fabricius KE, Langdon C, Uthicke S, Humphrey C, Noonan S, De'ath G, Okazaki R, Muehllehner N, Glas MS, Lough JM, De 'ath G, Okazaki R, Muehllehner N, Glas MS, Lough JM (2011) Losers and winners in coral reefs acclimatized to elevated carbon dioxide concentrations. Nat Clim Chang 1:165–169

Gardner TA, Cote IM, Gill JA, Grant A, Watkinson AR (2003) Long-Term Region-Wide Declines in Caribbean Corals. Science 301:958–960

Gattuso JP, Pichon M, Delesalle B, Canon C, Frankignoulle M (1996) Carbon fluxes in coral reefs. I. Lagrangian measurement of community metabolism and resulting air-sea CO2 disequilibrium. Mar Ecol Prog Ser 145:109–121

Glynn PW (1993) Coral reef bleaching: ecological perspectives. Coral Reefs 12:1–17

Graham NAJ, Cinner JE, Norström A V., Nyström M (2014) Coral reefs as novel ecosystems: embracing new futures. Curr Opin Environ Sustain 7:9–14

de Groot R, Brander L, van der Ploeg S, Costanza R, Bernard F, Braat L, Christie M, Crossman N, Ghermandi A, Hein L, Hussain S, Kumar P, McVittie A, Portela R, Rodriguez LC, ten Brink P, van Beukering P (2012) Global estimates of the value of ecosystems and their services in monetary units. Ecosyst Serv 1:50–61

Grottoli AG, Warner ME, Levas SJ, Aschaffenburg MD, Schoepf V, Mcginley M, Baumann J, Matsui Y (2014) The cumulative impact of annual coral bleaching can turn some coral species winners into losers. Glob Chang Biol 20:3823–3833

Harney JN, Fletcher CH (2003) A budget of carbonate framework and sediment production, Kailua Bay, Oahu, Hawaii. J Sediment Res 73:856–868

Hemer MA, Fan Y, Mori N, Semedo A, Wang XL (2013) Projected changes in wave climate from a multi-model ensemble. Nature Climate Change 3(5): 471

Hoegh-Guldberg O, Mumby PJ, Hooten A, Steneck RS, Greenfield P, Gomez E, Harvell CD, Sale PF, Edwards AJ, Caldeira K, Knowlton N, Eakin CM, Iglesias-Prieto R, Muthiga N, Bradbury RH, Dubi A, Hatziolos ME (2007) Coral reefs under rapid climate change and ocean acidification. Science 318:1737–1742

van Hooidonk R, Maynard J, Tamelander J, Gove J, Ahmadia G, Raymundo L, Williams G, Heron SF, Planes S (2016) Local-scale projections of coral reef futures and implications of the Paris Agreement. Sci Rep 6:39666

Hubbard DK, Miller AI, Scaturo D (1990) Production and cycling of calcium carbonate in a shelf-edge reef system (St. Croix, U.S. Virgin Islands): Applications to the nature of reef systems in the fossil record. J Sediment Petrol 60:335–360

Hughes TP, Anderson KD, Connolly SR, Heron SF, Kerry JT, Lough JM, Baird AH, Baum JK, Berumen ML, Bridge TC, Claar DC, Eakin CM, Gilmour JP, Graham NAJ, Harrison H, Hobbs JPA, Hoey AS, Hoogenboom M, Lowe RJ, McCulloch MT, Pandolfi JM, Pratchett M, Schoepf V, Torda G, Wilson SK (2018a) Spatial and temporal patterns of mass bleaching of corals in the Anthropocene. Science 359:80–83

Hughes TP, Barnes ML, Bellwood DR, Cinner JE, Cumming GS, Jackson JBC, Kleypas J, Leemput Van De IA, Lough JM, Morrison TH, Palumbi SR (2017) Coral reefs in the Anthropocene. Nature 546:82

Hughes TP, Kerry JT, Baird AH, Connolly SR, Dietzel A, Eakin CM, Heron SF, Hoey AS, Hoogenboom MO, Liu G, McWilliam MJ, Pears RJ, Pratchett MS, Skirving WJ, Stella JS, Torda G (2018b) Global warming transforms coral reef assemblages. Nature 556:492

Jackson JBC, Donovan MK, Cramer KL, Lam V (2014) Status and Trends of Caribbean Coral Reefs : 1970-2012. Glob Coral Reef Monit Netw

Jokiel PL, Coles SL (1977) Effects of Temperature on the Mortality and Growth of Hawaiian Rccf Corals. Mar Biol 43:201–208

Kayanne H, Hata H, Kudo S, Yamano H, Watanabe A, Ikeda Y, Nozaki K, Kato K, Negishi A, Saito H (2005) Seasonal and bleaching-induced changes in coral reef metabolism and CO_2 flux. Global Biogeochem Cycles 19:1–11

Kleypas JA, Buddemeier RW, Gattuso JP (2001) The future of coral reefs in an age of global change. Int J Earth Sci 90:426–437

Knowlton N, Brainard RE, Fisher R, Moews M, Plaisance L, Caley MJ (2010) Coral Reef Biodiversity. In: McIntyre A. (eds) Life in the World's Oceans: Diversity, Distribution, and Abundance. Wiley-Blackwell, Oxford, pp 65–77

Kuffner IB, Toth LT (2016) A geological perspective on the degradation and conservation of western Atlantic coral reefs. Conserv Biol 30:706–715

Langdon C, Gattuso J-P, Andersson A (2010) Measurements of calcification and dissolution of benthic organisms and communities. Guid to best Pract Ocean Acidif Res data Report 213–232

Lange ID, Perry CT (2019) Bleaching impacts on carbonate production in the Chagos Archipelago: influence of functional coral groups on carbonate budget trajectories. Coral Reefs

Loya Y, Sakai K, Yamazato K, Nakano Y, Sambali H, Van Woesik R (2001) Coral bleaching: The winners and the losers. Ecol Lett 4:122–131

McMahon A, Santos IR, Cyronak T, Eyre BD (2013) Hysteresis between coral reef calcification and the seawater aragonite saturation state. Geophys Res Lett 40:4675–4679

Moberg F, Folke C (1999) Ecological goods and services of coral reef ecosystems. Ecol Econ 29:215–233

Montaggioni L, Braithwaite C (2009) Chapter Five Patterns of Carbonate Production and Deposition on Reefs. Elsevier B.V.,

Page HN, Courtney TA, Collins A, Carlo EH De, Andreas A, Andreas J, Page HN (2017) Net Community Metabolism and Seawater Carbonate Chemistry Scale Non-Intuitively with Coral Cover. Front Mar Sci 4:1–17

Perry CT, Alvarez-filip L, Graham NAJ, Mumby PJ, Wilson SK, Kench PS, Derek P, Morgan KM, Slangen ABA, Damian P (2018) Loss of coral reef growth capacity to track future increases in sea-level. Nature 558:396–400

Perry CT, Edinger EN, Kench PS, Murphy GN, Smithers SG, Steneck RS, Mumby PJ (2012) Estimating rates of biologically driven coral reef framework production and erosion: A new census-based carbonate budget methodology and applications to the reefs of Bonaire. Coral Reefs 31:853–868

Perry CT, Filip LA (2018) Changing geo-ecological functions of coral reefs in the Anthropocene. Funct Ecol 1–13

Perry CT, Kench PS, Smithers SG, Riegl B, Yamano H, O'Leary MJ (2011) Implications of reef ecosystem change for the stability and maintenance of coral reef islands. Glob Chang Biol 17:3679–3696

Perry CT, Morgan KM, Yarlett RT (2017) Reef Habitat Type and Spatial Extent as Interacting Controls on Platform-Scale Carbonate Budgets. Front Mar Sci 4:1–13

Perry CT, Murphy GN, Kench PS, Smithers SG, Edinger EN, Steneck RS, Mumby PJ (2013) Caribbean-wide decline in carbonate production threatens coral reef growth. Nat Commun 4:1402

Perry CT, Steneck RS, Murphy GN, Kench PS, Edinger EN, Smithers SG, Mumby PJ (2015) Regional-scale dominance of non-framework building corals on Caribbean reefs affects carbonate production and future reef growth. Glob Chang Biol 21:1153–1164

Pratchett MS, Anderson KD, Hoogenboom MO, Widman E, Baird AH, Pandolfi JM, Edmunds PJ, Lough JM (2015) Spatial, temporal and taxonomic variation in coral growth - implications for the structure and function of coral reef ecosystems. Oceanogr Mar Biol An Annu Rev 53:215–296

Reaka-Kudla ML (1997) The Global Biodiversity of Coral Reefs: A comparison with Rain Forests. Biodiversity II: Understanding and Protecting Our Biologiclal Resources. The National Academy of Sciences, pp 49–50

Schönberg CHL, Fang JKH, Carreiro-Silva M, Tribollet A, Wisshak M (2017) Bioerosion: The other ocean acidification problem. ICES J Mar Sci 74:895–925

Smith S, Kinsey D (1976) Calcium Carbonate Production, Coral Reef Growth, and Sea Level Change. Science 194:937–939

Smith S V. (1973) Carbon Dioxide Dynamics: a Record of Organic Carbon Production, Respiration, and Calcification in the Eniwetok Reef Flat Community 1. Limnol Oceanogr 18:106–120

Smith S V, Key G (1975) Carbon Dioxide and Metabolism in Marine Environments Carbon. Limnol Oceanogr 20:493–495

Stearn W, Scoffin TP, Martindale W (1977) Calcium carbonate budget of a fringing reef on teh west coast of Barbados. Bull Mar Sci 27:479–510

Toth LT, Stathakopoulos A, Kuffner IB, Ruzicka RR, Colella MA, Shinn EA (2019) The unprecedented loss of Florida's reef-building corals and the emergence of a novel coral-reef assemblage. 0:1–14

Tuck ME, Kench PS, Ford MR, Masselink G (2019) Physical modelling of the response of reef islands to sea-level rise. Geology 47:1–4

Watanabe A, Kayanne H, Hata H, Kudo S, Nozaki K, Kato K, Negishi a, Ikeda Y, Yamano H (2006) Analysis of the seawater CO_2 system in the barrier reef-lagoon system of Palau using total alkalinity-dissolved inorganic carbon diagrams. Limnol Oceanogr 51:1614–1628

Williams GJ, Norström A V, Wedding LM, Graham NAJ, Nyström M, Jouffray JB, Gove JM, Heenan A (2019) Coral reef ecology in the Anthropocene. Funct Ecol 1014–1022

Van Woesik R, Sakai K, Ganase A, Loya Y (2011) Revisiting the winners and the losers a decade after coral bleaching. Mar Ecol Prog Ser 434:67–76

Woodhead AJ, Williams GJ, Hicks CC, Norström A V, Graham NAJ (2019) Coral reef ecosystem services in the Anthropocene. Funct Ecol 1–12

CHAPTER 2

Evaluating measurements of coral reef net ecosystem calcification rates

Courtney TA & Andersson AJ

Coral Reefs
https://doi.org/10.1007/s00338-019-01828-2

REPORT

Evaluating measurements of coral reef net ecosystem calcification rates

T. A. Courtney[1] · **A. J. Andersson**[1]

Received: 10 January 2019 / Accepted: 5 June 2019

Abstract Monitoring the rates and drivers of coral reef net ecosystem calcification (NEC) under anthropogenic environmental change is critical for predicting associated changes in reef structures and ecosystem services. However, NEC studies to date show weak agreement between studies and notably reveal no relationship between NEC and benthic calcifier cover. In this study, we tested for the sensitivity of calculated NEC to uncertainties in seawater depths and residence times (± 83% relative to 6 m and 6 h, respectively) using a coral reef total alkalinity (A_T) simulator (reefCA$_T$S) and found that these errors can interact to drive large asymmetric uncertainties ranging from − 91% to + 1000% in NEC. Furthermore, numerical simulations of hypothetical NEC for coral populations occupying reefs with increasing structural complexity (rugosity = 1–4) showed that the effects of reef-scale rugosity on NEC can be as important as benthic community composition. As a result, uncertainties in seawater depth, residence time, and/or reef structural complexity are enough to mask any potential real correlation between NEC and percent calcifier cover in the field. To improve comparability and validity of NEC studies, we recommend that future studies place a high degree of scrutiny on measurements of seawater hydrodynamics, report all NEC equation parameters ± uncertainties, and ideally include benthic community composition and structural complexity data to further explore the relationship between NEC and calcifier cover.

Keywords Coral reef · Net ecosystem calcification · Structural complexity · Rugosity · Ecosystem services · Climate change · Biogeochemistry · Ecosystem monitoring

Topic Editor Morgan S. Pratchett

Electronic supplementary material The online version of this article (https://doi.org/10.1007/s00338-019-01828-2) contains supplementary material, which is available to authorized users.

✉ T. A. Courtney
traviscourtney@gmail.com

[1] Scripps Institution of Oceanography, University of California, San Diego, La Jolla, CA, USA

Introduction

Coral reefs are currently undergoing rapid declines in coral cover globally (Gardner et al. 2003; Bruno and Selig 2007; Jackson et al. 2014), which can decrease coral reef growth and shoreline protection for coastal human populations around the world (Harris et al. 2018; Perry et al. 2018; Storlazzi et al. 2018). Monitoring coral reef growth (i.e., coral reef growth = calcification − $CaCO_3$ dissolution + $CaCO_3$ sediment import − $CaCO_3$ sediment export [Chave et al. 1972; Stearn et al. 1977; Kleypas et al. 2001]) is therefore necessary to predict potential changes in the maintenance of coral reef $CaCO_3$ structures and the resulting ecosystem services these structures provide (Kleypas et al. 2001; Edmunds et al. 2016; Courtney et al. 2018; Cyronak et al. 2018; Perry et al. 2018). However, accurate and precise measurements of modern coral reef growth have proved a challenging task.

Reef growth can be directly measured from reef sediment cores (Aronson and Precht 2001; Montaggioni 2005) or by long-term changes in bathymetric mapping (Yates et al. 2017). However, these methods lack the temporal resolution to track higher frequency changes in reef growth and metabolic performance associated with shifting benthic community compositions and oceanographic forcing,

which are increasingly important given the current status of coral reef declines. Alternatively, census-based $CaCO_3$ budget methodology is one approach used to approximate annual net coral reef $CaCO_3$ production by assigning annual rates of $CaCO_3$ production and erosion to benthic survey data, but by definition generally omits the net import/export of $CaCO_3$ terms required to fully calculate reef growth (Chave et al. 1972; Stearn et al. 1977; Hubbard et al. 1990; Perry et al. 2012, 2018). These methods can be rapidly applied across a range of coral reef systems, but typically rely on literature-derived annual mean $CaCO_3$ production/erosion rates that are assumed to be constant across geographic and environmental conditions (Perry et al. 2012). As a result, these census-based budgets often fail to capture sub-annual variability in net reef $CaCO_3$ production (Courtney et al. 2016) and site-specific variability in rates of $CaCO_3$ production and erosion. Another approach to estimate net coral reef $CaCO_3$ production utilizes chemistry-based methods (i.e., net ecosystem calcification [NEC] = calcification–$CaCO_3$ dissolution) that address these shortcomings by measuring alkalinity anomalies ($\Delta A_T = A_{Tinitial} - A_{Tfinal}$ where A_{Tfinal} represents the seawater total alkalinity that has been modified by the coral reef from its initial value of $A_{Tinitial}$) as a proxy for net removal of Ca^{2+} and dissolved inorganic carbon (DIC) by NEC on time-scales of approximately hours to days (Broecker and Takahashi 1966).

While a broad range of NEC methods exists, they all rely on difficult to constrain measurements of seawater hydrodynamics that mediate the length of time and total amount of the seawater that has been in contact with and modified by the benthos to calculate NEC from alkalinity anomalies (Broecker and Takahashi 1966; Smith and Key 1975; Gattuso et al. 1996; Silverman et al. 2007; Venti et al. 2012; Zhang et al. 2012; Falter et al. 2013; Lowe and Falter 2015; Courtney et al. 2016). Historically, studies have utilized slack tides, temporal isolation during low tide, unidirectional flow regimes (Eularian or Lagrangian), enclosures, or calculated atoll seawater residence times to estimate NEC (Broecker and Takahashi 1966; Smith and Key 1975; Kinsey 1985; Gattuso et al. 1996). The advantages and disadvantages of these earlier methods have previously been discussed by Kinsey (1985), but see also more recent eddy covariance and benthic gradient flux methods (Long et al. 2015; Takeshita et al. 2016).

Typically, NEC is calculated from measurements of seawater alkalinity anomaly (ΔA_T), density (ρ), depth (z), and residence time (τ) as per the following equation (Smith and Key 1975; Langdon et al. 2010):

$$\mathrm{NEC} = \frac{\Delta A_T \rho z}{2\tau} \quad (1)$$

Of these parameters, seawater A_T can be precisely measured within $\pm$ 2 μmol kg^{-1} using established sampling and analytical methods (Dickson et al. 2007) and seawater density can be precisely measured or calculated from seawater temperature, salinity, and pressure via the seawater equation of state to within $\pm$ 0.002 kg m^{-3} (McDougall and Barker 2011; Roquet et al. 2015). LIDAR (Light Detection and Ranging)-produced digital elevation models (Yates et al. 2017) allow for precise measurements of reef-scale seawater depths (z) and advancements in current profiler technologies (DeCarlo et al. 2017), numerical models (Lowe et al. 2009), and chemistry-based seawater residence times (Venti et al. 2012; Muehllehner et al. 2016) have improved our ability to quantify coral reef hydrodynamics. However, precisely determining the z and τ of the hydrochemical footprint (i.e., spatial area and length of time over which the water has been modified by the benthos) associated with the measured ΔA_T remains a significant challenge owing to the spatiotemporally complex hydrodynamics of coral reef environments, which consequently can generate potentially large uncertainties in NEC calculated from z and τ via Eq. 1 (Venti et al. 2012; Zhang et al. 2012; Falter et al. 2013; Lowe and Falter 2015; Courtney et al. 2016). For example, Shamberger et al. (2011) and Courtney et al. (2018) used seawater flow rates and residence times, respectively, to calculate NEC using similar ΔA_T and hydrodynamic conditions at overlapping portions of the Kāne'ohe Bay reef flat, but the differences in characterizing this flow were the primary driver of diverging NEC rates by approximately an order of magnitude between the two studies (Courtney et al. 2018). Thus, we suggest that the uncertainties associated with constraining the z and τ of the hydrochemical footprint require further investigation to ensure greater consistency and comparability of NEC between studies.

Intuitively, increasing cover of calcifiers (e.g., the typical dominant reef calcifiers are scleractinian corals, red coralline algae, molluscs, *Halimeda* calcifying algae, and benthic foraminifera [Montaggioni and Braithwaite 2009]) should positively correlate with increasing NEC due to increasing $CaCO_3$ production rates. This relationship is inherent in census-based studies (but note that this is in part an artifact of the budget methodology [Perry et al. 2012]) and has been observed in a chemistry-based mesocosm study (Page et al. 2017), but field-based NEC rates show no relationship with calcifier cover (DeCarlo et al. 2017). This lack of an observed relationship between calcifier cover and NEC in the field could be due to mechanistic factors such as altered calcification rates under local environmental conditions (DeCarlo et al. 2017) or competitive interactions (Tanner 1995, 1997; McWilliam et al. 2018), the provisioning of additional surface area to calcifiers by

three-dimensional reef-scale structural complexity (Hubbard et al. 1990; Pichon 1997; Szmant 1997, 2002; Perry et al. 2012), underreported calcifier cover owing to difficulties in surveying under canopies (Goatley and Bellwood 2011), relative proportion of faster and slower calcifiers (Chave et al. 1972; Pichon 1997; Szmant 2002; Perry et al. 2015), and/or the effects of $CaCO_3$ dissolution and chemical $CaCO_3$ bioerosion (Andersson and Gledhill 2013; Eyre et al. 2018). Alternatively, the previously described difficulties associated with constraining complex seawater hydrodynamics over coral reef environments and resulting NEC uncertainties can be large (Falter et al. 2013) and we hypothesize that these potentially large and underreported NEC uncertainties may be masking any potential real correlation between NEC and calcifier cover.

To test this hypothesis, we developed a coral reef total alkalinity simulator (reefCA$_T$S) to calculate expected ΔA_T for a given NEC under varying seawater depths and residence times and to perform a sensitivity analysis of how errors in seawater depth and residence time affect calculated NEC. We then further calculated a range of expected NEC for given coral cover, community composition, and reef structural complexity drawing from census-based and mesocosm/enclosure NEC studies to serve as a reference for evaluating future NEC studies.

Materials and methods

The coral reef total alkalinity simulator (reefCA$_T$S) is a simple box model consisting of a seawater reservoir overlying a coral reef community that measures the change in seawater A_T owing to NEC. The purpose of this study was not to fully simulate the dynamic physical and biogeochemical processes occurring over a reef flat (e.g., see Falter et al. [2013]), but instead to generate the simplest example of a calcifying benthic community chemically modifying the overlying seawater chemistry (Fig. 1) to (1) calculate ΔA_T for a range of seawater depths and residence times with calcification by two representative coral species and (2) isolate the sensitivity of NEC calculations to uncertainties associated with constraining seawater depth (z) and residence time (τ).

reefCA$_T$S model overview

Seawater hydrodynamics were simplified by assuming a steady state of seawater flux into (SW_{in}; kg h^{-1}) and out of (SW_{out}) the seawater reservoir (i.e., SW_{in} = SW_{out}) with a fixed 1 km^2 planar area and constant parameterized depth that assumes no influence of tides and waves on the volume of seawater in this reservoir. Furthermore, seawater was assumed to only flow into the reef seawater reservoir from

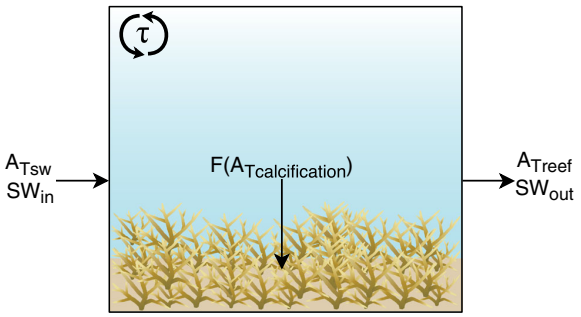

Fig. 1 reefCA$_T$S diagram shows the parameterized fluxes of seawater total alkalinity (A_T) into and out of the 1-km^2 planar area coral reef seawater reservoir with volume controlled by parameterizing reservoir depth (z). A_{Tsw} is the total alkalinity of the seawater flowing into the box (SW_{in}), which is instantaneously mixed for the duration of the seawater residence time (τ). A_{Treef} is the total alkalinity of the seawater flowing out of the reef box (SW_{out}), z is the depth which controls the volume of seawater in the reef box, and $F(A_{Tcalcification})$ is the total alkalinity flux out of the reef seawater owing to model parameterized calcification

source water of constant A_T (A_{Tin}; μmol kg^{-1}) that was completely and instantaneously mixed and remained for a fixed residence time before flowing out of this reservoir (Fig. 1). Alkalinity flux owing to calcification [$F(A_{Tcalcification})$; μmol h^{-1}] was parameterized based on literature values (see subsequent section) and was the sole process changing A_T within the seawater reservoir. No other processes (e.g., no $CaCO_3$ dissolution, no heating/cooling, and no evaporation/precipitation) modified seawater properties. The mass balance of total alkalinity in the seawater reservoir was represented by the following differential equation:

$$\frac{dA_{Treef}}{dt} = SW_{in} \times [A_{Tin}] - SW_{out} \times [A_{Treef}] - F(A_{Tcalcification}), \quad (2)$$

and thus, at steady state:

$$0 = SW_{in} \times [A_{Tin}] - SW_{out} \times [A_{Treef}] - F(A_{Tcalcification}) \quad (3)$$

The seawater residence time (τ; h) was defined as the ratio of the total mass of seawater in the reservoir (M_{SWreef}; kg) over the seawater inflow or outflow, assuming a steady state:

$$\tau = \frac{M_{SWreef}}{SW_{in}} = \frac{za\rho}{SW_{in}} \quad (4)$$

where z is the depth of the reef seawater reservoir (m), a is the area of the reef (m^2), and ρ is the density of seawater (kg m^{-3}). Thus, the differential equation for the rate of change of reef seawater total alkalinity (dA_{Treef}/dt; μmol kg^{-1} h^{-1}) can be expressed as:

$$\frac{dA_{Treef}}{dt} = \frac{A_{Tin} - A_{Treef}}{\tau} - \frac{F(A_{Tcalcification})}{za\rho} \quad (5)$$

This equation (Eq. 5) was solved at 0.1-h time steps using the *ode45* ordinary differential equation solver in the statistical software *R* (R Core Team 2017) package *deSolve* (Soetaert et al. 2010). Each model simulation was run for 2500 h to ensure a steady state in the reef seawater reservoir before calculation of the alkalinity anomaly ($\Delta A_T = A_{Tin} - A_{Treef}$) and NEC via Eq. 1.

Parameterized values

All reefCA_TS runs were calculated using a 1 km × 1 km planar reef area with fixed calcification rates for a range of seawater depths (1–11 m at 1 m intervals) and residence times (1–11 h at 1 h intervals) to simulate a broad range of coral reef hydrodynamic states and resulting ΔA_T. Fixed calcification rates were used to avoid confounding the results of this analysis with diel variability in calcification rates. A rate of 33.8 mmol m^{-2} h^{-1} by 100% coral cover of *Acropora nasuta* (calcification = 29.6 kg $CaCO_3$ m^{-2} yr^{-1} sensu Morgan and Kench [2012]) was used because it represents an approximate upper rate for calcifying reef corals (Pratchett et al. 2015). While the subsequent sensitivity analyses were based on 100% cover *A. nasuta* calcification rates, additional simulations were conducted using a calcification rate of 15.7 mmol m^{-2} h^{-1} that represents calcification by 100% cover of the more slowly calcifying *Porites lobata* (calcification = 13.8 kg $CaCO_3$ m^{-2} yr^{-1} sensu Morgan and Kench [2012]) to serve as an additional reference for expected ΔA_T. For reference of the values used in this study, the 1–11 m seawater depths used in this study are within the range of mean (± standard deviation) depths for typical reef flats (1.3 ± 0.5 m) and channels (6.3 ± 9.8 m) from Falter et al. (2013). Similarly, the 1–11 h residence times in this study are within the range of 1.4–14.7 h it would take for seawater to transit and be biogeochemically modified by a typical reef flat assuming mean (± standard deviation) unidirectional, depth-averaged flow rates of 0.16 ± 0.06 m s^{-1} and reef flat widths of 3.7 ± 2.6 km from Falter et al. (2013). However, it is important to note that recirculation patterns, oscillating seawater flows, and reef morphologies are capable of generating longer and spatially variable seawater residence times than predicted from mean unidirectional flow rates across a reef flat, which consequently can drive greater and more spatially variable coral reef ΔA_T (Lowe et al. 2009; Venti et al. 2012; Zhang et al. 2012; Falter et al. 2013; Lowe and Falter 2015; Muehllehner et al. 2016). To address this potential for longer residence times and better represent lower coral cover systems, we included additional ΔA_T simulations with residence times ranging from 1 to 144 h, depths ranging from 1 to 11 m, and 10% coral cover calcification rates (i.e., 10% *A. nasuta* or 10% *P. lobata*) occupying a planar 1 km^2 reef area. Models were parameterized using mean surface ocean total alkalinity (A_T = 2310 µmol kg^{-1}) and average seawater density (ρ = 1023 kg m^{-3}) for the upper 50 m at station ALOHA from the Hawai'i Ocean Time-series for 1988–2017 (hahana.soest.hawaii.edu/hot/hot-dogs).

Sensitivity analysis

The model simulation for a seawater depth of 6 m and residence time of 6 h using the fixed 33.8 mmol m^{-2} h^{-1} calcification rate by 100% cover *A. nasuta* calcification resulted in a ΔA_T of 66 µmol kg^{-1}. This ΔA_T was then used to calculate NEC (Eq. 1) using the actual seawater depth and residence time and for a range of erroneous seawater depths (1–11 m) and residence times (1–11 h). While we do not know the actual range of typical errors in seawater depth and residence time across NEC studies, these simulated ranges were calculated as the percent error relative to the model parameterized reference value such that z = 6 ± 5 m (± 83%) and τ = 6 ± 5 h (± 83%) to generalize these results to other NEC studies with varying mean seawater depths and residence times. Similarly, erroneously calculated NEC from the sensitivity analysis of this study was determined as the percent error relative to the actual parameterized reefCA_TS NEC. The resulting errors in NEC were assessed with respect to (1) seawater depth, (2) residence time, or (3) both seawater depth and residence time.

Literature review

A literature review of NEC supplementing the work of DeCarlo et al. (2017) with more recent studies and separating studies conducted in mesocosms and enclosures from field-based studies was then performed to further test for linear scaling of NEC with calcifier cover (see supplementary NEC review datasheet). Linear models between NEC (previous studies were converted to mmol $CaCO_3$ m^{-2} h^{-1}) and percent calcifier cover were fitted using the function *lm* and assessed using ANOVA for the mesocosm/enclosure and field-based studies separately to test for linear correlations between NEC and calcifier cover.

Effects of reef structural complexity on NEC

Additional calculations were made to assess the effects of reef structural complexity and coral community composition on NEC. We used rugosity (R) = linear/planar distance along the reef surface with typical ranges of R = 1–4 (Graham and Nash 2013) to model the effects of structural

complexity on NEC in this study. Single-species benthic communities of 0–100% *A. nasuta* and *P. lobata*, respectively, were simulated over reef-scale rugosities ranging from 1 to 4 to simulate potential upper bounds of NEC for reef sites of varying structural complexity occupied by a rapidly calcifying coral (*A. nasuta*) and a more slowly calcifying coral (*P. lobata*). These simulations allow us to explore the interactions between calcification rates and reef structural complexity (Pichon 1997; Szmant 1997, 2002; Perry et al. 2012; Graham and Nash 2013; Pratchett et al. 2015) to calculate expected NEC for hypothetical coral reef ecosystems.

Results

reefCA$_T$S alkalinity anomalies

The reefCA$_T$S runs for a range of seawater depths (1–11 m) and residence times (1–11 h) for the parameterized 33.8 mmol m^{-2} h^{-1} calcification rate (100% cover *A. nasuta* planar reef) generated ΔA_T ranging from 6 µmol kg^{-1} (1 h, 11 m simulation) to 726 µmol kg^{-1} (11 h, 1 m simulation) (Table 1). Simulations for the parameterized 15.7 mmol m^{-2} h^{-1} calification rate (100% cover *P. lobata* planar reef) yielded ΔA_T ranging from 3 µmol kg^{-1} (1 h, 11 m simulation) to 338 µmol kg^{-1} (11 h, 1 m simulation) (Table 1). The longer residence time simulations for the 10% *A. nasuta* and 10% *P. lobata* planar reefs with depths of 1 to 11 m and residence times of 1 to 144 h followed a similar pattern (Table 2). In essence, the ΔA_T is dependent on the ratio of calcification rate to seawater volume wherein shallower seawater depths have exponentially decreasing seawater volumes that are more intensely chemically modified by calcification and result in greater ΔA_T (Tables 1, 2). Longer seawater residence times allow for a greater contact time between the overlying seawater and underlying calcifiers, resulting in greater seawater ΔA_T (Tables 1, 2).

reefCA$_T$S sensitivity analysis

The *A. nasuta* simulations evaluating the effect of erroneous depths show that errors of ± 83% in z relative to the actual parameterized depth of 6 m (i.e., 1–11 m) yielded erroneously calculated NEC increasing linearly from − 83% to + 83% (5.6–61.9 mmol m^{-2} h^{-1}) relative to the actual rate of 33.8 mmol m^{-2} h^{-1} (Fig. 2a). Conversely, *A. nasuta* simulations evaluating the effect of erroneous residence times show that errors of ± 83% in τ relative to the actual parameterized residence time of 6 h (i.e., 1–11 h) yielded erroneously calculated NEC exponentially decreasing from + 500% (202.6 mmol m^{-2} h^{-1}) to − 45% (18.4 mmol m^{-2} h^{-1}) relative to the actual rate of 33.8 mmol m^{-2} h^{-1} (Fig. 2b). Thus, underestimates of τ produced greater NEC errors (i.e., − 83% τ = + 500% NEC) than overestimates of τ (i.e., + 83% τ = − 45% NEC, Fig. 2b). Simulations in which both of these simulated errors in seawater depth (± 83%) and residence time (± 83%) were made concurrently resulted in a mean (± SE) NEC error of + 65 ± 18% owing to the nonlinear range of erroneously calculated NEC from − 91% to + 1000% (3.1–371.4 mmol m^{-2} h^{-1}) relative to the actual NEC of 33.8 mmol m^{-2} h^{-1} (Fig. 2). Equivalently, the percent error in NEC owing to any combination of errors in z and τ can further be generalized by solving the % error NEC equation for those terms:

Table 1 Seawater total alkalinity anomalies (ΔA_T; µmol kg^{-1}) expressed across the range of seawater depths (z = 1–11 m) and residence times (τ = 1–11 h) explored in this study. ΔA_T represents $A_{Tsw} - A_{Treef}$ after the reefCA$_T$S runs for the respective seawater depth and residence times have reached steady state for fixed calcification rates of 100% cover by *Acropora nasuta* (33.8 mmol m^{-2} h^{-1}, bold) and *Porites lobata* (15.7 mmol m^{-2} h^{-1}, italics) occupying a 1 km^2 planar reef flat. Coral calcification rates are sensu Morgan and Kench (2012)

	Residence time (h)										
	1	2	3	4	5	6	7	8	9	10	11
Depth (m)											
1	**66**	**132**	**198**	**264**	**330**	**396**	**462**	**528**	**594**	**660**	**726**
	31	*62*	*92*	*123*	*154*	*185*	*215*	*246*	*277*	*308*	*338*
2	**33**	**66**	**99**	**132**	**165**	**198**	**231**	**264**	**297**	**330**	**363**
	15	*31*	*46*	*62*	*77*	*92*	*108*	*123*	*138*	*154*	*169*
3	**22**	**44**	**66**	**88**	**110**	**132**	**154**	**176**	**198**	**220**	**242**
	10	*21*	*31*	*41*	*51*	*62*	*72*	*82*	*92*	*103*	*113*
4	**16**	**33**	**49**	**66**	**82**	**99**	**115**	**132**	**148**	**165**	**181**
	8	*15*	*23*	*31*	*38*	*46*	*54*	*62*	*69*	*77*	*85*
5	**13**	**26**	**40**	**53**	**66**	**79**	**92**	**106**	**119**	**132**	**145**
	6	*12*	*18*	*25*	*31*	*37*	*43*	*49*	*55*	*62*	*68*
6	**11**	**22**	**33**	**44**	**55**	**66**	**77**	**88**	**99**	**110**	**121**
	5	*10*	*15*	*21*	*26*	*31*	*36*	*41*	*46*	*51*	*56*
7	**9**	**19**	**28**	**38**	**47**	**57**	**66**	**75**	**85**	**94**	**104**
	4	*9*	*13*	*18*	*22*	*26*	*31*	*35*	*40*	*44*	*48*
8	**8**	**16**	**25**	**33**	**41**	**49**	**58**	**66**	**74**	**82**	**91**
	4	*8*	*12*	*15*	*19*	*23*	*27*	*31*	*35*	*38*	*42*
9	**7**	**15**	**22**	**29**	**37**	**44**	**51**	**59**	**66**	**73**	**81**
	3	*7*	*10*	*14*	*17*	*21*	*24*	*27*	*31*	*34*	*38*
10	**7**	**13**	**20**	**26**	**33**	**40**	**46**	**53**	**59**	**66**	**73**
	3	*6*	*9*	*12*	*15*	*18*	*22*	*25*	*28*	*31*	*34*
11	**6**	**12**	**18**	**24**	**30**	**36**	**42**	**48**	**54**	**60**	**66**
	3	*6*	*8*	*11*	*14*	*17*	*20*	*22*	*25*	*28*	*31*

Table 2 Seawater total alkalinity anomalies (ΔA_T; μmol kg^{-1}) expressed across the range of seawater depths (z = 1–11 m) and longer residence times (τ = 1–144 h). ΔA_T represents $A_{Tsw} - A_{Treef}$ after the reefCA$_T$S runs for the respective seawater depth and residence times have reached steady state for fixed calcification rates of 10% cover by *Acropora nasuta* (33.8 mmol m^{-2} h^{-1}, bold) and 10% cover by *Porites lobata* (15.7 mmol m^{-2} h^{-1}, italics) occupying a 1 km^2 planar reef flat. Coral calcification rates are sensu Morgan and Kench (2012)

	Residence time (h)							
	1	3	6	12	24	48	96	144
Depth (m)								
1	**7**	**20**	**40**	**79**	**158**	**317**	**633**	**950**
	3	*9*	*18*	*37*	*74*	*148*	*295*	*443*
2	**3**	**10**	**20**	**40**	**79**	**158**	**317**	**475**
	2	*5*	*9*	*18*	*37*	*74*	*148*	*221*
3	**2**	**7**	**13**	**26**	**53**	**106**	**211**	**317**
	1	*3*	*6*	*12*	*25*	*49*	*98*	*148*
4	**2**	**5**	**10**	**20**	**40**	**79**	**158**	**238**
	1	*2*	*5*	*9*	*18*	*37*	*74*	*111*
5	**1**	**4**	**8**	**16**	**32**	**63**	**127**	**190**
	1	*2*	*4*	*7*	*15*	*30*	*59*	*89*
6	**1**	**3**	**7**	**13**	**26**	**53**	**106**	**158**
	1	*2*	*3*	*6*	*12*	*25*	*49*	*74*
7	**1**	**3**	**6**	**11**	**23**	**45**	**90**	**136**
	0	*1*	*3*	*5*	*11*	*21*	*42*	*63*
8	**1**	**2**	**5**	**10**	**20**	**40**	**79**	**119**
	0	*1*	*2*	*5*	*9*	*18*	*37*	*55*
9	**1**	**2**	**4**	**9**	**18**	**35**	**70**	**106**
	0	*1*	*2*	*4*	*8*	*16*	*33*	*49*
10	**1**	**2**	**4**	**8**	**16**	**32**	**63**	**95**
	0	*1*	*2*	*4*	*7*	*15*	*30*	*44*
11	**1**	**2**	**4**	**7**	**14**	**29**	**58**	**86**
	0	*1*	*2*	*3*	*7*	*13*	*27*	*40*

$$\%_{err}NEC = \left(\frac{\tau z_{err}}{z\tau_{err}} - 1\right) \times 100 \quad (6)$$

where z and τ are the actual seawater depth and residence time and z_{err} and τ_{err} are the erroneously measured seawater depth and residence time.

Scaling of NEC with calcifier cover

Linear models between NEC and percent calcifier cover from previous studies revealed a statistically significant linear correlation for studies conducted in mesocosms and enclosures (NEC ± SE [mmol m^{-2} h^{-1}] = 0.10 ± 0.02 × % calcifier cover + 0.03 ± 1.2; R^2 = 0.68, df = 13, F = 27.7, p = 0.0002; Fig. 3a), but not for field-based studies (R^2 = 0.054, df = 29, F = 1.7, p = 0.21; Fig. 3b). Hypothetical scaling of NEC for 0–100% cover of *A. nasuta* and *P. lobata* for planar reefs (R = 1) revealed that many literature-based NEC studies exceed expected *A. nasuta* calcification rates (Fig. 3b). However, increases in reef-scale structural complexity would increase the expected NEC for a 1 m^2 planar area with the highest structural complexity (R = 4) yielding maximum NEC of 135.0 mmol m^{-2} h^{-1} for 100% *A. nasuta* coral cover and 63.0 mmol m^{-2} h^{-1} for 100% *P. lobata* coral cover (Fig. 4). Structurally complex reefs at the reef scale (R = 3–4) occupied by 100% *P. lobata* yielded greater NEC (47.2 and 63.0 mmol m^{-2} h^{-1}, respectively) than planar reefs (R = 1) occupied by 100% *A. nasuta* (NEC = 33.8 mmol m^{-2} h^{-1}; Fig. 4).

Discussion

Coral reefs are structurally complex environments that complicate accurate calculations of seawater hydrodynamics and thereby challenge precise calculations of NEC (Lowe et al. 2009; Falter et al. 2013; Lowe and Falter 2015). However, reducing NEC uncertainty is critical for monitoring the rates and drivers of reef-scale calcification to understand current and future maintenance of coral reef $CaCO_3$ structures in a changing ocean (Kleypas et al. 2001; Silverman et al. 2009; Albright et al. 2015; Edmunds et al. 2016; Courtney et al. 2018; Cyronak et al. 2018; Perry et al. 2018). Here we have synthesized findings from in situ coral calcification rate data, $CaCO_3$ budget methodologies, and NEC from previous studies with a biogeochemical modeling approach to improve our understanding of ΔA_T, uncertainties in NEC, and the relationship between NEC and calcifier cover. In doing so, the reefCA$_T$S runs provide a range of ΔA_T for the given parameterized *Acropora nasuta* and *Porites lobata* calcification rates under varying seawater depths and residence times (Tables 1, 2). The true uncertainty of characterizing seawater depth, residence time, and calculated NEC remains a significant challenge and warrants additional investigations in the field. Nonetheless, the uncertainty analysis in this study generalizes to any combination of errors in z and τ via Eq. 6 and can therefore be used to calculate % NEC error with respect to z_{err} and τ_{err} for any study.

Assuming that there is an equal probability of either overestimating or underestimating seawater depth and residence time (i.e., normal distribution of errors in z and τ centered around the actual z and τ, respectively), the mean modeled + 65 ± 18% NEC error in these simulations initially suggests studies may therefore be more likely to overestimate NEC owing to the greater uncertainties in NEC associated with underestimating seawater residence time. Furthermore, residence times can vary across a given coral reef system from hours up to days (or longer),

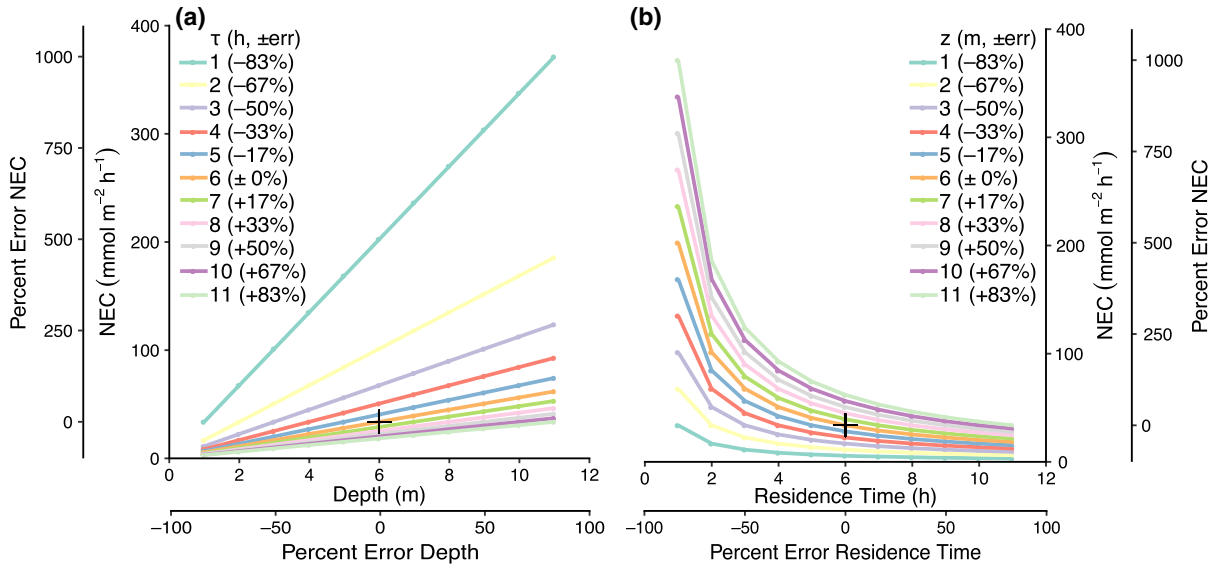

Fig. 2 Net ecosystem calcification (NEC) is erroneously calculated for a range of seawater depths (z = 1–11 m, ± 83% error) and residence times (τ = 1–11 h, ± 83% error) using the reefCA$_T$S generated alkalinity anomaly for calcification by 100% cover *Acropora nasuta* (z = 6 m, τ = 6 h). Each panel shows the erroneously calculated NEC values relative to the actual NEC rate (+) as a function of (a) depth for each residence time (colored lines) and (b) residence time for each depth (colored lines). Primary x-axes report erroneous (a) depth and (b) residence time, whereas primary y-axes show calculated NEC. Secondary axes report percent errors in depth, residence time, and calculated NEC

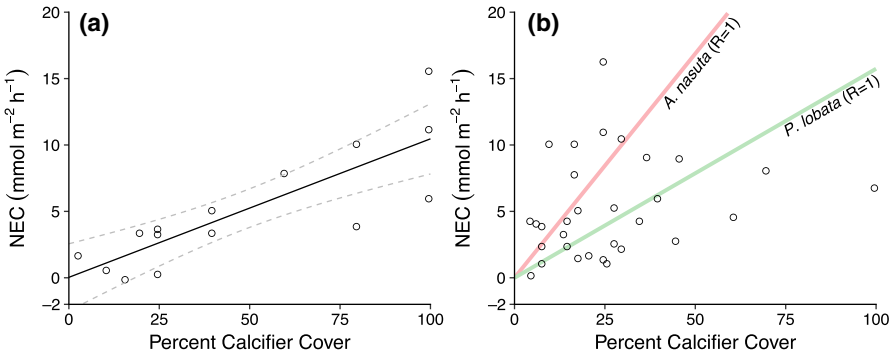

Fig. 3 Literature-derived values of net ecosystem calcification (NEC) as a function of percent calcifier cover (black circles) based on results from (a) mesocosm and enclosure experiments and (b) in situ measurements. (a) Significant positive linear correlation between NEC and percent calcifier cover in mesocosms and enclosures is denoted by the black line (± 95% confidence intervals in gray dashed lines). (b) The expected calcification rates for 0–50% cover of *A. nasuta* (pink line) and 0–100% *P. lobata* (green line) overlying a planar reef (rugosity, R = 1) are plotted relative to in situ NEC rates

suggesting the uncertainty in attributing ΔA_T measurements to residence times for calculation of NEC could be similarly large (Lowe et al. 2009; Venti et al. 2012; Zhang et al. 2012; Falter et al. 2013; Lowe and Falter 2015; Muehllehner et al. 2016). To provide a scalable example for how these potential differences in residence times could impact calculated NEC rates, an erroneous residence time of 6 h that in fact is 6 d results in a 2300% error in NEC (i.e., based on Eq. 6: $\%_{err}$NEC = [144 h/6 h − 1] × 100; Zhang et al. 2012; Courtney et al. 2018). Collectively, these findings suggest that residence time is likely the greatest source of error in NEC calculated from Eq. 1.

The capacity for the large modeled errors in NEC owing to errors in seawater depth and residence time in this study leads us to conclude that even relatively modest uncertainties less than the ± 83% in seawater depth and residence time have the potential to mask any real relationship between NEC and calcifier cover in the field. For example, the large errors in NEC (− 91% to + 1000%; 3.1–371.4 mmol m^{-2} h^{-1}) from the reefCA$_T$S sensitivity

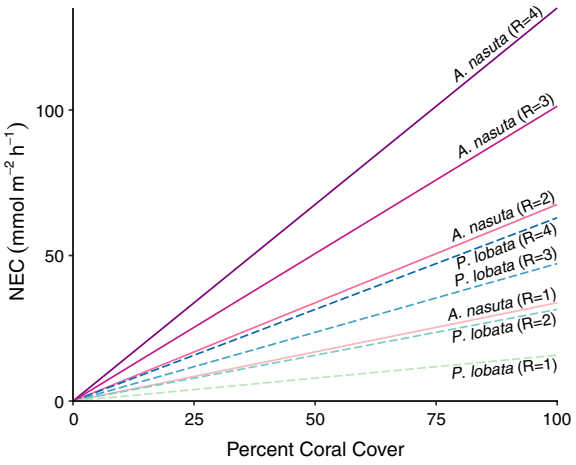

Fig. 4 Net ecosystem calcification (NEC) rates were simulated for 0–100% cover communities of *Acropora nasuta* (solid lines) and *Porites lobata* (dashed lines) corals occupying reefs with a range of structural complexities from planar (rugosity, R = 1) to highly structurally complex (R = 4) utilizing coral calcification rates from Morgan and Kench (2012)

analysis are approximately an order of magnitude greater than the 100% calcifier cover NEC of 10.5 ± 2.6 mmol m^{-2} h^{-1} (mean ± 95% confidence interval) extrapolated from the literature review of mesocosms and enclosures. Interestingly, this 100% calcifier cover NEC from mesocosm and enclosure studies agrees well with 100% coral/algae cover NEC of 10 kg $CaCO_3$ m^{-2} y^{-1} (11.4 mmol m^{-2} h^{-1}) hypothesized by Chave et al. (1972) and observed by Kinsey (1979, 1981), but is less than the maximum daytime NEC (44 mmol m^{-2} h^{-1}) recorded by DeCarlo et al. (2017) in Dongsha Atoll. Further research may therefore be necessary to explore a potential upper bound for coral reef NEC rates.

However, we further found that many in situ NEC studies from the literature exceeded our simulated planar reef 100% *Acropora* rates (Fig. 4) leading us to explore the influence of reef-scale structural complexity as an explanatory variable. For example, the finding that the more slowly calcifying *Porites lobata* occupying structurally complex reefs (R = 3–4) can generate higher NEC than an equivalent cover of *Acropora nasuta* occupying a planar substrate (Fig. 4) suggests that reef-scale structural complexity may be as important as benthic community composition for driving NEC. It is important to note that while reef structural complexity and benthic community composition are often linked, larger-scale reef rugosities are maintained even for degraded reefs (Richardson et al. 2017). This suggests that natural or artificial re-colonization of reef-scale structurally complex reefs by stress-tolerant corals may act to stabilize potentially declining NEC associated with declining coral cover and shifting coral communities (Gardner et al. 2003; Bruno and Selig 2007; Jackson et al. 2014; Perry et al. 2015; Hughes et al. 2018) and projected increases in $CaCO_3$ dissolution (Andersson and Gledhill 2013; Eyre et al. 2018) under global environmental change.

While it is not possible to directly assess the validity of NEC from previous studies with the results presented here, the insights gained in this study provide a framework for improving the validity and comparability of future NEC rates and their uncertainties. First and foremost, the model results of this study highlight the potential for extremely large errors in NEC primarily owing to uncertainties in constraining the seawater depth and residence time associated with the ΔA_T of the hydrochemical footprint. To improve comparability of NEC between sites and studies, we recommend that studies provide a detailed report of all parameters ± uncertainties of the NEC calculation (Eq. 1) and especially ΔA_T to improve our collective understanding of NEC and ΔA_T in coral reefs. Ideally future studies could leverage traditional NEC methods with any combination of established model-based approaches (Falter et al. 2013), dye/chemical tracers of seawater hydrodynamics (Falter et al. 2008; Venti et al. 2012; Muehllehner et al. 2016), eddy covariance/benthic gradient flux measurements (Long et al. 2015; Takeshita et al. 2016), and/or expectations of NEC for a given calcifier cover (Fig. 3a, Fig. 4). To further evaluate the potential correlation between NEC and calcifier cover, we suggest future studies report NEC along with preexisting or contemporaneous measurements of benthic community composition and reef structural complexity.

Monitoring coral reef calcification will prove to be a key aspect for understanding and predicting potential changes in coral reef structures and the ecosystem services they provide (Kleypas et al. 2001; Edmunds et al. 2016; Courtney et al. 2018; Cyronak et al. 2018). NEC calculations are a convenient tool for monitoring real-time coral reef calcification under changing environmental conditions and benthic communities, but here we have shown that a high level of scrutiny should be placed on measuring the seawater depth and residence time of the hydrochemical footprint due to their potentially large contributions to calculated NEC error. While the true uncertainty of NEC represents a difficult and ongoing challenge, incorporating secondary approaches and/or expectations from the simulations presented here can provide greater confidence in our ability to accurately monitor reef-scale calcification and further explore the relationship between NEC and calcifier cover in the field.

Acknowledgements We are grateful to Tyler Cyronak for providing insightful discussions of chemistry-based NEC measurements, Carlos Minces for inspiration of the reefCA_TS models, and two anonymous

reviewers who improved this manuscript with their helpful insights. Funding was provided by NSF DGE-1650112 (TAC) and NSF OCE 12-55042 (AJA). All data from the literature review of previous NEC studies are presented in the supplementary NEC review datasheet.

Author contributions TAC and AJA conceived the study. TAC constructed the reefCA_TS model simulations and wrote the first draft of the manuscript with input from AJA.

Compliance with ethical standards

Conflict of interest On behalf of all authors, the corresponding author states that there is no conflict of interest.

References

Albright R, Benthuysen J, Cantin N, Caldeira K, Anthony K (2015) Coral reef metabolism and carbon chemistry dynamics of a coral reef flat. Geophys Res Lett 42:3980–3988

Andersson AJ, Gledhill D (2013) Ocean Acidification and Coral Reefs: Effects on Breakdown, Dissolution, and Net Ecosystem Calcification. Ann Rev Mar Sci 5:321–348

Aronson RB, Precht WF (2001) White band diseases and the changing face of Caribbean coral reefs. Hydrobiologia 460:25–38

Broecker WS, Takahashi T (1966) Calcium carbonate precipitation on the Bahama Banks. J Geophys Res 71:1575

Bruno JF, Selig ER (2007) Regional decline of coral cover in the Indo-Pacific: Timing, extent, and subregional comparisons. PLoS One 2:e711

Chave KE, Smith SV, Roy KJ (1972) Carbonate production by coral reefs. Mar Geol 12:123–140

Courtney TA, Andersson AJ, Bates NR, Collins A, Cyronak T, de Putron SJ, Eyre BD, Garley R, Hochberg EJ, Johnson R, Musielewicz S, Noyes TJ, Sabine CL, Sutton AJ, Toncin J, Tribollet A (2016) Comparing Chemistry and Census-Based Estimates of Net Ecosystem Calcification on a Rim Reef in Bermuda. Front Mar Sci 3:181

Courtney TA, De Carlo EH, Page HN, Bahr KD, Barro A, Howins N, Tabata R, Terlouw G, Rodgers KS, Andersson AJ (2018) Recovery of reef-scale calcification following a bleaching event in Kāne'ohe Bay, Hawai'i. Limnol Oceanogr Lett 3:1–9

Cyronak T, Andersson AJ, Langdon C, Albright R, Bates NR, Caldeira K, Carlton R, Corredor JE, Dunbar RB, Enochs I, Erez J, Eyre BD, Gattuso JP, Gledhill D, Kayanne H, Kline DI, Koweek DA, Lantz C, Lazar B, Manzello D, McMahon A, Meléndez M, Page HN, Santos IR, Schulz KG, Shaw E, Silverman J, Suzuki A, Teneva L, Watanabe A, Yamamoto S (2018) Taking the metabolic pulse of the world's coral reefs. PLoS One 13:1–17

DeCarlo TM, Cohen AL, Wong GTF, Shiah F, Lentz SJ, Davis KA, Shamberger KEF, Lohmann P (2017) Community production modulates coral reef pH and the sensitivity of ecosystem calcification to ocean acidification. J Geophys Res Ocean 122:745–761

Dickson AG, Sabine CL, Christian JR (2007) Guide to Best Practices for Ocean CO_2 Measurements. PICES Spec Publ 3(3):191

Edmunds PJ, Comeau S, Lantz C, Andersson A, Briggs C, Cohen A, Gattuso JP, Grady JM, Gross K, Johnson M, Muller EB, Ries JB, Tambutté S, Tambutté E, Venn A, Carpenter RC (2016) Integrating the Effects of Ocean Acidification across Functional Scales on Tropical Coral Reefs. Bioscience 66:350–362

Eyre BD, Cyronak T, Drupp P, De Carlo EH, Sachs JP, Andersson AJ (2018) Coral reefs will transition to net dissolving before end of century. Science 359(6378):908–911

Falter JL, Lowe RJ, Atkinson MJ, Monismith SG, Schar DW (2008) Continuous measurements of net production over a shallow reef community using a modified Eulerian approach. J Geophys Res Ocean 113:1–14

Falter JL, Lowe RJ, Zhang Z, McCulloch M (2013) Physical and Biological Controls on the Carbonate Chemistry of Coral Reef Waters: Effects of Metabolism, Wave Forcing, Sea Level, and Geomorphology. PLoS One 8(1):e53303

Gardner TA, Côté IM, Gill JA, Grant A, Watkinson AR (2003) Long-Term Region-Wide Declines in Caribbean Corals. Science 301(5635):958–960

Gattuso JP, Pichon M, Delesalle B, Canon C, Frankignoulle M (1996) Carbon fluxes in coral reefs. I. Lagrangian measurement of community metabolism and resulting air-sea CO_2 disequilibrium. Mar Ecol Prog Ser 145:109–121

Goatley CHR, Bellwood DR (2011) The roles of dimensionality, canopies and complexity in ecosystem monitoring. PLoS One 6:e27307

Graham NAJ, Nash KL (2013) The importance of structural complexity in coral reef ecosystems. Coral Reefs 32:315–326

Harris DL, Rovere A, Casella E, Power H, Canavesio R, Collin A, Pomeroy A, Webster JM, Parravicini V (2018) Coral reef structural complexity provides important coastal protection from waves under rising sea levels. Sci Adv 4(2):eaao4350

Hubbard DK, Miller AI, Scaturo D (1990) Production and cycling of calcium carbonate in a shelf-edge reef system (St. Croix, U.S. Virgin Islands): Applications to the nature of reef systems in the fossil record. J Sediment Petrol 60:335–360

Hughes TP, Kerry JT, Baird AH, Connolly SR, Dietzel A, Eakin CM, Heron SF, Hoey AS, Hoogenboom MO, Liu G, McWilliam MJ, Pears RJ, Pratchett MS, Skirving WJ, Stella JS, Torda G (2018) Global warming transforms coral reef assemblages. Nature 556(7702):492

Jackson JBC, Donovan MK, Cramer KL, Lam V (2014) Status and Trends of Caribbean Coral Reefs : 1970–2012. IUCN, Glob Coral Reef Monit Netw

Kinsey DW (1979) Carbon turnover and accumulation by coral reefs. Doctoral dissertation, University of Hawai'i

Kinsey DW (1981) The Pacific/Atlantic reef growth controversy. Proc Fourth Int Coral Reef Symp Manila 1:493–498

Kinsey DW (1985) Metabolism, calcification and carbon production: 1 systems level studies. Fifth Int Coral Reef Congr 4:505–526

Kleypas JA, Buddemeier RW, Gattuso JP (2001) The future of coral reefs in an age of global change. Int J Earth Sci 90:426–437

Langdon C, Gattuso J-P, Andersson A (2010) Measurements of calcification and dissolution of benthic organisms and communities. Guide to Best Pract Ocean Acidif Res Data Report 213–232

Long MH, Charette MA, Martin WR, Mccorkle DC (2015) Oxygen metabolism and pH in coastal ecosystems: Eddy Covariance Hydrogen ion and Oxygen Exchange System (ECHOES). Limnol Oceanography Methods 13:438–450

Lowe RJ, Falter JL (2015) Oceanic Forcing of Coral Reefs. Ann Rev Mar Sci 7:43–66

Lowe RJ, Falter JL, Monismith SG, Atkinson MJ (2009) A numerical study of circulation in a coastal reef-lagoon system. J Geophys Res Ocean 114:1–18

McDougall TJ, Barker PM (2011) Getting started with TEOS-10 and the Gibbs Seawater (GSW) Oceanographic Toolbox. SCOR/IAPSO WG127

McWilliam M, Hoogenboom MO, Baird AH, Kuo C, Madin JS, Hughes TP (2018) Biogeographical disparity in the functional

diversity and redundancy of corals. Proc Natl Acad Sci 115(12):3084–3089
Montaggioni LFF (2005) History of Indo-Pacific coral reef systems since the last glaciation: Development patterns and controlling factors. Earth-Science Rev 71:1–75
Montaggioni LF, Braithwaite CJR (2009) Quaternary coral reef systems: history, development processes and controlling factors. Elsevier 5
Morgan KM, Kench PS (2012) Skeletal extension and calcification of reef-building corals in the central Indian Ocean. Mar Environ Res 81:78–82
Muehllehner N, Langdon C, Venti A, Kadko D (2016) Dynamics of carbonate chemistry, production, and calcification of the Florida Reef Tract (2009–2010): Evidence for seasonal dissolution. Global Biogeochem Cycles 30:661–688
Page HN, Courtney TA, Collins A, De Carlo EH, Andersson AJ (2017) Net Community Metabolism and Seawater Carbonate Chemistry Scale Non-Intuitively with Coral Cover. Front Mar Sci 4:1–17
Perry CT, Edinger EN, Kench PS, Murphy GN, Smithers SG, Steneck RS, Mumby PJ (2012) Estimating rates of biologically driven coral reef framework production and erosion: A new census-based carbonate budget methodology and applications to the reefs of Bonaire. Coral Reefs 31:853–868
Perry CT, Steneck RS, Murphy GN, Kench PS, Edinger EN, Smithers SG, Mumby PJ (2015) Regional-scale dominance of non-framework building corals on Caribbean reefs affects carbonate production and future reef growth. Glob Chang Biol 21:1153–1164
Perry CT, Alvarez-Filip L, Graham NA, Mumby PJ, Wilson SK, Kench PS, Manzello DP, Morgan KM, Slangen AB, Thomson DP, Januchowski-Hartley F (2018) Loss of coral reef growth capacity to track future increases in sea-level. Nature 558(7710):396
Pichon M (1997) Coral reef metabolism in the Indo-Pacific: the broader picture. 8th Int Coral Reef Symp 1:977–980
Pratchett MS, Anderson KD, Hoogenboom MO, Widman E, Baird AH, Pandolfi JM, Edmunds PJ, Lough JM (2015) Spatial, temporal and taxonomic variation in coral growth - implications for the structure and function of coral reef ecosystems. Oceanogr Mar Biol An Annu Rev 53:215–296
R Core Team (2017) R: A language and environment for statistical computing. R Foundation for Statistical Computing, Vienna, Austria URL: http//wwwR-project.org/
Richardson LE, Graham NAJ, Hoey AS (2017) Cross-scale habitat structure driven by coral species composition on tropical reefs. Sci Rep 7:7557
Roquet F, Madec G, Mcdougall TJ, Barker PM (2015) Accurate polynomial expressions for the density and specific volume of seawater using the TEOS-10 standard. Ocean Model 90:29–43
Shamberger KEF, Feely RA, Sabine CL, Atkinson MJ, DeCarlo EH, Mackenzie FT, Drupp PS, Butterfield DA (2011) Calcification and organic production on a Hawaiian coral reef. Mar Chem 127:64–75
Silverman J, Lazar B, Erez J (2007) Effect of aragonite saturation, temperature, and nutrients on the community calcification rate of a coral reef. J Geophys Res Ocean. https://doi.org/10.1029/2006JC003770
Silverman J, Lazar B, Cao L, Caldeira K, Erez J (2009) Coral reefs may start dissolving when atmospheric CO_2 doubles. Geophys Res Lett 36:1–5
Smith SV, Key GS (1975) Carbon Dioxide and Metabolism in Marine Environments. Limnol Oceanogr 20:493–495
Soetaert K, Petzoldt T, Setzer RW (2010) Package deSolve: Solving Initial Value Differential Equations in R. J Stat Softw
Stearn W, Scoffin TP, Martindale W (1977) Calcium carbonate budget of a fringing reef on the west coast of Barbados. Bull Mar Sci 27:479–510
Storlazzi CD, Gingerich SB, Van Dongeren A, Cheriton OM, Swarzenski PW, Quataert E, Voss CI, Field DW, Annamalai H, Piniak GA, McCall R (2018) Most atolls will be uninhabitable by the mid-21st century because of sea-level rise exacerbating wave-driven flooding. Sci Adv 4: eaap9741
Szmant AM (1997) Nutrient effects on coral reefs: a hypothesis on the importance of topographic and trophic complexity to reef nutrient dynamics. Proc 8th Int Coral Reef Symp, Panama 1527–1532
Szmant AM (2002) Nutrient Enrichment on Coral Reefs: Is It a Major Cause of Coral Reef Decline? Estuaries 25:743–766
Takeshita Y, Mcgillis W, Briggs EM, Carter AL, Donham EM, Martz TR, Price NN, Smith JE (2016) Assessment of net community production and calcification of a coral reef using a boundary layer approach. J Geophys Res Ocean 121:5655–5671
Tanner E (1995) Competition between scleractinian corals and macroalgae: An experimental investigation of coral growth, survival and reproduction. Journal of Experimental Marine Biology and Ecology 190:151–168
Tanner JE (1997) Interspecific competition reduces fitness in scleractinian corals. Journal of Experimental Marine Biology and Ecology 214:19–34
Venti A, Kadko D, Andersson AJ, Langdon C, Bates NR (2012) A multi-tracer model approach to estimate reef water residence times. Limnol Oceanogr Methods 10:1078–1095
Yates KK, Zawada DG, Smiley NA, Tiling-Range G (2017) Divergence of seafloor elevation and sea level rise in coral reef ecosystems. Biogeosciences 14:1739–1772
Zhang Z, Falter J, Lowe R, Ivey G (2012) The combined influence of hydrodynamic forcing and calcification on the spatial distribution of alkalinity in a coral reef system. J Geophys Res Ocean 117:1–18

Chapter 2, in full, is a reprint of the material as it appears in Courtney TA & Andersson AJ. Evaluating measurements of coral reef net ecosystem calcification rates. *Coral Reefs* 2019. The dissertation author was the primary investigator and author of this paper.

CHAPTER 3

Comparing Chemistry and Census-based Estimates of Net Ecosystem Calcification on a Rim Reef in Bermuda

Courtney TA, Andersson AJ, Bates NB, Collins A, Cyronak T, de Putron SJ, Eyre BD, Garley R, Hochberg EJ, Johnson R, Musielewicz S, Noyes T, Sabine CL, Sutton AJ, Toncin J, Tribollet A

frontiers in Marine Science

ORIGINAL RESEARCH
published: 23 September 2016
doi: 10.3389/fmars.2016.00181

Comparing Chemistry and Census-Based Estimates of Net Ecosystem Calcification on a Rim Reef in Bermuda

Travis A. Courtney[1], Andreas J. Andersson[1], Nicholas R. Bates[2], Andrew Collins[2], Tyler Cyronak[1], Samantha J. de Putron[2], Bradley D. Eyre[3], Rebecca Garley[2], Eric J. Hochberg[2], Rodney Johnson[2], Sylvia Musielewicz[4,5], Tim J. Noyes[2], Christopher L. Sabine[5], Adrienne J. Sutton[4,5], Jessy Toncin[6] and Aline Tribollet[6]*

[1] *Geosciences Research Division, Scripps Institution of Oceanography, University of California, San Diego, La Jolla, CA, USA,* [2] *Bermuda Institute of Ocean Sciences, St. George's, Bermuda,* [3] *Center for Coastal Biogeochemistry, School of Environment, Science, and Engineering, Southern Cross University, Lismore, NSW, Australia,* [4] *Joint Institute for the Study of the Atmosphere and Ocean, University of Washington, Seattle, WA, USA,* [5] *Pacific Marine Environmental Laboratory, National Oceanic and Atmospheric Administration, Seattle, WA, USA,* [6] *Institut de Recherche pour le Développement, Institut Pierre Simon Laplace - Laboratoire d'Océanographie et du Climat, Université Pierre-et-Marie-Curie, Paris, France*

OPEN ACCESS

Edited by:
Jessica Carilli, University of Massachusetts Boston, USA

Reviewed by:
Christopher Paul Jury, Hawai'i Institute of Marine Biology, USA
Chris Perry, University of Exeter, UK

***Correspondence:**
Travis A. Courtney
traviscourtney@gmail.com

Specialty section:
This article was submitted to Coral Reef Research, a section of the journal Frontiers in Marine Science

Received: *02 June 2016*
Accepted: *06 September 2016*
Published: *23 September 2016*

Citation:
Courtney TA, Andersson AJ, Bates NR, Collins A, Cyronak T, de Putron SJ, Eyre BD, Garley R, Hochberg EJ, Johnson R, Musielewicz S, Noyes TJ, Sabine CL, Sutton AJ, Toncin J and Tribollet A (2016) Comparing Chemistry and Census-Based Estimates of Net Ecosystem Calcification on a Rim Reef in Bermuda. Front. Mar. Sci. 3:181. doi: 10.3389/fmars.2016.00181

Coral reef net ecosystem calcification (NEC) has decreased for many Caribbean reefs over recent decades primarily due to changes in benthic community composition. Chemistry-based approaches to calculate NEC utilize the drawdown of seawater total alkalinity (TA) combined with residence time to calculate an instantaneous measurement of NEC. Census-based approaches combine annual growth rates with benthic cover and reef structural complexity to estimate NEC occurring over annual timescales. Here, NEC was calculated for Hog Reef in Bermuda using both chemistry and census-based NEC techniques to compare the mass-balance generated by the two methods and identify the dominant biocalcifiers at Hog Reef. Our findings indicate close agreement between the annual 2011 census-based NEC 2.35 ± 1.01 kg $CaCO_3 \bullet m^{-2} \bullet y^{-1}$ and chemistry-based NEC 2.23 ± 1.02 kg $CaCO_3 \bullet m^{-2} \bullet y^{-1}$ at Hog Reef. An additional record of Hog Reef TA data calculated from an autonomous CO_2 mooring measuring pCO_2 and modeled pH_{total} every 3-h highlights the dynamic temporal variability in coral reef NEC. This ability for chemistry-based NEC techniques to capture higher frequency variability in coral reef NEC allows the mechanisms driving NEC variability to be explored and tested. Just four coral species, *Diploria labyrinthiformis*, *Pseudodiploria strigosa*, *Millepora alcicornis*, and *Orbicella franksi*, were identified by the census-based NEC as contributing to 94 ± 19% of the total calcium carbonate production at Hog Reef suggesting these species should be highlighted for conservation to preserve current calcium carbonate production rates at Hog Reef. As coral cover continues to decline globally, the agreement between these NEC estimates suggest that either method, but ideally both methods, may serve as a useful tool for coral reef managers and conservation scientists to monitor the maintenance of coral reef structure and ecosystem services.

Keywords: coral reef, net ecosystem calcification, budget, accretion, dissolution, calcium carbonate, biogeochemistry

INTRODUCTION

Coral reefs provide a great multitude of ecosystem goods and services to humanity including renewable food and material resources, shoreline protection, and nutrient cycling (e.g., Smith, 1978; Salvat, 1992; Spurgeon, 1992; Done et al., 1996; Moberg and Folke, 1999; de Groot et al., 2012). However, tropical reef coral cover is currently declining due to a combination of local and global pressures (i.e., overfishing, sedimentation, disease, warming, and acidification) with ∼80% declines in coral cover observed across the Caribbean since the mid-1970s (Gardner et al., 2003). These declines in overall Caribbean coral cover are combined with an overall loss of reef structural complexity (Alvarez-Filip et al., 2009) and coral community shifts toward more slowly calcifying and less-structurally complex opportunistic coral species (Alvarez-Filip et al., 2013). Consequently, losses in coral cover, and changes in coral community composition have resulted in decreased net coral reef calcium carbonate ($CaCO_3$) production across the Caribbean (Perry et al., 2013, 2015). While hermatypic scleractinian corals are typically the dominant coral reef $CaCO_3$ producers (Vecsei, 2004), coral reef net ecosystem calcification (NEC) is the sum of gross calcification and gross $CaCO_3$ dissolution (Chave et al., 1972). Coral reef accretion and maintenance of geomorphic structure therefore depends on NEC as well as the net import, export, and erosion of $CaCO_3$ material (e.g., Scoffin, 1992; Milliman, 1993; Kleypas et al., 2001; Perry et al., 2008; Montaggioni and Braithwaite, 2009; Tribollet and Golubic, 2011; Perry et al., 2012).

The topic of spatial scale is of particular importance for the study of ecological phenomenon (Levin, 1992 and references therein) including coral reef calcification (e.g., Kinsey, 1985; Andréfouët and Payri, 2000; Vecsei, 2004; Edmunds et al., 2016). Measurements of coral reef calcification range from organismal to ecosystem and global scales (see discussion in Edmunds et al., 2016). By necessity, measuring $CaCO_3$ production at organism scales (e.g., Bak, 1976; Jokiel et al., 1978) fundamentally utilize different approaches than studies examining entire reef and global scales (e.g., Kinsey, 1979; Milliman, 1993; Kleypas, 1997; Vecsei, 2004). Coral reef $CaCO_3$ production at sub-reef to reef scales has historically been measured via census or accretion-based $CaCO_3$ budget approaches (e.g., Chave et al., 1972 and references therein; Stearn et al., 1977; Hubbard et al., 1990; Eakin, 1996; Harney and Fletcher, 2003; Perry et al., 2012, 2013) and chemistry-based alkalinity anomaly approaches (e.g., Broecker and Takahashi, 1966; Smith and Key, 1975; Smith and Kinsey, 1976; Gattuso et al., 1996; and summarized in Atkinson, 2011; Andersson and Gledhill, 2013).

Census-based budgets utilize bottom-up approaches to sum up the calcification by individual $CaCO_3$ producers whereas chemistry-based budgets provide a top-down integrated measurement of the entire reef NEC. Interestingly, $CaCO_3$ production on coral reefs in the Atlantic has historically been measured using census and accretion based approaches while chemistry-based approaches have been more widely used in the Pacific Ocean (Kinsey, 1981). Montaggioni and Braithwaite (2009) summarized the literature finding that global coral reef calcification estimates range from 1 to 10 kg $CaCO_3 \bullet m^2 \bullet y^{-1}$ using census-based methods and from 0.5 to 10 kg $CaCO_3 \bullet m^2 \bullet y^{-1}$ based on alkalinity anomaly methods thereby concluding that the two methods are generally in close agreement. Measurements of census-based and chemistry-based $CaCO_3$ production at One Tree Island, Great Barrier Reef were scaled to the entire reef using remote sensing with a remarkably small 0.3% difference between the two methods (Hamylton et al., 2013). Thus, a robust comparison of these two methods at the same reef site allows the bottom-up census-based budget of NEC to be weighed against the top-down chemistry-based NEC, resulting in a more thorough understanding of the mechanisms of $CaCO_3$ production and maintenance of structure in coral reef environments.

In this study, NEC was calculated using census-based and chemistry-based budgets from September 2010 to September 2012 for Hog Reef (32°27′26.39″N, 64°50′5.10″W), located on the northwestern rim reef of Bermuda between deeper oceanic waters and shallower sandy back-reef environments (**Figure 1**). The Bermuda platform is a reef system surrounded by deep oceanic waters located in the North Atlantic sub-tropical gyre and at the current latitudinal limit for tropical coral reef ecosystems (Kleypas et al., 1999; Andersson et al., 2014). The history of Bermuda NEC measurements (e.g., Bates, 2002; Bates et al., 2010) and characterization of Bermuda platform seawater residence times (Venti et al., 2012) further make Hog Reef an ideal location to conduct a chemistry-based NEC study. Briefly, calcifying organism growth rates, microborer $CaCO_3$ dissolution rates, and $CaCO_3$ sand dissolution rates were multiplied by their respective benthic area to produce a census-based NEC budget with seasonal variability at Hog Reef. NEC was calculated using chemistry-based alkalinity anomaly of reef seawater relative to offshore seawater via water samples taken monthly from Hog Reef. Seasonal and diel NEC variability was estimated by TA calculated from seawater measurements taken every 3 h by an autonomous pCO_2 mooring at Hog Reef. These estimates of coral reef NEC provide valuable insight into the net balance between calcification and $CaCO_3$ dissolution, thus serving as an important tool for monitoring the maintenance of coral reef structure and ecosystem services as coral reef function and health continue to change globally.

METHODS

Census Based Budget Formation

Reef Surveys

The census-based budgets were modeled after the standardized methods outlined in the *ReefBudget* project (Perry et al., 2012). Video transects were conducted in August 2010 at Hog Reef as part of an ecological monitoring project consisting of five permanent 30-m transects stationed at ca. 8 m depth at the reef site. For each transect, a video camera was pointed perpendicular to the benthos at a constant distance to film a 1-m wide band to the left side of each transect generating 5 • 30 m^2 transects. Each video transect was analyzed for percent cover by coral species, gorgonian, zoanthid, sponge, sessile invertebrates,

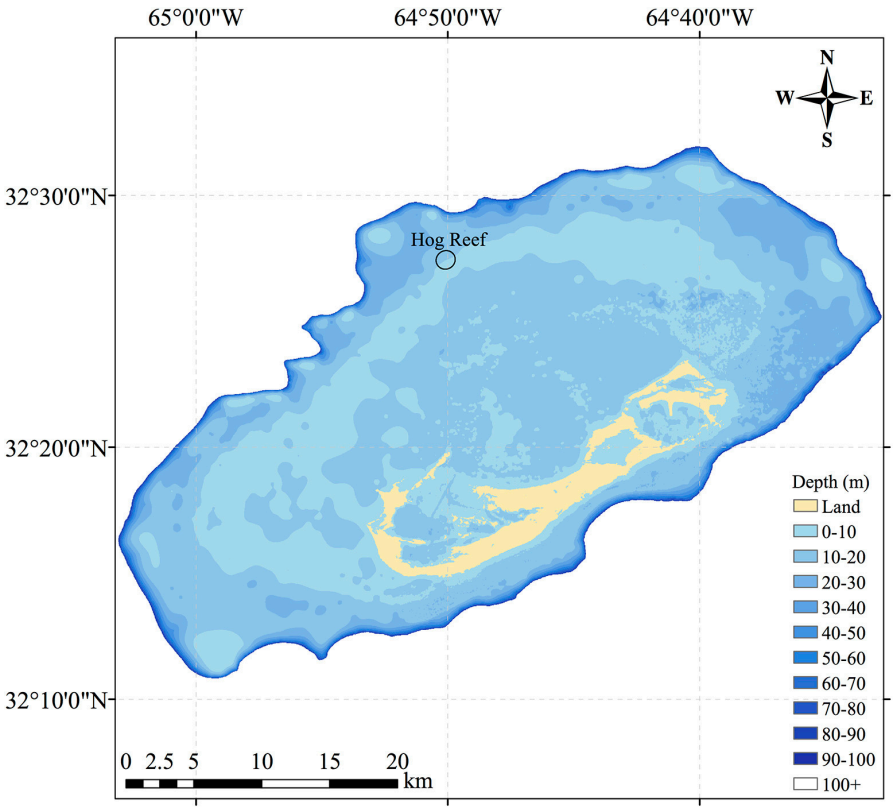

FIGURE 1 | Map of the Bermuda coral reef platform showing Hog Reef, located on the northwestern portion of the rim reef. The black ellipse at Hog Reef represents the estimated effective footprint for the benthic community influence on the overlying seawater chemistry.

macroalgae, turf algae, calcifying algae, dead coral, unknown organisms, rock, rubble, and sand (**Figure 2**). Notably, mean percent cover (±standard deviation) of hard scleractinian corals at the survey site was 27 ± 5%. Due to the structural complexity of the reef environment, reef rugosity (Spatial Scales I and II in Dahl, 1973) was calculated for each site to determine the total abundance of benthic organisms occupying a given planar area of the reef environment (Dahl, 1973). The Segmented Line and Measure tools in *ImageJ* were used to calculate reef rugosity from the ratio of reef profile distance and horizontal planar distance for each photograph ($n = 12$) resulting in a mean (± standard deviation) rugosity of 1.5 ± 0.2. Hog Reef has a very complex three-dimensional structure consisting of many small caves and overhangs that is not currently measurable using traditional rugosity approaches (e.g., Dahl, 1973) and precludes some aspects of the benthos beneath underlying canopies from being surveyed in the planar video transects (Goatley and Bellwood, 2011). This additional structural complexity therefore underestimates this study's survey of benthic foraminifera, coralline algae, cryptic Porifera sponges, cryptic corals, and additional organisms or uncolonized substrate occurring in these unsampled microenvironments.

In situ Calcification Rates

In situ calcification rates for *Diploria labyrinthiformis* and *Porites astreoides* corals and literature reported annual mean calcification rates aggregated in the *ReefBudget* data analysis sheets (Perry et al., 2012) for all other corals and calcifying algae were used in the formation of the census-based budget. Colonies of *D. labyrinthiformis* ($n = 17$) and *P. astreoides* ($n = 14$) were collected from Hog Reef and mounted on tiles at Hog Reef from September 2010 to September 2012 to calculate *in situ* calcification rates for the duration of the experiment. During the growth rate study, each coral was weighed every 2–3 months using the buoyant weight method (Jokiel et al., 1978) with a correction term for seawater density at the time of measurement and subtraction of the weight of the tile and *Z-SPAR A-788* epoxy used to mount the coral to the tile. Mean initial coral weights (±standard deviation) were 358 ± 122 g for *D. labyrinthiformis* and 419 ± 124 g for *P. astreoides*. Mean calcification rates for each growth interval were calculated as the change in weight (mg) per day over each growth interval. Calcification rates were normalized to surface area using the foil method conducted at the end of the growth rate experiment (Marsh, 1970). Mean (±standard deviation) individual coral

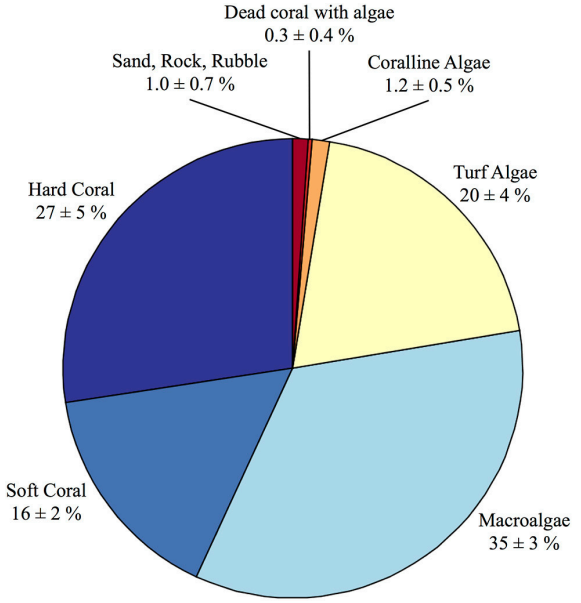

FIGURE 2 | Summary of percent cover (±standard deviation) from the benthic surveys conducted at Hog Reef. The benthic survey percent cover data was used in conjunction with the effective footprint analysis to scale the benthic composition onto larger spatial patterns of rocky reef-dominated (94.9 ± 0.2%) and sand-dominated (5.1 ± 0.2%) substrates at Hog Reef.

colony surface areas in the growth rate experiment were 195 ± 31 cm^2 for *D. labyrinthiformis* and 164 ± 48 cm^2 for *P. astreoides*.

Seasonal Variability in Calcification

Temporal variability in *D. labyrinthiformis* and *P. astreoides* growth rates was determined by dividing growth rates at each weight interval by the mean growth rates over the approximately 2-year growth rate experiments to yield standardized growth rate values. These standardized growth rates through time were fit with a single-term Fourier model using the Curve Fitting Tool in MATLAB to model the seasonal variability in growth rates (±95% confidence intervals):

$$f(x) = 1.01 \pm 0.05 - (0.37 \pm 0.13)\cos[x(5.79 \pm 0.22)] - (0.29 \pm 0.15)\sin[x(5.79 \pm 0.22)] \quad (1)$$

where x is the date in decimal years centered at the year 2010 and f(x) is the proportional, standardized seasonal variation of the mean annual growth rate. This seasonal variability relationship was used to scale the literature-derived annual mean coral and calcifying algal growth rates from the *ReefBudget* data analysis sheets (Perry et al., 2012) to approximate seasonal variability in the census-based data for comparison to the continuous chemistry-based budgets in this study.

Similarly, the *in situ* measured growth rates for *D. labyrinthiformis* and *P. astreoides* were fit with single-term Fourier models using the Curve Fitting Tool in MATLAB to construct continuous estimations of calcification rates for the duration of the 2-year experiment. The equation for *D. labyrinthiformis* growth rates (± 95% confidence intervals) is:

$$f(x) = 3.12 \pm 0.17 - (0.86 \pm 0.56)\cos[x(5.83 \pm 0.30)] - (0.97 \pm 0.47)\sin[x(5.83 \pm 0.30)] \quad (2)$$

where x is the date in decimal years centered at the year 2010 and f(x) is the seasonal variation of the *D. labyrinthiformis* annual growth rate (kg $CaCO_3 \bullet m^{-2} \bullet y^{-1}$). The equation for *P. astreoides* growth rates (± 95% confidence intervals) is:

$$f(x) = 2.53 \pm 0.19 - (1.32 \pm 0.39)\cos[x(5.71 \pm 0.30)] - (0.53 \pm 0.70)\sin[x(5.71 \pm 0.30)] \quad (3)$$

where x is the date in decimal years centered at the year 2010 and f(x) is the seasonal variation of the *P. astreoides* annual growth rate (kg $CaCO_3 \bullet m^{-2} \bullet y^{-1}$). The Fourier fitted continuous growth rates for *D. labyrinthiformis* and *P. astreoides* were used to model the seasonal-variability of the census-based budget.

Summation of Net Calcification

Calcification rates of each calcifying species were multiplied by reef rugosity and percent cover of each species from the benthic surveys to determine species-level calcification at Hog Reef. These species-level calcification rates were summed to obtain the net calcification (kg $CaCO_3 \bullet m^{-2} \bullet y^{-1}$) by the benthic community at Hog Reef. Regrettably, calcification by benthic foraminifera, which could represent up to 50% of the sand composition at Hog Reef (unpublished data), was not included in the budget due to the lack of benthic survey data on these species. Despite large abundance in the sand, Bermuda reef benthic foraminifera $CaCO_3$ production was previously estimated to be 0.080 kg $CaCO_3 \bullet m^{-2} \bullet y^{-1}$ (Langer et al., 1997), supporting earlier findings that the contributions by benthic foraminifera on coral reef NEC are an order of magnitude smaller than the $CaCO_3$ produced by non-Acroporid corals (Chave et al., 1972). Calcification by suborder holaxonia sea fans and sea rods (16 ± 2% cover ± standard deviation of the benthic survey data; **Figure 2**) were also excluded from this analysis due to the high variability of calcified material within individuals (Esford and Lewis, 1990) and a lack of reliable linear extension rate measurements to pair with the percent cover survey data. Of the other dominant biocalcifying components of coral reef environments listed by Montaggioni and Braithwaite (2009), Mollusca were insufficiently surveyed to reliably estimate Mollusca calcification from the benthic survey data.

Net $CaCO_3$ Dissolution

Calcium carbonate dissolution at Hog Reef was measured as the sum of $CaCO_3$ dissolution by sediments, microborers, and sponges. Sediment $CaCO_3$ dissolution at Hog Reef was directly measured over a full diel cycle in summer 2015 (July) via the alkalinity anomaly measured in three independent benthic chambers following methods outlined in Cyronak et al. (2013b). Net sediment $CaCO_3$ dissolution (±standard deviation) for the

sand at Hog Reef was -0.39 ± 0.11 kg $CaCO_3 \bullet m^{-2} \bullet yr^{-1}$. Given the lack of data for any temporal variability in sediment $CaCO_3$ dissolution at Hog Reef, this rate was assumed to be constant throughout the year and was multiplied by the percent sediment cover from the survey data at Hog Reef. No sponges were recorded in our transect data thereby precluding net $CaCO_3$ dissolution by sponges from the calculation of this budget. Mean (±standard deviation) microborer $CaCO_3$ dissolution rates of -0.21 ± 0.09 kg $CaCO_3 \bullet m^{-2} \bullet yr^{-1}$ were determined from scanning electron microscopy of subsections from 3 experimental coral blocks cut from a single massive *Porites lobata* skeleton exposed at Hog Reef between September 2011 and September 2012 following methods outlined in Tribollet et al. (2009). These methods for estimating $CaCO_3$ dissolution differed from the *ReefBudget* calculations in that this study additionally included sediment dissolution, which is typically absent from census-based budgets (Eyre et al., 2014), while mechanical bioerosion by fish and urchins were omitted from this study. This distinction between mechanical and chemical bioerosion was made such that the census budgets would reflect only the chemical balance of calcification and $CaCO_3$ dissolution to allow for a better comparison between the census-based and chemistry-based budgets outlined in this study.

Effective Reef Footprint and Hydrology

To best compare the census-based and chemistry-based estimates of NEC, an effective reef footprint (i.e., the spatial extent of benthic community influence on water chemistry) was calculated to link the benthos to overlying water column carbonate chemistry. The mean water flow of the tidally driven currents at Hog Reef was integrated over a complete tidal cycle to estimate the spatial area of the benthos that a typical parcel of reefwater travels over a tidal cycle. This calculated area of reef therefore represents the estimated areal footprint over which the NEC carbonate chemistry signal has been integrated in the seawater. The estimated footprint was used with aerial imagery and digital elevation model data to calculate the percent hard reef vs. sandy substrate and an average water depth for calculations of the census based and chemistry based Hog Reef NEC.

A *Nortek AS Aquadopp Profiler* was mounted at approximately 12 m depth to measure current speeds in 0.5 m depth bins from surface to bottom at a frequency of 1.0 MHz from 18 July 2015 to 26 July 2015. In the absence of continuous current measurements during the ca. 2-year study, this later current profiler deployment was used to record many tidal cycles of the predominately tidally driven flow regime at Hog Reef with the caveat that typical current profiles may vary over longer time scales due to changing wind and storm activity. Calculations using potential changes in flow regime beyond the typically tidal influence have relatively small impacts on measured census-based and chemistry-based NEC due to the correspondingly small changes in percent hard reef substrate and depth of the effective reef footprint. To avoid the tidal influence on the occasional aerial exposure of the uppermost surface current bins, only bins from 0.4 to 10.9 m distance from the profiler were analyzed. Current speeds were converted into *u* and *v* components and averaged across depth bins from 0.4 to 10.9 m to yield the average water column velocity for the duration of the deployment. An hourly low-pass Lanczos filter was used on the top-bottom averaged *u* and *v* components to filter out higher frequency turbulence from the current data. A principal components analysis was performed on the filtered top-bottom averaged *u* and *v* data following procedures outlined in Glover et al. (2011) to identify the primary (PC1) and orthogonal (PC2) principal components of seawater current. PC1 ($2.89\ cm \bullet s^{-1}$ at 335°) therefore represents the mean speed and direction of the dominant current flow and PC2 ($2.75\ cm \bullet s^{-1}$ at 245°) represents the mean speed of the flow 90° to PC1. These components of current velocity were scaled by a tidal period of 12.4167 h to yield a typical distance traveled by a parcel of water over a complete tidal cycle. The tidally scaled magnitudes and directions of these principal components (PC1: 1.29 km 335°; PC2: 1.23 km 245°) were centered at the Hog Reef PMEL $MAPCO_2$ mooring to estimate an elliptical effective footprint (**Figure 1**) for the benthic community influence on seawater chemistry.

The coordinates for the effective footprint were imported into *ArcMap*® software and layered onto a Bermuda 1 arc-second sea level digital elevation model (Sutherland et al., 2014) and Bermuda marine aerial imagery (Bermuda Zoological Society, 1997). The *ArcMap*® Zonal Statistics as Table tool was used to calculate the mean (±standard deviation) depth from the digital elevation model for the elliptical Hog Reef footprint as 10.3 ± 3.3 m. The elliptical footprint was used to crop and export the marine aerial imagery from *ArcMap*® software to *ImageJ* (Schneider et al., 2012) for analysis of percent cover by larger-scale reef and sand patches in the effective footprint. The image contrast was enhanced and converted to 8-bit grayscale before applying a black-and-white threshold with additional manual paintbrush tool interpretation of reef composition from the photograph such that areas of reef became black pixels and areas of sand became white pixels. The histogram of the ellipse was analyzed to determine the percent of black and percent of white pixels resulting in 94.9% hard reef and 5.1% sand composition. Because the reef survey data was collected over the dominantly reef section, the census-based budget data was scaled to represent 94.9% of the budget area and sand $CaCO_3$ dissolution rates were applied to the remaining 5.1% sand-covered portion of the effective reef footprint. Notably, this scaling of the transect data to the effective reef footprint resulted in a mean (±uncertainty) of 26 ± 5% hard coral cover for Hog Reef.

Chemistry Based Budget Formation

Carbonate Chemistry Bottle Samples

Hog Reef seawater bottle samples were analyzed for total alkalinity (TA) to calculate the chemistry based NEC in this study. All water samples were collected approximately monthly using a 5-L Niskin bottle at 0.5–1.0 m depth according to best practices (Dickson et al., 2007). Samples were stored using 200 mL-*Kimax* glass sample bottles, fixed using 100 µL saturated solution of $HgCl_2$, and subsequently analyzed for TA using a *VINDTA 3S* system and DIC using *VINDTA 3C* and *AIRICA* systems (Marianda Inc). The accuracy and precision of TA analyses were verified against certified reference material (CRM) provided by the laboratory of Prof. A. Dickson of Scripps Institution

of Oceanography. Analysis of replicate CRMs yielded a typical accuracy and precision of ±2–4 μmol•kg^{-1} for both TA and DIC. Temperature (accuracy ± 0.15°C) and salinity (accuracy ± 1%) for all samples were measured using a *YSI 556 Handheld Multiparameter Instrument*. Additional seawater samples were collected for 66% of all bottle samples and analyzed for salinity using an *Autosal Salinometer* (accuracy < ± 0.002). These salinometer salinity values were preferentially used over the *YSI* salinity measurements in the analysis for this project.

Offshore seawater bottle samples were collected approximately monthly at the Bermuda Atlantic Time-series Study (BATS; 31°50′N, 64°10′W) and analyzed for temperature, salinity, and TA. BATS is located ∼80 km southeast of Bermuda and represents typical surface seawater of the Sargasso Sea making BATS carbonate chemistry samples an ideal offshore reference for calculation of NEC in this study (Bates et al., 2001, 2010; Bates, 2002; Yeakel et al., 2015). BATS TA samples were collected in 200 mL-*Kimax* glass bottles, fixed with $HgCl_2$, and sealed until analysis at Bermuda Institute of Ocean Sciences (Bates et al., 2012). TA was analyzed by a *VINDTA 2S* System (*Marianda Inc*) with typical replicate accuracy and precision of <0.2% determined daily using CRMs. TA for the Hog Reef and BATS bottle samples were normalized to the mean salinity of 36.59 g•kg^{-1} measured at Hog Reef. Because the BATS bottle samples were not collected at the same time as the Hog Reef samples, the BATS bottle samples were linearly interpolated to match the monthly Hog Reef seawater sampling dates for analysis of NEC in this study.

Hog Reef MAPCO$_2$ Mooring Carbonate Chemistry

Hog Reef seawater pCO_2 and modeled pH_{total} were used to calculate TA every 3 h to estimate variability in Hog Reef NEC at higher frequencies than the ca. monthly Hog Reef seawater bottle samples. Seawater pCO_2, atmospheric pressure, temperature, and salinity were measured every 3 h by the NOAA PMEL MAPCO$_2$ mooring stationed at Hog Reef (32°27′26.39″N, 64°50′5.10″W). The MAPCO$_2$ mooring utilizes a *Battelle Memorial Institute* CO_2 system to measure CO_2 mole fraction and a *Sea-Bird 16plus v2 plus* to measure seawater temperature and salinity (Sutton et al., 2014). The *Sea-Bird* sensors failed after a few months during both deployments of the MAPCO$_2$ mooring in this study due to extensive biofouling. Mooring salinity records were thus completed using linearly interpolated salinity data from the monthly Hog Reef seawater samples. Daily averaged temperature from four *HOBO* loggers (mean standard deviation ± 0.11°C between loggers) deployed at Hog Reef recording temperature every 8-min were used for the duration of this study. An average of the daily temperature values for the day before and the day after a brief, 4-day interval lacking temperature record in mid-July were used to fill that same 4-day interval to maintain a continuous temperature record during the study.

Hog Reef seawater TA and DIC bottle samples were used to calculate seawater pH_{total} and pCO_2 for each bottle sample. The high correlation between bottle sample pH_{total} and pCO_2 was used to predict seawater pH_{total} from MAPCO$_2$ mooring pCO_2. The combination of 3-h temporally resolved MAPCO$_2$ mooring pCO_2 and pH_{total} allowed Hog Reef TA to be calculated every 3 h at Hog Reef. Hog Reef seawater TA and DIC bottle samples were used to calculate seawater carbonate chemistry using CO2SYS for MATLAB (van Heuven et al., 2011) using temperature and salinity measured at the time of sampling, the pH_{total}, K_1 and K_2 dissociation constants by Mehrbach et al. (1973) refit by Dickson and Millero (1987), K_{HSO4}- by Dickson (1990), and total boron by Uppström (1974). Calculated pH_{total} was highly linearly correlated ($R^2 = 0.998$; $p < 0.0001$) with $\log(pCO_2)$ resulting in the following equation (± standard error):

$$pH_{total} = (-0.393 \pm 0.003) \times \log[pCO_2\,(\mu atm)] + (10.40 \pm 0.02) \quad (4)$$

The highly linear correlation between $\log(pCO_2)$ and pH_{total} over the range of values in this study allowed us to use the above equation to model pH_{total} as a function of the Hog Reef mooring pCO_2 data to create a 3-h temporal resolution pH_{total} record. The Hog Reef mooring pCO_2 and modeled pH_{total} data were used to calculate TA with *CO2SYS for MATLAB* (van Heuven et al., 2011) using the HOBO temperature and interpolated seawater bottle salinity data, and the same set of constants previously described. TA from this output was normalized to the mean salinity of 36.59 measured at Hog Reef to compare with the BATS bottle samples normalized to that same salinity. The BATS bottle samples (collected approximately monthly) were linearly interpolated to match the modeled TA data (calculated every 3-h) for analysis of higher frequency measurements of NEC in this study. We recognize using this modeled TA dataset yields some additional uncertainty relative to direct TA measurements; however, the higher frequency variability captured by this method provides valuable insight on the range of Hog Reef NEC over shorter timescales than would otherwise be possible from traditional bottle samples.

Seawater density for the MAPCO$_2$ mooring and bottle sample data were calculated using the TEOS-10 Gibbs Seawater (GSW) oceanographic toolbox (McDougall and Barker, 2011). For the bottle samples, seawater density was calculated using salinity of the bottles, temperature at the time of bottle sampling, and atmospheric pressure at the time of sampling (from the Bermuda Weather Service (2016) and MAPCO$_2$ mooring). For the MAPCO$_2$ mooring, seawater density was calculated from the MAPCO$_2$ and interpolated seawater bottle salinity data, *HOBO* logger temperature data, and MAPCO$_2$ pressure sensor data.

Net Ecosystem Calcification

NEC represents the effects of gross calcification and gross $CaCO_3$ dissolution integrated over a water column of given density (ρ), depth (z), and residence time (τ) as per the following equation (Smith and Key, 1975; Langdon et al., 2010):

$$NEC = \frac{\rho z(TA_{offshore} - TA_{reef})}{2\tau} \quad (5)$$

NEC was calculated for the discrete TA bottle samples and the MAPCO$_2$ mooring TA data relative to interpolated BATS offshore TA data, bottle and MAPCO$_2$ mooring seawater density data, depth of the effective footprint from *ArcGIS*, and a

mean residence time (± standard deviation) of 2.5 ± 0.4 days calculated at the nearby North Rock rim reef site using a multi-tracer approach (Venti et al., 2012). Trapezoidal numerical integration was used to calculate annual NEC for the bottle samples. Regrettably, a full annual cycle was not measured by the $MAPCO_2$ data (0.91 years) for the duration of this study (September 2010–September 2012). Trapezoidal numerical integration was thus applied to the mooring NEC data, bottle sample NEC data, and census-based NEC data over the longest $MAPCO_2$ mooring data record (0.91 year time period from February 2011 to January 2012) to allow for a direct comparison of the methods without temporal bias. The census-based NEC, seawater bottle chemistry-based NEC, and mooring chemistry-based NEC are hereafter referred to as the census NEC, bottle NEC, and mooring NEC throughout the remainder of this manuscript.

Propagation of Uncertainty

Uncertainty for the census, bottle, and mooring NEC budgets was estimated using standard procedures for propagation of uncertainties summarized by Ku (1966). Standard deviations for all measured and calculated data were used to propagate uncertainties with a few exceptions. Uncertainties in species-level growth rates from the literature were not included in this analysis. Uncertainty of measured TA ($\pm 4\,\mu mol \bullet kg^{-1}$) was obtained from replicate measures of CRMs. An uncertainty of $\pm 21\,\mu mol \bullet kg^{-1}$ was used for the uncertainty in $MAPCO_2$ mooring pH-pCO_2 predicted TA values. The mean difference between measured bottle TA and corresponding $MAPCO_2$ mooring pH-pCO_2 predicted TA at the time of water bottle sampling was $20.5\,\mu mol \bullet kg^{-1}$, which is also consistent with an uncertainty of $\pm 21\,\mu mol \bullet kg^{-1}$ estimated by Millero (2007) using ship-based pCO_2 and pH measurements. Subjective uncertainty for the Hog Reef footprint percent composition of reef and sand was estimated to be ±2% based on repeated *ImageJ* analysis of Hog Reef benthic composition.

RESULTS

Census Based Budget Formation

The mean census NEC (±uncertainty) for the entire length of the approximately 2-year *in situ* calcification study was 2.21 ± 1.01 kg $CaCO_3 \bullet m^{-2} \bullet y^{-1}$ (**Table 1**; **Figure 3**). Calcification (±uncertainty) accounted for 2.53 ± 0.99 kg $CaCO_3 \bullet m^{-2} \bullet y^{-1}$ and $CaCO_3$ dissolution (±uncertainty) was −0.32 ± 0.13 kg $CaCO_3 \bullet m^{-2} \bullet y^{-1}$ (**Tables 1**, **2**; **Figure 4**). The percentage (±uncertainty) of total calcification for *D. labyrinthiformis* (15 ± 3%), *Pseudodiploria strigosa* (29 ± 10%), *Millepora alcicornis* (26 ± 12%), and *Orbicella franksi* (24 ± 9%) show they are the dominant $CaCO_3$ producers (94 ± 19% for all four species) at Hog Reef (**Table 1**; **Figure 4**). Although measured rates of sand $CaCO_3$ dissolution were higher than microborer $CaCO_3$ dissolution rates per unit area, the smaller total area of sands resulted in areal $CaCO_3$ dissolution (± uncertainty) being dominated by microborers (93 ± 57%) with sand $CaCO_3$ dissolution (7 ± 4%) making up the remainder (**Table 2**; **Figure 4**). Integrated census NEC (±uncertainty) for 2011 was 2.35 ± 1.01 kg $CaCO_3 \bullet m^{-2} \bullet y^{-1}$ and from 2011.2 to 2012.1 was 2.28 ± 1.01 kg $CaCO_3 \bullet m^{-2} \bullet y^{-1}$ (**Table 3**).

Chemistry Based Budget Formation

The mean bottle NEC (±uncertainty) for the entire length of the approximately 2-year *in situ* calcification study was 2.85 ± 1.02 kg $CaCO_3 \bullet m^{-2} \bullet y^{-1}$ (**Table 3**). The integrated bottle NEC for 2011 was 2.23 ± 1.02 kg $CaCO_3 \bullet m^{-2} \bullet y^{-1}$ and from 2011.2 to 2012.1 was 2.46 ± 1.02 kg $CaCO_3 \bullet m^{-2} \bullet y^{-1}$ (**Table 3**). Similarly, the mean mooring NEC (±uncertainty) was 3.73 ± 1.34 kg $CaCO_3 \bullet m^{-2} \bullet y^{-1}$ (**Table 3**). There was insufficient data to calculate mooring NEC for 2011 using the $MAPCO_2$ data with the interval 2011.2–2012.1 representing the longest continuous record for the mooring NEC data. The integrated mooring NEC estimate for this interval was 4.09 ± 1.34 kg $CaCO_3 \bullet m^{-2} \bullet y^{-1}$ (**Table 3**).

TABLE 1 | Summary table of calcification at Hog Reef.

Calcifying organism	Mean survey %-cover	Mean reef %-cover	*ReefBudget* calcification rates (kg $CaCO_3 \bullet m^{-2} \bullet y^{-1}$)	Mean study interval rates (kg $CaCO_3 \bullet m^{-2} \bullet y^{-1}$)	Mean reef calcification (kg $CaCO_3 \bullet m^{-2} \bullet y^{-1}$)	% of Total Hog Reef calcification
Diploria labyrinthiformis	9 ± 2	9 ± 1	4.64	3.00	0.38 ± 0.08	15 ± 3
Pseudodiploria strigosa	10 ± 3	9 ± 3	5.34	5.13	0.7 ± 0.2	30 ± 10
Favia fragum	0.04 ± 0.09	0.04 ± 0.09	9.76	9.38	0.01 ± 0.01	0.2 ± 0.5
Madracis decactis	0.04 ± 0.09	0.04 ± 0.09	33.46	32.16	0.02 ± 0.04	0.7 ± 1.6
Millepora alcicornis	1.8 ± 0.8	1.6 ± 0.7	28.10	27.01	0.7 ± 0.3	30 ± 10
Montastraea cavernosa	0.6 ± 0.6	0.6 ± 0.5	9.07	8.72	0.08 ± 0.07	3 ± 3
Orbicella franksi	5 ± 2	5 ± 2	9.06	8.71	0.6 ± 0.2	24 ± 9
Porites astreoides	1.1 ± 0.3	1.0 ± 0.3	6.32	2.36	0.04 ± 0.01	1.4 ± 0.5
Coralline algae	1.2 ± 0.5	1.2 ± 0.5	0.18	0.17	0.003 ± 0.001	0.12 ± 0.05

Percent cover (± standard deviation) from the benthic surveys and estimated reef footprint are reported alongside literature calcification rates aggregated by ReefBudget and the mean calcification rate over the entire study period after taking into account seasonal variability in calcification rates and using in situ calcification rate data for D. labyrinthiformis and P. astreoides. Mean calcification rates and percent of total calcification (± uncertainties) are reported for each species.

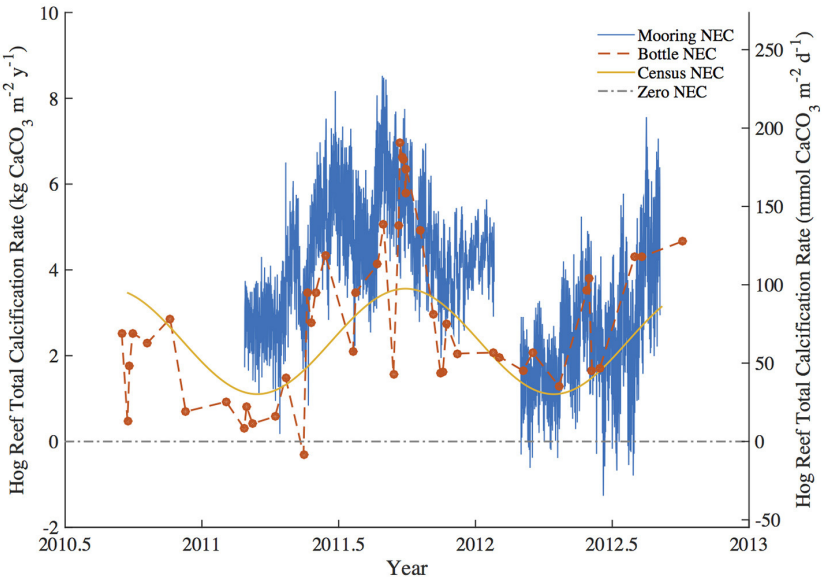

FIGURE 3 | Summary figure of Hog Reef Net Ecosystem Calcification (NEC) using the mooring NEC, bottle NEC, and census NEC approaches for the study period. The dashed zero-NEC line indicates the tipping point between net calcification (above the line) and net $CaCO_3$ dissolution (below the line).

TABLE 2 | Summary table of $CaCO_3$ dissolution at Hog Reef.

$CaCO_3$ dissolution type	Mean survey %-cover	Mean reef %-cover	Mean $CaCO_3$ dissolution rate (kg $CaCO_3 \bullet m^{-2} \bullet y^{-1}$)	Mean reef $CaCO_3$ dissolution (kg $CaCO_3 \bullet m^{-2} \bullet y^{-1}$)	% of Total Hog Reef $CaCO_3$ dissolution
Microborer	99.3 ± 0.4	95 ± 2	−0.21 ± 0.09	−0.3 ± 0.1	90 ± 60
Sand	0.7 ± 0.4	5 ± 2	−0.39 ± 0.11	−0.02 ± 0.01	7 ± 4

Percent cover from the benthic surveys (±standard deviation) and calculated from the estimated reef footprint (±uncertainty) are reported for substrate available to dissolution by microboring communities (dominated by pioneer chlorophytes such as Phaeophila sp. and Ostreobium sp.) and sand $CaCO_3$ dissolution. $CaCO_3$ dissolution rates (± standard deviation), mean $CaCO_3$ dissolution (± uncertainty), and percentage of total $CaCO_3$ dissolution (± uncertainty) are expressed for microborer and sand dissolution at Hog Reef.

DISCUSSION

Annual NEC for 2011 calculated by the census NEC (2.35 ± 1.01 kg $CaCO_3 \bullet m^{-2} \bullet y^{-1}$) and by the bottle NEC (2.23 ± 1.02 kg $CaCO_3 \bullet m^{-2} \bullet y^{-1}$) are in close agreement. Chemistry-based NEC estimates measure NEC via the TA anomaly technique thereby recording the integrated signal of calcification and $CaCO_3$ dissolution occurring within the reef ecosystem. These findings that the census-based budget are in close agreement with the bottle chemistry NEC suggest that the summation of the components of coral reef calcification and $CaCO_3$ dissolution are representative of the total balance between calcification and $CaCO_3$ dissolution occurring at Hog Reef.

Annual NEC calculated for 2011 for Hog Reef using census (2.35 ± 1.01 kg $CaCO_3 \bullet m^{-2} \bullet y^{-1}$) and bottle-based (2.23 ± 1.02 kg $CaCO_3 \bullet m^{-2} \bullet y^{-1}$) methods in addition to other census-based NEC studies from the Caribbean (Stearn et al., 1977; Mallela and Perry, 2007; Perry et al., 2013) generally fall within the 20–250 mmol $CaCO_3 \bullet m^{-2} \bullet d^{-1}$ (0.73–9.13 kg $CaCO_3 \bullet m^{-2} \bullet y^{-1}$) range of average global coral reef flat NEC (Atkinson, 2011; **Figure 5**). The relationship between percent hard coral cover and reef NEC in this study is in general agreement with trends observed in other census-based studies of Caribbean reefs (Stearn et al., 1977; Mallela and Perry, 2007; Perry et al., 2013; **Figure 5**). Notably, the annual Hog Reef census NEC and bottle NEC are in close agreement with the census NEC calculated for a Bonaire reef (2.31 ± 1.05 kg $CaCO_3 \bullet m^{-2} \bullet y^{-1}$) with analogous hard coral cover (Hog Reef: 26 ± 5%; Bonaire reef: 25.0 ± 4.5%) and depth (Hog Reef: 10.3 ± 3.3 m; Bonaire Reef: 10 m; Perry et al., 2013; **Figure 5**). Collectively, these findings support earlier claims by Montaggioni and Braithwaite (2009) and measurements by Hamylton et al. (2013) that net coral reef calcification estimates using chemistry and census-based approaches are generally in close agreement.

To test for any temporal bias in the NEC rates calculated from daytime bottle sampling of NEC, the autonomous MAPCO$_2$ mooring recorded seawater pCO_2 every 3-h allowing for a higher temporal resolution of NEC to be measured. The mooring NEC values reveal the seasonal cycles and diel variability in NEC with generally higher NEC values of 4.10 ± 1.34 kg $CaCO_3 \bullet m^{-2} \bullet y^{-1}$

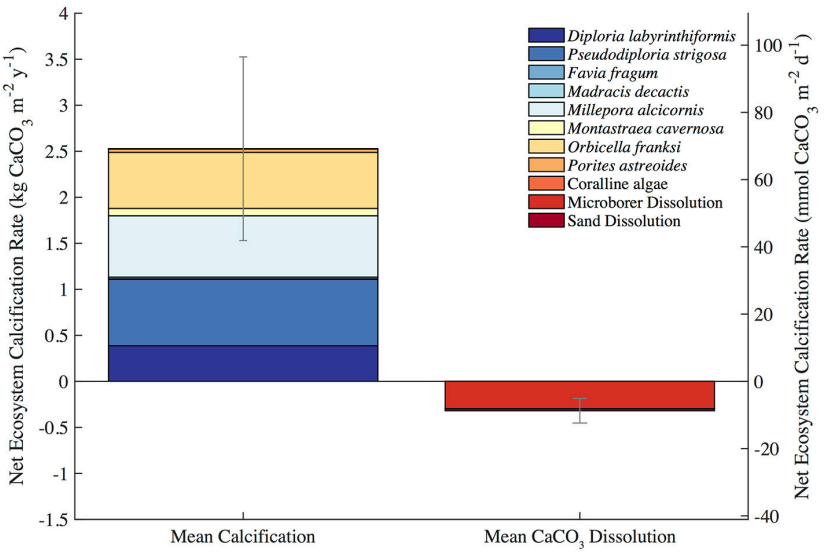

FIGURE 4 | Census-based summary of mean calcification and mean $CaCO_3$ dissolution. *D. labyrinthiformis*, *P. strigosa*, *M. alcicornis*, and *O. franksi* are the dominant biocalcifiers and microborer activity dominates $CaCO_3$ dissolution at Hog Reef.

TABLE 3 | NEC summary table for each method.

Method	Mean NEC (kg $CaCO_3 \bullet m^{-2} \bullet y^{-1}$)	NEC 2011 (kg $CaCO_3 \bullet m^{-2} \bullet y^{-1}$)	NEC 2011.2-2012.1 (kg $CaCO_3 \bullet m^{-2} \bullet y^{-1}$)
Census NEC	2.21 ± 1.01	2.35 ± 1.01	2.28 ± 1.01
Bottle NEC	2.85 ± 1.02	2.23 ± 1.02	2.46 ± 1.02
Mooring NEC	3.73 ± 1.34	Insufficient data	4.10 ± 1.34

NEC (±uncertainty) is calculated as the mean NEC over the entire study period, integrated annual NEC for 2011, and integrated annual NEC for the first mooring deployment.

compared to 2.35 ± 1.01 kg $CaCO_3 \bullet m^{-2} \bullet y^{-1}$ and 2.46 ± 1.02 kg $CaCO_3 \bullet m^{-2} \bullet y^{-1}$ for the census NEC and bottle NEC respectively during the same initial mooring deployment from 2011.2 to 2012.1 (**Table 3**; **Figures 3**, **6**). These mooring NEC values may be higher due to additional uncertainty generated by modeling TA from $MAPCO_2$ mooring pH-pCO_2 and/or could relate to higher frequency variability in reef processes. The absolute mooring NEC values should therefore be treated with some caution, but the range nonetheless highlights the dynamic variability of Hog Reef NEC. Interestingly, agreement between the census and chemistry-based NEC methods varies over the 2-year period further highlighting the dynamic variability of coral reef environments (**Figure 3**). This may be in part due to unmeasured temporal variability in the rates of dissolution by microborers and sediments, species-level differences in seasonal calcification responses, higher frequency variability in calcification rates than the 2-month intervals measured by the *in situ* growth rate experiments, and or changes in seawater residence time resulting from changes in wind and currents. Mean annual $CaCO_3$ dissolution by microborers was used for the census NEC; however, recent work has shown that $CaCO_3$ dissolution of new substrates by microborers varies nonlinearly due to succession of microboring communities over time and a combination of biotic and abiotic factors (Vogel et al., 2000; Carreiro-Silva et al., 2005; Aline, 2008; Tribollet et al., 2009; Grange et al., 2015). Similarly, sediment $CaCO_3$ dissolution rates were measured once in the summer and thus do not account for any potential temporal variability in $CaCO_3$ dissolution rates. Further research should be conducted to quantify shorter temporal scale variability in growth rates of biocalcifiers, $CaCO_3$ dissolution rates, and changes in coral reef seawater residence time to better understand these changes and the factors driving variable NEC (Venti et al., 2012; Teneva et al., 2013).

The census NEC in this study was limited by the high structural complexity (i.e., caves and overhangs) of Hog Reef, lack of calcification by suborder holaxonia and phyla Mollusca, and potential differences in biocalcification rates in Bermuda relative to literature reported rates for the tropical Caribbean. The limitations imposed by "canopy effects" present in the planar video surveys of structurally complex Hog Reef (Goatley and Bellwood, 2011) lead to underestimates of calcification by benthic foraminifera, bryozoans, corals, and coralline algae as well as underestimates of $CaCO_3$ dissolution by cryptic bioeroders (Hutchings, 1986), uncolonized substrate, and sediments occurring in unsampled caves. A prior estimate of Bermuda coral reef benthic foraminifera $CaCO_3$ production (0.080 kg $CaCO_3 \bullet m^{-2} \bullet y^{-1}$; Langer et al., 1997) is significantly less than the census NEC (2.35 ± 1.01 kg $CaCO_3 \bullet m^{-2} \bullet y^{-1}$) suggesting the absence of benthic foraminifera has a small influence on the Hog Reef NEC estimate. Additionally, the lack of published calcification rates for suborder holaxonia sea fans and sea rods and absence of phyla Mollusca and

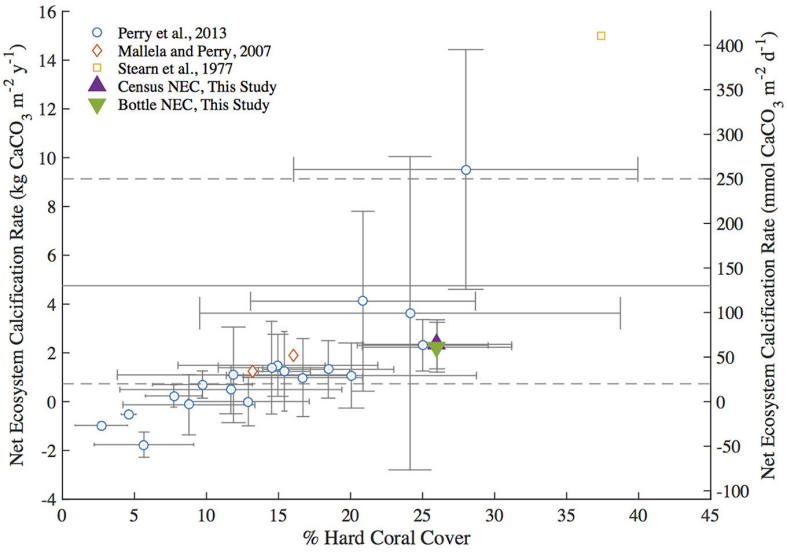

FIGURE 5 | Summary plot of Caribbean Reef percent hard coral cover vs. Net Ecosystem Calcification (NEC) adapted from Perry et al. (2013). Census NEC and bottle NEC are the 2011 integrated NEC values from this study. The gray dashed lines represent the upper and lower bounds of typical global coral reef flat NEC and the solid gray line indicates the mean global coral reef flat NEC from Atkinson (2011).

Echinodermata in the benthic survey data further underestimate total calcification occurring at Hog Reef. Because Bermuda is located at the edge of the latitudinal limit for coral reefs, it remains unclear how the cooler waters may systematically reduce calcification rates of all biocalcifiers in Bermuda relative to literature reported rates for more tropical Caribbean reefs. Annual *in situ* calcification rates for 2011 in this study for *D. labyrinthiformis* (3.02 kg $CaCO_3 \bullet m^{-2} \bullet y^{-1}$) and *P. astreoides* (2.70 kg $CaCO_3 \bullet m^{-2} \bullet y^{-1}$) were 35 and 57% lower respectively than calcification rates aggregated by *ReefBudget* for Caribbean corals at 10 m-depth (Perry et al., 2012). Similarly reduced growth rates in Bermuda relative to elsewhere in the Caribbean were observed for *P. strigosa*, *D. labyrinthiformis*, *P. astreoides*, and *Scolymia cubensis* (Tomascik and Logan, 1990; Logan and Tomascik, 1991; Logan et al., 1994). These findings that calcification rates are potentially lower in Bermuda suggest that the Caribbean *ReefBudget* calcification rates (Perry et al., 2012) used for many of the calcifying species in this study overestimate Hog Reef NEC. While this study was unable to quantify the contributions by each of these components, the close agreement between the census NEC and the bottle NEC suggest the net effect of these uncertainties on NEC may cancel out or are small relative to the other components of the census-based budget.

The bottle and mooring NEC in this study were limited by the ability to measure residence time, reef depth, and TA of reef seawater relative to source seawater. Estimations of NEC via the alkalinity anomaly method are particularly sensitive to changes in residence time and flow rates of the seawater overlying the reef community (Venti et al., 2012; Zhang et al., 2012; Falter et al., 2013; Teneva et al., 2013). Controlled volume experiments and numerical models further elucidate the necessity in measuring the height of the resulting mixed water column when calculating NEC (Zhang et al., 2012; Falter et al., 2013; Teneva et al., 2013). Prior work on residence times for nearby North Channel by Venti et al. (2012) and Bermuda platform bathymetry data from Sutherland et al. (2014) constrained these uncertainties in residence time and depth such that bottle and mooring NEC could be estimated for Hog Reef. To test for the contributions of uncertainty in residence time and seawater depth in this study, a sensitivity analysis was performed on the bottle NEC to test for a range of variability introduced within one standard deviation of mean residence times and depth of the effective reef footprint of Hog Reef (**Figure 7**). The source seawater TA for Bermuda rim reefs is well characterized by BATS making Hog Reef an ideal location to estimate chemistry-based NEC. Reef seawater TA for the bottle NEC estimates was directly measured ($\pm 4\ \mu mol \bullet kg^{-1}$) while mooring NEC in this study requires reef seawater TA to be calculated from measured pCO_2 and modeled pH_{total} (estimated $\pm 21\ \mu mol \bullet kg^{-1}$ from Millero, 2007). The resulting error between bottle NEC (± 1.02 kg $CaCO_3 \bullet m^{-2} \bullet y^{-1}$) and mooring NEC ($\pm 1.34$ kg $CaCO_3 \bullet m^{-2} \bullet y^{-1}$) reveals that the uncertainty introduced from predicting mooring TA is less than the combined uncertainties in seawater residence time and depth. This collectively shows that uncertainty in bottle and mooring NEC estimates are only as good as the ability to quantify the residence time and volume of the seawater overlying the benthic community.

The balance between coral reef calcification and $CaCO_3$ dissolution is of particular concern to the persistence of coral reef structure and other ecosystem services (Eyre et al., 2014). Coral community shifts and declining coral cover have already

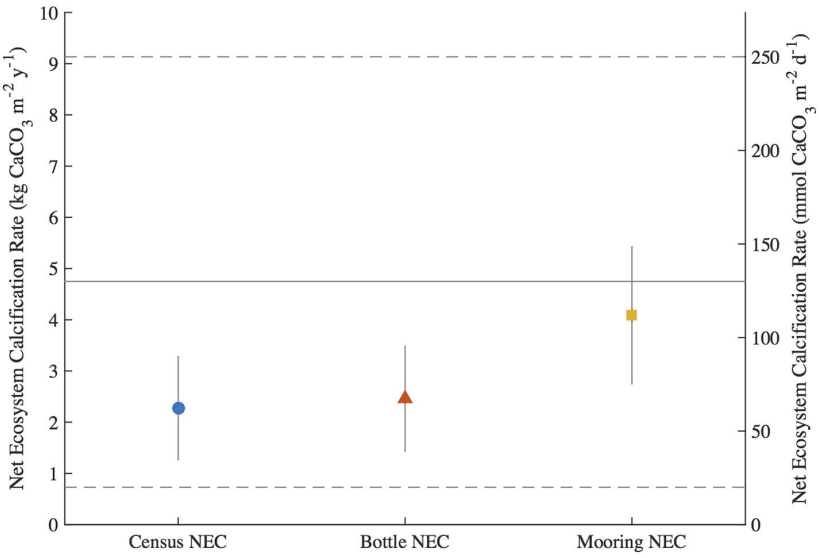

FIGURE 6 | Integrated Net Ecosystem Calcification (NEC) (±uncertainty) during the first mooring deployment from 2011.2 to 2012.1 for the census NEC, bottle NEC, and mooring NEC. The solid gray line and dashed gray lines represent the mean and range of NEC, respectively, for reef flats globally from Atkinson (2011).

decreased Caribbean reef NEC with a tipping point from positive to negative net $CaCO_3$ production occurring when hard coral cover falls below ca. 10% (Perry et al., 2013, 2015). In this study, census-based estimates of calcification greatly exceeded $CaCO_3$ dissolution at Hog Reef (**Figure 4**); however, chemistry based estimates reveal occasional measurements of net $CaCO_3$ dissolution occurring in spring and mid-summer (**Figure 3**). Despite larger-scale patterns of coral cover decline in the Caribbean over the most recent decades (Gardner et al., 2003), mean Bermuda rim reef hard coral cover has remained approximately constant over that time period (Dodge et al., 1982; CARICOMP, 2000; Linton and Fisher, 2004; MEP, 2007; Smith et al., 2013; Jackson et al., 2014). Because coral cover has remained approximately constant, any decadal-scale changes in calcification and $CaCO_3$ dissolution are therefore more likely to have changed due to changing rates and not changing benthic community composition. Notably, recent studies have shown that coral reef $CaCO_3$ dissolution is stimulated by changing climate and ocean chemistry (Andersson et al., 2009; Tribollet et al., 2009; Cyronak et al., 2013a; Reyes-Nivia et al., 2013) suggesting that even at constant coral cover, increased $CaCO_3$ dissolution could drive declines in net $CaCO_3$ production at Hog Reef. Further research should be conducted to see how these rates have changed in response to changing climate and ocean chemistry to better understand potential calcification-$CaCO_3$ dissolution tipping points for the rim reefs of Bermuda.

Continued global declines in coral cover and changing coral community composition highlight the importance for NEC measurements to be included in coral reef monitoring projects to assess the ability of a given coral reef to maintain positive $CaCO_3$ production and therefore reef structure and function. Because NEC measures the capacity for *in situ* coral reef $CaCO_3$ production (Perry et al., 2012, 2013), it must be considered within the context of additional import, export, and erosion of $CaCO_3$ material if the monitoring goal is to directly measure net coral reef accretion (e.g., Scoffin, 1992; Milliman, 1993; Kleypas et al., 2001; Perry et al., 2008, 2012; Montaggioni and Braithwaite, 2009; Tribollet and Golubic, 2011). To date, much attention has been given to reef accretion processes highlighting the importance of additionally studying the dynamics of erosive processes, especially dissolution of $CaCO_3$ in sediment and by microborers, sponges, and other bioeroders. Although sediment dissolution was only a small component of the total dissolution in this study due to the small percentage surface area of sands, other reefs have a much larger percentage surface area of sands making sediment $CaCO_3$ dissolution a more important component of the $CaCO_3$ budget at those reefs (Cyronak et al., 2013a; Cyronak and Eyre, 2016). Nonetheless, census and chemistry-based NEC estimates represent relatively non-invasive means of measuring coral reef $CaCO_3$ production capacity. Census-based NEC and the relative $CaCO_3$ production contributions by the dominant biocalcifying species for Caribbean coral reefs can be estimated from benthic survey data using standardized methods and literature reported rates from the *ReefBudget* project (Perry et al., 2012). Notably, *D. labyrinthiformis*, *P. strigosa*, *M. alcicornis*, and *O. franksi* contribute 94 ± 19% of the total calcification at Hog Reef (**Table 1**, **Figure 4**) suggesting conservation measures should focus on those four species to preserve positive $CaCO_3$ production at Hog Reef. Chemistry-based NEC estimates require well-constrained estimates of

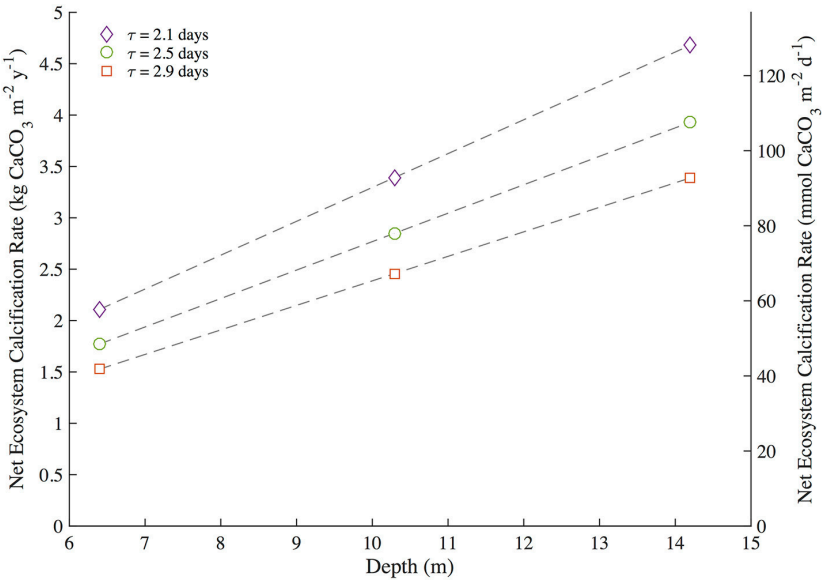

FIGURE 7 | Sensitivity analysis for bottle NEC at Hog Reef during the 2-year study period. Bottle Net Ecosystem Calcification (NEC) was calculated iteratively using mean depth ± one standard deviation (10.3 ± 3.3 m) and mean residence time ± one standard deviation (2.5 ± 0.4 days) to determine the sensitivity of NEC to the interacting uncertainty and variability of these measurements.

seawater residence time, bathymetry, source seawater TA, and reef seawater TA to capture the entire sum of calcification and $CaCO_3$ dissolution over shorter time scales (e.g., Langdon et al., 2010 and references therein). These shorter time scale NEC measurements allow the mechanisms (i.e., Smith and Buddemeier, 1992: temperature, light, carbonate chemistry, hydrodynamics, nutrients, salinity, and sea level) driving NEC to be further explored (Silverman et al., 2007; Shaw et al., 2012, 2015; Albright et al., 2015), thus providing a greater understanding of coral reef NEC and how coral reef $CaCO_3$ production may be affected by global change. The results of this study conducted at Hog Reef suggest that either method may be used with remarkable agreement over annual time scales (Hog Reef, 2011 census NEC 2.35 ± 1.01 kg $CaCO_3 \bullet m^{-2} \bullet y^{-1}$ vs. bottle NEC 2.23 ± 1.02 kg $CaCO_3 \bullet m^{-2} \bullet y^{-1}$) depending on the available resources and goals of the reef-monitoring agency. When used in conjunction, the census and chemistry-based NEC approaches corroborate estimates of NEC to provide species-level estimates of $CaCO_3$ production (census NEC; **Table 1**, **Figure 4**) while highlighting temporal variability (chemistry NEC; **Figure 3**) in coral reef $CaCO_3$ production.

CONCLUSIONS

The present study reveals that 2011 annual census NEC (2.35 ± 1.01 kg $CaCO_3 \bullet m^{-2} \bullet y^{-1}$) and bottle NEC (2.23 ± 1.02 kg $CaCO_3 \bullet m^{-2} \bullet y^{-1}$) at Hog Reef are in close agreement. Census-based budgets allow for NEC to be subdivided into the individual contributions by species or substrate on calcification and $CaCO_3$ dissolution over annual time scales and revealed that the vast majority of $CaCO_3$ production at Hog Reef (94 ± 19%) was by *D. labyrinthiformis*, *P. strigosa*, *M. alcicornis*, and *O. franksi*. Alternatively, chemistry-based estimates capture the NEC of the entire reef at shorter temporal timescales allowing the high temporal variability of coral reef NEC to be analyzed relative to the potential drivers causing NEC to vary. Varying agreement between census-based and chemistry-based NEC was found during the ca. 2-year study interval further highlighting the dynamic nature of NEC and calling for further investigation of the mechanisms driving variability in biocalcification, dissolution, and seawater residence times at Hog Reef. These findings collectively suggest that either method, but ideally both methods, may be used to estimate coral reef NEC depending on the goals or available resources of the coral reef-monitoring project and that high temporal variability in coral reef environments must always be considered when studying biogeochemical processes such as calcification and $CaCO_3$ dissolution.

AUTHOR CONTRIBUTIONS

TAC and AJA designed the NEC study, analyzed the results, and wrote the manuscript. AJA, AC, TC, SdP, BE, RG, EH, RJ, SM, TN, CS, AJS, JT, and AT collected and provided data for various components of the NEC study. All authors commented on and approved the final draft of this manuscript.

FUNDING

NSF OCE 09-28406 (AJA, NB, SdP); NSF OCE 12-55042 (AJA); NSF OCE 14-16518 (AJA, RJ); ARC DP150102092 (BE, AJA); French Ministry of Ecology MEDDE- Program MIDACOR (AT); NOAA Office of Oceanic and Atmospheric Research (AS, CS).

ACKNOWLEDGMENTS

James J. Leichter is gratefully acknowledged for providing guidance and insight into developing methods for determining the effective footprint based on the acoustic current profiler data. We thank Mandy Shailer from the Government of Bermuda for her assistance in providing us with the most up-to-date Bermuda platform bathymetry data. We thank Sandrine Caquineau for her assistance with scanning electron microscopy on the platform ALIZES (Centre IRD, Bondy, Fr). Additional BIOS and NOAA PMEL staff are gratefully acknowledged for their contributions to the data collection of various components of this project. Theodor Kindeberg provided comments that improved an earlier version of this manuscript. We additionally thank the two reviewers for their constructive comments and feedback. This work is PMEL contribution number 4504.

REFERENCES

Albright, R., Benthuysen, J., Cantin, N., Caldeira, K., and Anthony, K. (2015). Coral reef metabolism and carbon chemistry dynamics of a coral reef flat. *Geophys. Res. Lett.* 42, 3980–3988. doi: 10.1002/2015GL063488

Aline, T. (2008). Dissolution of dead corals by euendolithic microorganisms across the northern Great Barrier Reef (Australia). *Microb. Ecol.* 55, 569–580. doi: 10.1007/s00248-007-9302-6

Alvarez-Filip, L., Carricart-Ganivet, J. P., Horta-Puga, G., and Iglesias-Prieto, R. (2013). Shifts in coral-assemblage composition do not ensure persistence of reef functionality. *Sci. Rep.* 3:3486. doi: 10.1038/srep03486

Alvarez-Filip, L., Dulvy, N. K., Gill, J. A., Côté, I. M., and Watkinson, A. R. (2009). Flattening of Caribbean coral reefs: region-wide declines in architectural complexity. *Proc. Biol. Sci.* 276, 3019–3025. doi: 10.1098/rspb.2009.0339

Andersson, A. J., and Gledhill, D. (2013). Ocean acidification and coral reefs: effects on breakdown, dissolution, and net ecosystem calcification. *Ann. Rev. Mar. Sci.* 5, 321–348. doi: 10.1146/annurev-marine-121211-172241

Andersson, A. J., Kuffner, I. B., Mackenzie, F. T., Jokiel, P. L., Rodgers, K. S., and Tan, A. (2009). Net loss of $CaCO_3$ from a subtropical calcifying community due to seawater acidification: mesocosm-scale experimental evidence. *Biogeosciences* 6, 1811–1823. doi: 10.5194/bg-6-1811-2009

Andersson, A. J., Yeakel, K. L., Bates, N. R., and de Putron, S. J. (2014). Partial offsets in ocean acidification from changing coral reef biogeochemistry. *Nat. Clim. Chang.* 4, 56–61. doi: 10.1038/nclimate2050

Andréfouët, S., and Payri, C. (2000). Scaling-up carbon and carbonate metabolism of coral reefs using in-situ data and remote sensing. *Coral Reefs* 19, 259–269. doi: 10.1007/s003380000117

Atkinson, M. (2011). "Biogeochemistry of nutrients," in *Coral Reefs: An Ecosystem in Transition*, eds Z. Dubinsky and N. Stambler (Dordrecht: Springer), 199–206.

Bak, R. P. M. (1976). The growth of coral colonies and the importance of crustose coralline algae and burrowing sponges in relation with carbonate accumulation. *Netherlands J. Sea Res.* 10, 285–337. doi: 10.1016/0077-7579(76)90009-0

Bates, N. R. (2002). Seasonal variability of the effect of coral reefs on seawater CO_2 and air-sea CO_2 exchange. *Limnol. Oceanogr.* 47, 43–52. doi: 10.4319/lo.2002.47.1.0043

Bates, N. R., Amat, A., and Anderrsson, A. J. (2010). The interaction of carbonate chemistry and coral reel calcification: the carbonate chemistry coral reef ecosystem feedback (CREF) hypothesis. *Biogeosciences* 7, 2509–2530. doi: 10.5194/bg-7-2509-2010

Bates, N. R., Best, M. H. P., Neely, K., Garley, R., Dickson, A. G., and Johnson, R. J. (2012). Detecting anthropogenic carbon dioxide uptake and ocean acidification in the North Atlantic Ocean. *Biogeosciences* 9, 2509–2522. doi: 10.5194/bg-9-2509-2012

Bates, N. R., Samuels, L., and Merlivat, L. (2001). Biogeochemical and physical factors influencing seawater fCO_2 and air-sea CO_2 exchange on the Bermuda coral reef. *Limnol. Oceanogr.* 46, 833–846. doi: 10.4319/lo.2001.46.4.0833

Bermuda Weather Service (2016). *Climate Data for Bermuda*. Available online at: www.weather.bm/climate.asp

Bermuda Zoological Society (1997). *Marine Aerial Photography of Bermuda*. Flatts Village.

Broecker, W. S., and Takahashi, T. (1966). Calcium carbonate precipitation on the Bahama Banks. *J. Geophys. Res.* 71, 1575–1602. doi: 10.1029/JZ071i006p01575

CARICOMP (2000). "Status and temporal trends at CARICOMP coral reef sites," in *Proceedings of the 9th International Coral Reef Symposium*, Vol. 1, (Bali).

Carreiro-Silva, M., McClanahan, T. R., and Kiene, W. E. (2005). The role of inorganic nutrients and herbivory in controlling microbioerosion of carbonate substratum. *Coral Reefs* 24, 214–221. doi: 10.1007/s00338-004-0445-3

Chave, K. E., Smith, S. V., and Roy, K. J. (1972). Carbonate production by coral reefs. *Mar. Geol.* 12, 123–140. doi: 10.1016/0025-3227(72)90024-2

Cyronak, T., and Eyre, B. D. (2016). The synergistic effects of ocean acidification and organic metabolism on calcium carbonate ($CaCO_3$) dissolution in coral reef sediments. *Mar. Chem.* 183, 1–12. doi: 10.1016/j.marchem.2016.05.001

Cyronak, T., Santos, I. R., and Eyre, B. D. (2013a). Permeable coral reef sediment dissolution driven by elevated pCO_2 and pore water advection. *Geophys. Res. Lett.* 40, 4876–4881. doi: 10.1002/grl.50948

Cyronak, T., Santos, I. R., McMahon, A., and Eyre, B. D. (2013b). Carbon cycling hysteresis in permeable carbonate sands over a diel cycle: implications for ocean acidification. *Limnol. Oceanogr.* 58, 131–143. doi: 10.4319/lo.2013.58.1.0131

Dahl, A. L. (1973). Surface area in ecological analysis: quantification of benthic coral-reef algae. *Mar. Biol.* 23, 239–249. doi: 10.1007/BF00389331

de Groot, R., Brander, L., van der Ploeg, S., Costanza, R., Bernard, F., Braat, L., et al. (2012). Global estimates of the value of ecosystems and their services in monetary units. *Ecosyst. Serv.* 1, 50–61. doi: 10.1016/j.ecoser.2012.07.005

Dickson, A. G. (1990). Standard potential of the reaction: AgCl(s) + 1/2 H2(g) = Ag(s) + HCl(aq), and the standard acidity constant of the ion HSO4- in synthetic seawater from 273.15 to 318.15 K. *J. Chem. Thermodyn.* 22, 113–127. doi: 10.1016/0021-9614(90)90074-Z

Dickson, A. G., and Millero, F. J. (1987). A comparison of the equilibrium constants for the dissociation of carbonic acid in seawater media. Deep Sea Res. Part A. *Oceanogr. Res. Pap.* 34, 1733–1743. doi: 10.1016/0198-0149(87)90021-5

Dickson, A. G., Sabine, C. L., and Christian, J. R. (2007). *Guide to Best Practices for Ocean CO_2 Measurements*. IOCCP Report no. 8, PICES Special Publication 3, International Ocean Carbon Coordination Project, Sopot, Poland. Available online at: cdiac.ornl.gov/oceans/ Handbook_2007.html

Dodge, R. E., Logan, A., and Antonius, A. (1982). Quantitative reef assessment studies in Bermuda: a comparison of methods and preliminary results. *Bull. Mar. Sci.* 32, 745–760.

Done, T. J., Ogden, J. C., Wiebe, W. J., and Rosen, B. R. (1996). "Biodiversity and ecosystem function of coral reefs," in *Heywood VH Global Biodiversity Assessment*, eds H. A. Mooney, J. H. Cushman, E. Medina, O. E. Sala, and E.-D. Schulze (Cambridge University Press for United Nations Environment Programme), 393–429.

Eakin, C. M. (1996). Where have all the carbonates gone? A model comparison of calcium carbonate budgets before and after the 1982–1983 El Nino at Uva Island in the eastern Pacific. *Coral Reefs* 15, 109–119. doi: 10.1007/bf01771900

Edmunds, P. J., Comeau, S., Lantz, C., Andersson, A., Briggs, C., Cohen, A., et al. (2016). Integrating the effects of ocean acidification across functional scales on tropical coral reefs. *BioScience* 66, 350–362. doi: 10.1093/biosci/biw023

Esford, L. E., and Lewis, J. C. (1990). Stiffness of Caribbean gorgonians (Coelenterata, Octocorallia) and Ca/Mg content of their axes. *Mar. Ecol. Prog. Ser. Oldendorf* 6, 189–200. doi: 10.3354/meps067189

Eyre, B. D., Andersson, A. J., and Cyronak, T. (2014). Benthic coral reef calcium carbonate dissolution in an acidifying ocean. *Nat. Clim. Chang.* 4, 969–976. doi: 10.1038/nclimate2380

Falter, J. L., Lowe, R. J., Zhang, Z., and McCulloch, M. (2013). Physical and biological controls on the carbonate chemistry of coral reef waters: effects of metabolism, wave forcing, sea level, and geomorphology. *PLoS ONE* 8:e53303. doi: 10.1371/journal.pone.0053303

Gardner, T. A., Côté, I. M., Gill, J. A., Grant, A., and Watkinson, A. R. (2003). Long-term region-wide declines in Caribbean corals. *Science* 301, 958–960. doi: 10.1126/science.1086050

Gattuso, J. P., Pichon, M., Delesalle, B., Canon, C., and Frankignoulle, M. (1996). Carbon fluxes in coral reefs. I. Lagrangian measurement of community metabolism and resulting air-sea CO_2 disequilibrium. *Mar. Ecol.Prog. Ser.* 145, 109–121. doi: 10.3354/meps145109

Glover, D. M., Jenkins, W. J., and Doney, S. C. (2011). *Modeling Methods for Marine Science*. Cambridge: Cambridge University Press.

Goatley, C. H., and Bellwood, D. R. (2011). The roles of dimensionality, canopies and complexity in ecosystem monitoring. *PLoS ONE* 6:e27307. doi: 10.1371/journal.pone.0027307

Grange, J. S., Rybarczyk, H., and Tribollet, A. (2015). The three steps of the carbonate biogenic dissolution process by microborers in coral reefs (New Caledonia). *Environ. Sci. Pollut. Res.* 22, 13625–13637. doi: 10.1007/s11356-014-4069-z

Hamylton, S., Silverman, J., and Shaw, E. (2013). The use of remote sensing to scale up measures of carbonate production on reef systems: a comparison of hydrochemical and census-based estimation methods. *Int. J. Remote Sens.* 34, 6451–6465. doi: 10.1080/01431161.2013.800654

Harney, J. N., and Fletcher, C. H. III. (2003). A budget of carbonate framework and sediment production, Kailua Bay, Oahu, Hawaii. *J. Sediment. Res.*73, 856–868. doi: 10.1306/051503730856

Hubbard, D. K., Miller, A. I., and Scaturo, D. (1990). Production and cycling of calcium carbonate in a shelf-edge reef system (St. Croix, U.S. Virgin Islands): applications to the nature of reef systems in the fossil record. *J. Sediment. R.* 60, 335–360. doi: 10.1306/212F9197-2B24-11D7-8648000102C1865D

Hutchings, P. A. (1986). Biological destruction of coral reefs. *Coral reefs* 4, 239–252. doi: 10.1007/BF00298083

Jackson, J. B. C., Donovan, M. K., Cramer, K. L., and Lam, V. (2014). *Status and Trends of Caribbean Coral Reefs: 1970-2012*. Gland: Global Coral Reef Monitoring Network; IUCN.

Jokiel, P. L., Maragos, J. E., and Franzisket, L. (1978). *Coral Growth: Buoyant Weight Technique. Coral Reefs: Research Methods*. Paris: UNESCO, 529–541.

Kinsey, D. W. (1979). *Carbon Turnover and Accumulation by Coral Reefs*. Doctoral dissertation, University of Hawai'i.

Kinsey, D. W. (1981). "The Pacific/Atlantic reef growth controversy," in *Proceedings of the 4th International Coral Reef Symposium*, Vol. 1, (Manila), 493–498.

Kinsey, D. W. (1985). "Metabolism, calcification and carbon production. I. System level studies," in *Proceedings of the 5th International Coral Reef Congress* (Tahiti), 503–542.

Kleypas, J. A. (1997). Modeled estimates of global reef habitat and carbonate production since the last glacial maximum. *Paleoceanography* 12, 533–545. doi: 10.1029/97PA01134

Kleypas, J. A., Buddemeier, R. W., and Gattuso, J. P. (2001). The future of coral reefs in an age of global change. *Int. J. Earth Sci.* 90, 426–437. doi: 10.1007/s005310000125

Kleypas, J. A., McManus, J. W., and Meñez, L. A. (1999). Environmental limits to coral reef development: where do we draw the line? *Am. Zool.* 39, 146–159.

Ku, H. H. (1966). Notes on the use of propagation of error formulas. *J. Res. Natl. Bur. Stand.* 70C, 263–273. doi: 10.6028/jres.070c.025

Langdon, C., Gattuso, J.-P., and Andersson, A. (2010). "Measurements of calcification and dissolution of benthic organisms and communities," in *Guide to Best Practices for Ocean Acidification Research and Data Reporting,* eds U. Riebesell, V. J. Fabry, L. Hansson, and J.-P. Gattuso (Luxembourg: Publications Office of the European Union), 215–232.

Langer, M. R., Silk, M. T., and Lipps, J. H. (1997). Global ocean carbonate and carbon dioxide production; the role of reef Foraminifera. *J. Foraminiferal Res.* 27, 271–277. doi: 10.2113/gsjfr.27.4.271

Levin, S. A. (1992). The problem of pattern and scale in ecology: the Robert H. MacArthur award lecture. *Ecology* 73, 1943–1967. doi: 10.1007/978-1-4615-1769-6_15

Linton, D., and Fisher, T. (2004). *CARICOMP Caribbean Coastal Marine Productivity Program 1993-2003*. Kingston: Caricomp.

Logan, A., and Tomascik, T. (1991). Extension growth rates in two coral species from high-latitude reefs of Bermuda. *Coral Reefs* 10, 155–160. doi: 10.1007/BF00572174

Logan, A., Yang, L., and Tomascik, T. (1994). Linear skeletal extension rates in two species of Diploria from high-latitude reefs in Bermuda. *Coral Reefs* 13, 225–230. doi: 10.1007/BF00303636

Mallela, J., and Perry, C. T. (2007). Calcium carbonate budgets for two coral reefs affected by different terrestrial runoff regimes, Rio Bueno, Jamaica. *Coral Reefs* 26, 129–145. doi: 10.1007/s00338-006-0169-7

Marsh, J. A. Jr. (1970). Primary productivity of reef-building calcareous red algae. *Ecology* 51, 255–263. doi: 10.2307/1933661

McDougall, T. J., and Barker, P. M. (2011). *Getting Started with TEOS-10 and the Gibbs Seawater (GSW) Oceanographic Toolbox*. Sydney: SCOR/IAPSO WG 127, 1–28.

Mehrbach, C., Culberson, C. H., Hawley, J. E., and Pytkowicz, R. M. (1973). Measurement of the apparent dissociation constants of carbonic acid in seawater at atmospheric pressure. *Limnol. Oceanogr.* 18, 897–907. doi: 10.4319/lo.1973.18.6.0897

MEP (2007). *Marine Environmental Program Annual Report, 2006–2007*. Bermuda Institute of Ocean Sciences, 80.

Millero, F. J. (2007). The marine inorganic carbon cycle. *Chem. Rev.* 107, 308–341. doi: 10.1021/cr0503557

Milliman, J. D. (1993). Production and accumulation of calcium carbonate in the ocean: budget of a nonsteady state. *Glob. Biogeochem. Cycles* 7, 927–957. doi: 10.1029/93GB02524

Moberg, F., and Folke, C. (1999). Ecological goods and services of coral reef ecosystems. *Ecol. Econ.* 29, 215–233. doi: 10.1016/S0921-8009(99)00009-9

Montaggioni, L. F., and Braithwaite, C. J. R. (2009). *Quaternary Coral Reef Systems: History, Development Processes and Controlling Factors, Developments in Marine Geology*. Oxford: Elsevier.

Perry, C. T., Edinger, E. N., Kench, P. S., Murphy, G. N., Smithers, S. G., Steneck, R. S., et al. (2012). Estimating rates of biologically driven coral reef framework production and erosion: a new census-based carbonate budget methodology and applications to the reefs of Bonaire. *Coral Reefs* 31, 853–868. doi: 10.1007/s00338-012-0901-4

Perry, C. T., Murphy, G. N., Kench, P. S., Smithers, S. G., Edinger, E. N., Steneck, R. S., et al. (2013). Caribbean-wide decline in carbonate production threatens coral reef growth. *Nat. Commun.* 4, 1402. doi: 10.1038/ncomms2409

Perry, C. T., Spencer, T., and Kench, P. S. (2008). Carbonate budgets and reef production states: a geomorphic perspective on the ecological phase-shift concept. *Coral Reefs* 27, 853–866. doi: 10.1007/s00338-008-0418-z

Perry, C. T., Steneck, R. S., Murphy, G. N., Kench, P. S., Edinger, E. N., Smithers, S. G., et al. (2015). Regional-scale dominance of non-framework building corals on Caribbean reefs affects carbonate production and future reef growth. *Glob. Chang. Biol.* 21, 1153–1164. doi: 10.1111/gcb.12792

Reyes-Nivia, C., Diaz-Pulido, G., Kline, D., Guldberg, O. H., and Dove, S. (2013). Ocean acidification and warming scenarios increase microbioerosion of coral skeletons. *Glob. Chang. Biol.* 19, 1919–1929. doi: 10.1111/gcb.12158

Salvat, B. (1992). Coral reefs—a challenging ecosystem for human societies. *Glob. Environ. Change* 2, 12–18. doi: 10.1016/0959-3780(92)90032-3

Schneider, C. A., Rasband, W. S., and Eliceiri, K. W. (2012). NIH image to ImageJ: 25 years of image analysis. *Nat. Methods* 9, 671–675. doi: 10.1038/nmeth.2089

Scoffin, T. (1992). Taphonomy of coral reefs: a review. *Coral Reefs* 11, 57–77. doi: 10.1007/BF00357423

Shaw, E. C., McNeil, B. I., and Tilbrook, B. (2012). Impacts of ocean acidification in naturally variable coral reef flat ecosystems. *J. Geophys. Res. Oceans* 117, C03038. doi: 10.1029/2011JC007655

Shaw, E. C., Phinn, S. R., Tilbrook, B., and Steven, A. (2015). Natural in situ relationships suggest coral reef calcium carbonate production will decline with ocean acidification. *Limnol. Oceanogr.* 60, 777–788. doi: 10.1002/lno.10048

Silverman, J., Lazar, B., and Erez, J. (2007). Effect of aragonite saturation, temperature, and nutrients on the community calcification rate of a coral reef. *J. Geophys. Res. Oceans* 112, C05004. doi: 10.1029/2006JC003770

Smith, S. R., de Putron, S., Murdoch, T. J., Pitt, J. M., and Nagelkerken, I. (2013). "Biology and ecology of corals and fishes on the Bermuda Platform," in *Coral Reefs of the United Kingdom Overseas Territories*, ed C. R. C. Sheppard (Dordrecht: Springer), 135–151.

Smith, S. V. (1978). Coral-reef area and the contributions of reefs to processes and resources of the world's oceans. *Nature* 273, 225–226. doi: 10.1038/273225a0

Smith, S. V., and Buddemeier, R. W. (1992). Global change and coral reef ecosystems. *Annu. Rev. Ecol. Syst.* 23, 89–118. doi: 10.1146/annurev.es.23.110192.000513

Smith, S. V., and Key, G. S. (1975). Carbon dioxide and metabolism in marine environments. *Limnol. Oceanogr.* 20, 493–495. doi: 10.4319/lo.1975.20.3.0493

Smith, S. V., and Kinsey, D. W. (1976). Calcium carbonate production, coral reef growth, and sea level change. *Science* 194, 937–939. doi: 10.1126/science.194.4268.937

Spurgeon, J. P. (1992). The economic valuation of coral reefs. *Mar. Pollut. Bull.* 24, 529–536. doi: 10.1016/0025-326X(92)90704-A

Stearn, C. W., Scoffin, T. P., and Martindale, W. (1977). Calcium carbonate budget of a fringing reef on the West Coast of Barbados part I—zonation and productivity. *Bull. Mar. Sci.* 27, 479–510.

Sutherland, M. G., McLean, S. J., Love, M. R., Carignan, K. S., and Eakins, B. W. (2014). *Digital Elevation Models of Bermuda: Data Sources, Processing and Analysis*. Boulder, CO: NOAA National Geophysical Data Center, U.S. Dept. of Commerce, 7.

Sutton, A. J., Sabine, C. L., Maenner-Jones, S., Lawrence-Slavas, N., Meinig, C., Feely, R. A., et al. (2014). A high-frequency atmospheric and seawater pCO_2 data set from 14 open-ocean sites using a moored autonomous system. *Earth Syst. Sci. Data* 6, 353–366. doi: 10.5194/essd-6-353-2014

Teneva, L., Dunbar, R. B., Mucciarone, D. A., Dunckley, J. F., and Koseff, J. R. (2013). High-resolution carbon budgets on a Palau back—reef modulated by interactions between hydrodynamics and reef metabolism. *Limnol. Oceanogr.* 58, 1851–1870. doi: 10.4319/lo.2013.58.5.1851

Tomascik, T., and Logan, A. (1990). A comparison of peripheral growth rates in the recent solitary coral Scolymia cubensis (Milne-Edwards and Haime) from Barbados and Bermuda. *Bull. Mar. Sci.* 46, 799–806.

Tribollet, A., Godinot, C., Atkinson, M., and Langdon, C. (2009). Effects of elevated pCO_2 on dissolution of coral carbonates by microbial euendoliths. *Glob. Biogeochem. Cycles* 23, GB3008. doi: 10.1029/2008GB003286

Tribollet, A., and Golubic, S. (2011). "Reef bioerosion: agents and processes," in *Coral Reefs: An Ecosystem in Transition*, eds Z. Dubinsky and N. Stambler (Dordrecht: Springer), 435–449.

Uppström, L. R. (1974). The boron/chlorinity ratio of deep-sea water from the Pacific Ocean. *Deep Sea Res. Oceanogr. Abstr.* 21, 161–162. doi: 10.1016/0011-7471(74)90074-6

van Heuven, S., Pierrot, D., Rae, J. W. B., Lewis, E., and Wallace, D. W. R. (2011). *MATLAB Program Developed for CO_2 System Calculations*. *ORNL/CDIAC-105b*. Oak Ridge: Carbon Dioxide Information Analysis Center, Oak Ridge National Laboratory, U.S. Department of Energy.

Vecsei, A. (2004). A new estimate of global reefal carbonate production including the fore-reefs. *Glob. Planet. Change* 43, 1–18. doi: 10.1016/j.gloplacha.2003.12.002

Venti, A., Kadko, D., Andersson, A. J., Langdon, C., and Bates, N. R. (2012). A multi-tracer model approach to estimate reef water residence times. *Limnol. Oceanogr. Methods* 10, 1078–1095. doi: 10.4319/lom.2012.10.1078

Vogel, K., Gektidis, M., Golubic, S., Kiene, W. E., and Radtke, G. (2000). Experimental studies on microbial bioerosion at Lee Stocking Island, Bahamas and One Tree Island, Great Barrier reef, Australia: implications for paleoecological reconstructions. *Lethaia* 33, 190–204. doi: 10.1080/00241160025100053

Yeakel, K. L., Andersson, A. J., Bates, N. R., Noyes, T. J., Collins, A., and Garley, R. (2015). Shifts in coral reef biogeochemistry and resulting acidification linked to offshore productivity. *Proc. Natl. Acad. Sci. U.S.A.* 112, 14512–14517. doi: 10.1073/pnas.1507021112

Zhang, Z., Falter, J., Lowe, R., and Ivey, G. (2012). The combined influence of hydrodynamic forcing and calcification on the spatial distribution of alkalinity in a coral reef system. *J. Geophys. Res. Oceans* 117, C04034. doi: 10.1029/2011JC007603

Conflict of Interest Statement: The authors declare that the research was conducted in the absence of any commercial or financial relationships that could be construed as a potential conflict of interest.

Chapter 3, in full, is a reprint of the material as it appears in Courtney TA, Andersson AJ, Bates NB, Collins A, Cyronak T, de Putron SJ, Eyre BD, Garley R, Hochberg EJ, Johnson R, Musielewicz S, Noyes T, Sabine CL, Sutton AJ, Toncin J, Tribollet A. Comparing Chemistry and Census-based Estimates of Net Ecosystem Calcification on a Rim Reef in Bermuda. *Frontiers in Marine Science* 2016, 3:181. The dissertation author was the primary investigator and author of this paper.

CHAPTER 4

Environmental controls on modern scleractinian coral and reef-scale calcification

Courtney TA, Lebrato M, Bates NR, Collins A, de Putron SJ, Garley R, Johnson, R, Molinero JC, Noyes TJ, Sabine CL, Andersson AJ

APPLIED ECOLOGY

Environmental controls on modern scleractinian coral and reef-scale calcification

Travis A. Courtney,[1]* Mario Lebrato,[1,2] Nicholas R. Bates,[3,4] Andrew Collins,[3] Samantha J. de Putron,[3] Rebecca Garley,[3] Rod Johnson,[3] Juan-Carlos Molinero,[5] Timothy J. Noyes,[3] Christopher L. Sabine,[6] Andreas J. Andersson[1]

Modern reef-building corals sustain a wide range of ecosystem services because of their ability to build calcium carbonate reef systems. The influence of environmental variables on coral calcification rates has been extensively studied, but our understanding of their relative importance is limited by the absence of in situ observations and the ability to decouple the interactions between different properties. We show that temperature is the primary driver of coral colony (*Porites astreoides* and *Diploria labyrinthiformis*) and reef-scale calcification rates over a 2-year monitoring period from the Bermuda coral reef. On the basis of multimodel climate simulations (Coupled Model Intercomparison Project Phase 5) and assuming sufficient coral nutrition, our results suggest that *P. astreoides* and *D. labyrinthiformis* coral calcification rates in Bermuda could increase throughout the 21st century as a result of gradual warming predicted under a minimum CO_2 emissions pathway [representative concentration pathway (RCP) 2.6] with positive 21st-century calcification rates potentially maintained under a reduced CO_2 emissions pathway (RCP 4.5). These results highlight the potential benefits of rapid reductions in global anthropogenic CO_2 emissions for 21st-century Bermuda coral reefs and the ecosystem services they provide.

INTRODUCTION

Tropical coral reef ecosystems provide humanity with a range of direct (tourism and fishing), indirect (shoreline protection and fisheries recruitment), and nonuse (biodiversity and intrinsic value) ecosystem services (*1*). The structure of these ecosystems is maintained by net positive production of calcium carbonate ($CaCO_3$), with scleractinian corals accounting for the majority of the total coral reef $CaCO_3$ production (*2*). Current estimates suggest that there are fewer than 1000 zooxanthellate hermatypic scleractinian coral species sustaining the structural habitat that covers just 0.2% of the total ocean surface area and yet supports an estimated 35% of all species living in the global oceans (*3*).

The geologic record shows the onset of large and widespread coral reef accretion dating back to the late Triassic (~230 million years ago), when scleractinian corals are hypothesized to have first acquired photosynthetic zooxanthellae symbionts (*4*). This symbiosis allowed corals to expand geographic ranges (*4*) due to the algal symbionts providing upward of 100% of the daily respiratory carbon needed to sustain the modern coral host (*5*). The efficiency of this symbiosis allows corals to maintain primary productivity rates (8.0 to 40.0 g C m^{-2} day^{-1}) that are orders of magnitude higher than adjacent ocean water primary productivity (0.01 to 0.65 g C m^{-2} day^{-1}) (*5*).

Energy requirements for calcification initially suggest that photosynthesis is a key driver of coral calcification rates (*5*); however, coral calcification depends on a broad range of environmental variables, including seawater temperature, seawater carbonate chemistry, light and depth, food availability, nutrients, water flow rates, sedimentation, and competition (*2*). Although laboratory experiments have successfully established relationships between coral calcification rates and independently altered environmental parameters (for example, temperature, light, pH, and seawater saturation state with respect to aragonite, $\Omega_A = [Ca^{2+}][CO_3^{2-}]/K_{sp}$), comparatively fewer studies have explored the combined effects and/or the relative importance of these parameters under controlled laboratory conditions (*6*, *7*) or under naturally variable in situ conditions (*2*, *8*–*11*). The ability to measure and establish the relative importance of different drivers of calcification in the field is limited by the capacity to adequately monitor relevant properties simultaneously for extended periods of time (*12*) and to decouple the range of highly correlated and interdependent interactions between environmental factors (Fig. 1) (*8*). For example, temperature not only directly influences coral calcification rates but also strongly controls seawater pH and Ω_A, which are both hypothesized to be independently important drivers of coral calcification (Fig. 1) (*13*). Temperature is also directly related to light availability and season, which affect coral calcification directly via light-enhanced calcification (Fig. 1) (*2*, *10*) and indirectly via increased food availability resulting from seasonal patterns in oceanic primary production (Fig. 1) (*2*, *14*). Characterizing the mechanisms and the relative importance of different drivers of coral calcification rates both in the current natural environment and under future ocean warming and acidification is essential for understanding how coral reefs calcify at present and for predicting how calcification rates and coral reef accretion will change under predicted near-future conditions.

The Bermuda coral reef is located at the northern limit of coral reefs in the North Atlantic Ocean (Fig. 1). Because of its relatively high latitude (32°N), Bermuda experiences greater seasonal differences and variations in environmental parameters than reefs located closer to the equator (*15*). Therefore, the Bermuda coral reef provides an excellent natural laboratory to explore the relationships between coral calcification rates and multiple environmental parameters. Over a 2-year period (August 2010 to September 2012), in situ environmental properties {temperature, seawater carbonate chemistry [dissolved inorganic carbon (DIC), total alkalinity (TA), partial pressure of CO_2 (P_{CO_2}), pH_{sw}, Ω_A], light, chlorophyll *a*, and inorganic nutrients} were characterized alongside coral calcification rates by two scleractinian reef-building

[1]Scripps Institution of Oceanography, University of California, San Diego, La Jolla, CA 92093, USA. [2]Christian-Albrechts-University Kiel, Kiel, Germany. [3]Bermuda Institute of Ocean Sciences, St. George's, Bermuda. [4]Department of Ocean and Earth Science, National Oceanography Centre Southampton, University of Southampton, Southampton, UK. [5]GEOMAR Helmholtz Center for Ocean Research, Marine Ecology/Food Webs, Kiel, Germany. [6]Pacific Marine Environmental Laboratory, National Oceanic and Atmospheric Administration, Seattle, WA 98115, USA.
*Corresponding author. Email: traviscourtney@gmail.com

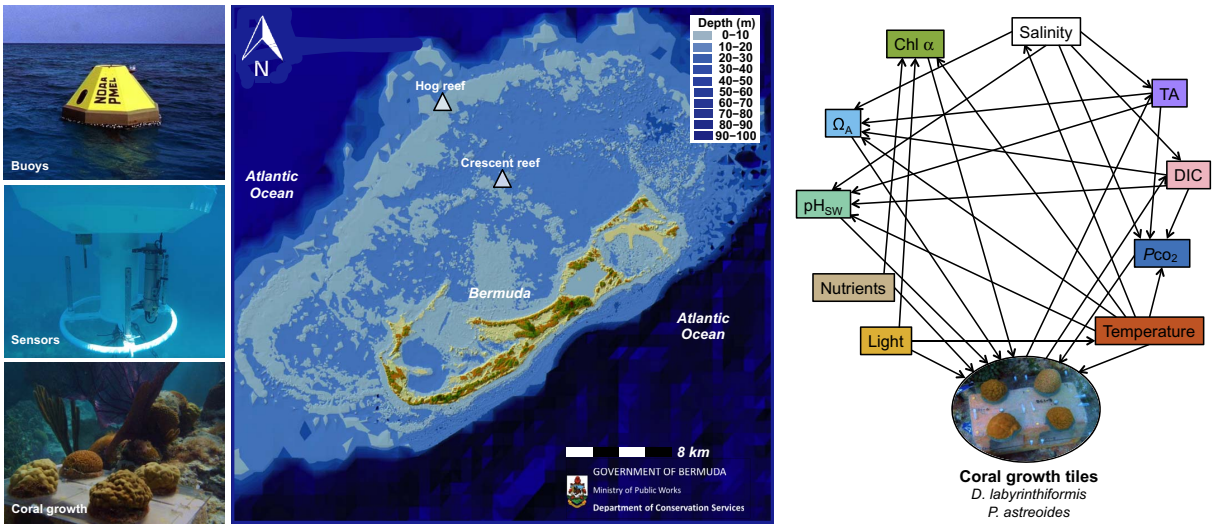

Fig. 1. Map of Bermuda study sites and environmental controls on calcification. The buoy, sensors, and in situ growth are presented next to a bathymetry map of Bermuda showing the locations of Hog Reef and Crescent Reef. Structural equation modeling (SEM) connections show the interactions between environmental drivers and their effect on coral calcification. Chl *α*, chlorophyll *a*. (The Bermuda Map is courtesy of M. Shailer of the Department of Conservation Services, Government of Bermuda.)

corals, *Porites astreoides* and *Diploria labyrinthiformis*, at two distinct reef environments. Colonies of *P. astreoides* and *D. labyrinthiformis* were transplanted onto tiles at a rim reef environment, Hog Reef, and an outer lagoon reef environment, Crescent Reef (n = 24 colonies per species per site; Fig. 1), and buoyant-weighed every 2 to 3 months to measure in situ calcification rates (*16*). In addition, net ecosystem calcification (NEC = gross calcification − gross $CaCO_3$ dissolution) for Hog Reef was calculated based on alkalinity anomalies (*17*) using monthly surface seawater TA samples and monthly offshore surface seawater TA from the Bermuda Atlantic Time-series Study (BATS) site (*18*) combined with estimates of seawater residence time (*19*). Assuming that calcification and $CaCO_3$ dissolution are the only processes significantly influencing salinity-normalized seawater TA, this variable serves as a direct proxy of NEC and changes in a ratio of 2:1 for every net mole of $CaCO_3$ deposited (*17*).

RESULTS

Observations of environmental controls and calcification

The data reveal a strong seasonal pattern in environmental variables and coral calcification rates over the 2-year study period (Fig. 2 and fig. S1). Light varied seasonally, with the lowest light intensity around January and the highest light intensity around June to July. Temperature lagged light intensity by 1 to 2 months, and maximum seawater temperatures were observed between August and October (Crescent Reef maximum temperature = 30.7° ± 0.1°C), whereas minimum seawater temperatures occurred from January to March (Hog Reef minimum temperature = 18.2° ± 0.1°C). Seasonal variability in seawater temperature and light was greater for Crescent Reef (Δ temperature = 12.4°C, Δ light = 13,500 lux) than for Hog Reef (Δ temperature = 11.9°C, Δ light = 6100 lux). Surface seawater Pco_2 was highest in the summer (Hog Reef maximum Pco_2 = 652 μatm), well exceeding equilibrium with the atmosphere, whereas pH_{sw} was lowest in the summer (Hog Reef minimum pH_{sw} = 7.93). The opposite trends were observed during winter (Hog Reef minimum Pco_2 = 303 μatm, maximum pH_{sw} = 8.14).

These observed seasonal variations in Pco_2 and pH_{sw} can mainly be explained by the seasonal variability in temperature (for example, warming explains 96 ± 3% of ΔPco_2 and 90 ± 3% of ΔpH_{sw} observed between 8 September 2010 and 25 February 2011). Seawater Ω_A did not follow a strong seasonal variation similar to Pco_2 and pH_{sw}, although minimum and maximum values were observed in the winter and summer, respectively, ranging from 3.09 to 3.93 at Hog Reef. Reef seawater DIC and TA were strongly depleted in the summer relative to offshore, reflecting the uptake of DIC and calcium used for reef-scale net organic carbon production and net calcification. Seasonal variability in seawater carbonate chemistry was greater for Hog Reef (ΔPco_2 = 349 μatm, ΔpH_{sw} = 0.22, $\Delta\Omega_A$ = 0.84) than for Crescent Reef (ΔPco_2 = 213 μatm, ΔpH_{sw} = 0.19, $\Delta\Omega_A$ = 0.70), primarily due to higher biomass relative to water volume driving greater reef metabolic effects on the water column at Hog Reef (that is, mean ± SE hard coral cover of 28 ± 1% versus 13 ± 1% at Crescent Reef) (*20*).

Notably, independently measured colony weight–normalized calcification rates of *P. astreoides* and *D. labyrinthiformis* colonies followed a similar seasonal variability with maximum rates observed from August to November and minimum rates observed from February to April. All forms of inorganic nitrogen, silica, and phosphorus remained low throughout the year but with occasional pulses (fig. S1). Monthly satellite chlorophyll *a* did not show strong seasonal variability at Hog Reef and Crescent Reef (fig. S1). Thus, maximum rates of both coral and reef-scale calcification appear to lag light intensity but coincide with maxima of seawater temperature, Pco_2, and Ω_A and minimum pH_{sw}. The seemingly paradoxical calcification maxima under seawater Pco_2 maximum and pH_{sw} minimum contradict the traditional understanding of the effects of seawater acidification on calcification (*13*), including a previous preliminary study conducted in the same area (*21*), but agree with recent studies that show that calcification can increase up to a threshold Pco_2 and pH if corals are adequately fed (*6*, *7*) or if Pco_2-pH conditions are within the natural variability experienced by the coral (*22*).

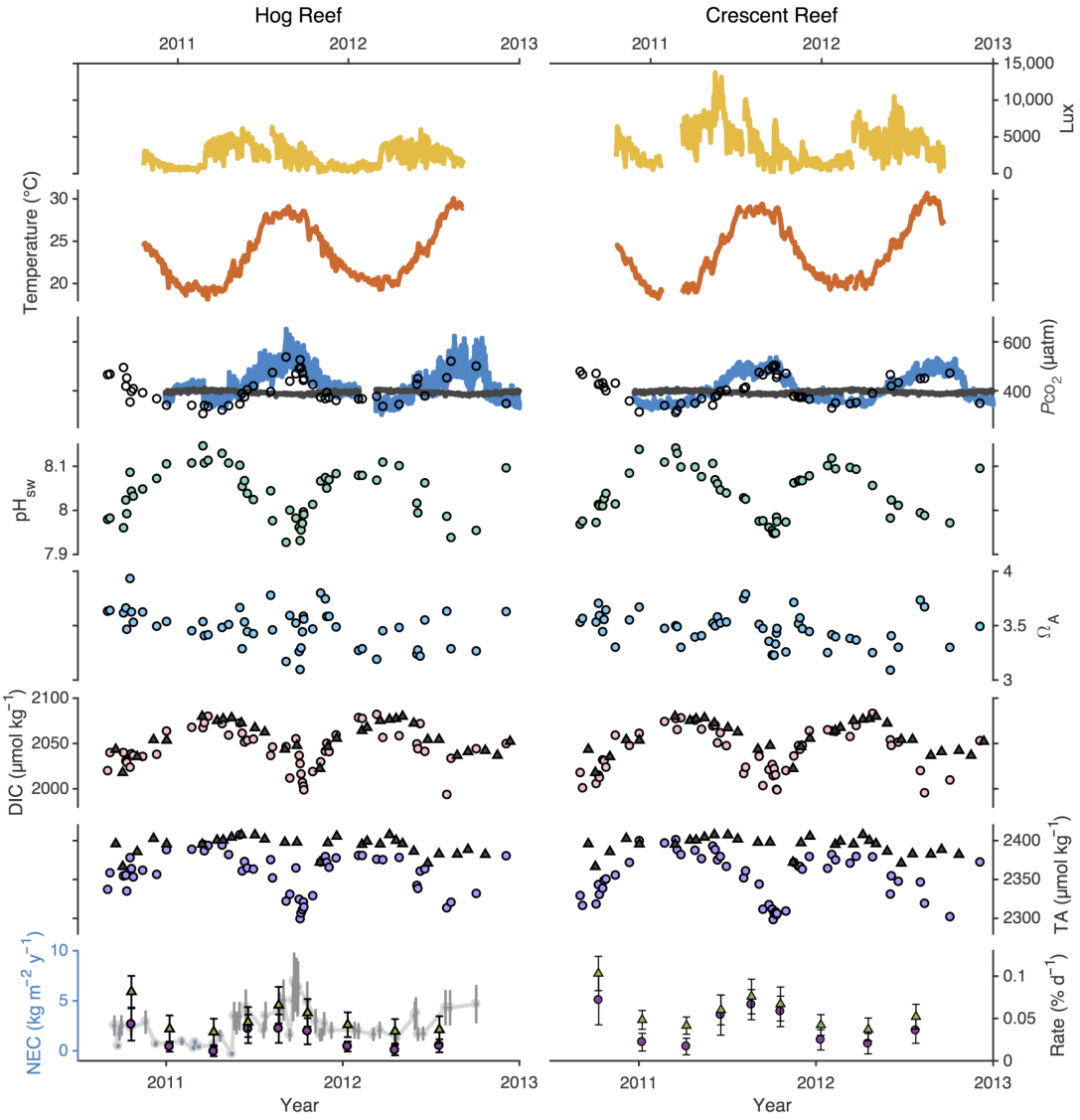

Fig. 2. Hog Reef and Crescent Reef environmental data and coral calcification rates. Both environmental parameters and calcification reveal strong seasonal trends in this high-latitude (32°N) coral reef system. For P_{CO_2} plots, blue denotes measured seawater P_{CO_2}, gray indicates measured atmospheric P_{CO_2}, and open circles represent seawater P_{CO_2} calculated from DIC and TA bottle samples. For TA and DIC plots, dark gray triangles represent BATS seawater DIC and TA, pink circles represent reef seawater DIC, and purple circles represent reef seawater TA. For the coral growth rate plots, purple circles represent *P. astreoides* and green triangles represent *D. labyrinthiformis* each with ±1 SD. Gray circles with the blue axis represent calculated NEC ± uncertainty.

Evaluating the relative importance of environmental controls on calcification

In an attempt to evaluate the relative importance and the interactive effects between environmental variables on colony and reef-scale calcification rates (Fig. 1), an SEM (Structural Equation Modeling) approach was used (*23*). This approach numerically solves the complex interactions between biotic and abiotic drivers of calcification to quantify both the direct and indirect effects of the measured environmental parameters on coral calcification. The model estimate for each reef driver (that is, temperature, pH_{sw}, Ω_A, P_{CO_2}, light, nutrients, and chlorophyll *a*) represents the change in SDs in calcification explained for each SD increase in reef driver (Fig. 3 and table S1). Temperature was the only variable with significant model estimates for both species at both reef sites and NEC at Hog Reef and yielded the greatest per-SD change in coral calcification rates with calcification across the five models, increasing by 2.1 to 4.3 SDs for a single SD increase in temperature. Compared to temperature, the model estimates for the other environmental parameters (pH_{sw}, Ω_A, P_{CO_2}, light, nutrients, and chlorophyll *a*) yielded smaller per-SD changes and failed to yield significant predictors for all five models (Fig. 3 and table S1). Notably, seawater pH_{sw} and Ω_A

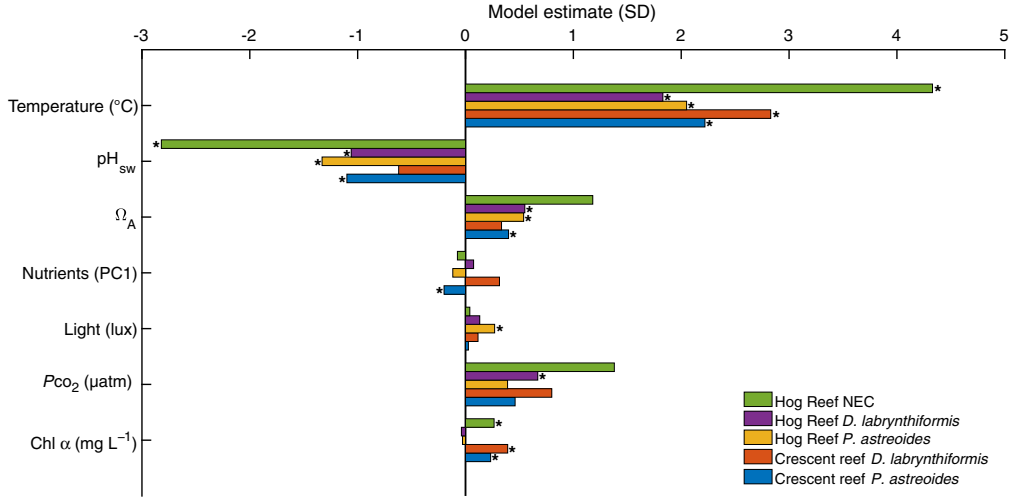

Fig. 3. Model estimates from the structural equation models. Each model estimate represents the SD change in calcification driven by a 1 SD increase in the given environmental parameter. Statistically significant model estimates ($P < 0.05$) are marked by stars.

produced significant predictors of calcification, but with pH_{sw} yielding significant, negative predictors of calcification (that is, decreasing pH is correlated with increasing calcification; see subsequent discussion) for four of the five SEM models at approximately one-half of the main effect of temperature (Fig. 3 and table S1). Chlorophyll *a* produced small but significant predictors of coral calcification at Crescent Reef and NEC at Hog Reef, whereas light, Pco_2, and nutrients each failed to yield significant predictors of calcification for more than one of the SEM models (Fig. 3 and table S1).

Because of the narrow range of Ω_A seasonal variability and highly coupled seawater pH and temperature observed during the in situ study, we performed an additional mesocosm experiment to further explore the effects of seawater carbonate chemistry on coral calcification. This mesocosm experiment was run in parallel with the in situ incubations for 3 months of the full 2-year in situ experiment using the same coral species and at three different seawater pH_{sw} conditions (mean pH_{sw} ± SD = 8.0 ± 0.1, 7.8 ± 0.1, and 7.6 ± 0.1). Linear models for the calcification rates of *P. astreoides* and *D. labyrinthiformis* failed to yield significant correlations between coral calcification rates and reduced seawater pH_{sw} (7.6 ± 0.1) or Ω_A (1.5 ± 0.5) relative to ambient conditions, when food was available (table S3). This finding adds to the growing literature finding that heterotrophy confers resistance to coral calcification under acidified conditions (*7*, *14*). In contrast, coral calcification rates during the mesocosm experiment appeared more strongly correlated with temperature, lending support to the findings from the 2-year in situ experiment that seasonal calcification rates of *P. astreoides* and *D. labyrinthiformis* from Bermuda are more strongly controlled by seawater temperature when adequate nutrition is available (*14*).

Predicting future coral reef calcification

To evaluate the effect of future warming on Bermudan *P. astreoides* and *D. labyrinthiformis* coral calcification rates, data from Coupled Model Intercomparison Project Phase 5 (CMIP5) multimodel climate simulations (*24*) using representative concentration pathways (RCPs) of +2.6, +4.5, +6.0, and +8.5 W m^{-2} radiative forcing relative to preindustrial levels (*25*) were used to simulate sea surface temperature (SST) warming rates over the 21st century in Bermuda (Fig. 4). Linear regressions of the CMIP5 model SST predictions relative to a +0.1°C $decade^{-1}$ rate of warming previously observed to increase calcification in high-latitude *Porites* corals (*26*) show that only the most conservative emissions pathway, RCP 2.6, yields a rate of warming (+0.05°C $decade^{-1}$) less than +0.1°C $decade^{-1}$, suggesting that coral calcification rates could continue to increase in Bermuda under this emissions pathway (Fig. 4A). The +0.4°C end-of-21st-century seawater warming predicted for Bermuda under RCP 2.6 was combined with linear calcification responses to temperature for *P. astreoides*, *D. labyrinthiformis*, and Hog Reef NEC from the 2-year in situ study to predict potential changes in calcification rates under this reduced emissions pathway. Assuming that these relationships remain fixed over the coming century, no thermal optima are exceeded, and other environmental controls remain constant, the models suggest that *P. astreoides* and *D. labyrinthiformis* could increase by ~2 to 4% and Hog Reef NEC could increase by ~6%. The onset of coral bleaching typically occurs when warming equates to a degree heating month (DHM), wherein monthly mean SSTs exceed the maximum monthly mean climatology by 1°C with more extreme bleaching and coral mortality occurring for an annual accumulation of two DHMs (*27*). The CMIP5 maximum summer temperatures relative to the time period 2006–2016 show that RCP 2.6 is the only emissions scenario in which Bermudan corals are predicted to escape regular, severe coral bleaching by the end of the century on the basis of the static 1°C DHM bleaching threshold (Fig. 4B).

DISCUSSION

The positive effects of temperature, Ω_A, and chlorophyll *a* (assuming this serves as a proxy for available coral nutrition) on coral calcification rates are consistent with previous laboratory and field studies (*2*, *6*, *7*, *10*–*13*), whereas the lack of correlation with light and the predicted positive effects owing to decreasing pH are inconsistent with anticipated results (*2*, *10*, *13*, *28*). However, one has to remain circumspect about these results because the SEM is not able to elucidate functional relationships and is most likely unable to decouple the dominant

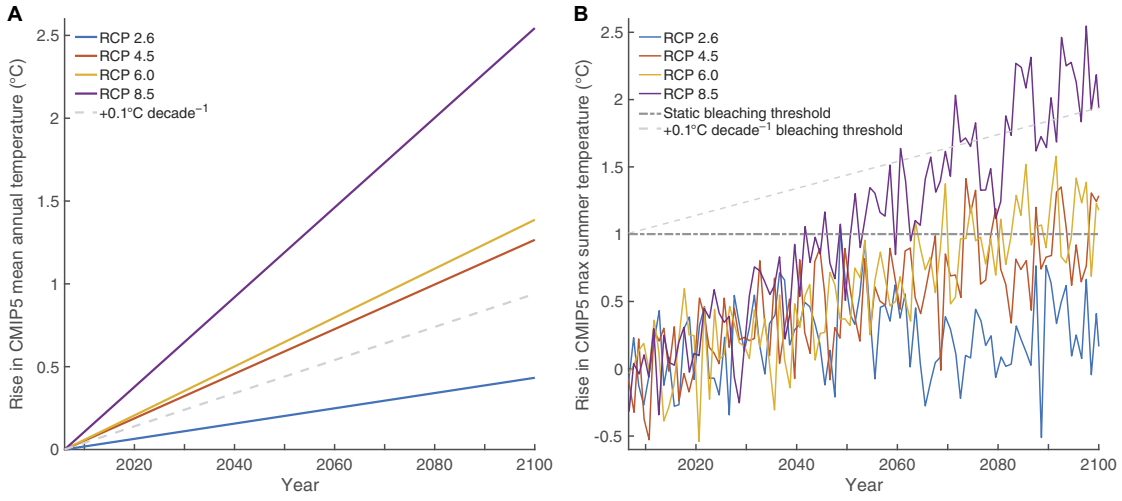

Fig. 4. Climate model projections for Bermuda. Monthly CMIP5 model SST data were aggregated for Bermuda under RCP emissions pathways. (**A**) Mean rise in monthly SSTs predicted for Bermuda until 2100. The dashed line represents the +0.1°C decade^{-1} rate of potential coral acclimatization based on increasing calcification rates observed in 20th-century East Indian Ocean *Porites* coral cores (*25*). (**B**) Rise in maximum summer temperatures for each RCP emissions pathway relative to the 1°C coral bleaching threshold above maximum summer 2006–2016 model climatology assuming no acclimatization (Static Bleaching Threshold) and assuming a +0.1°C decade^{-1} acclimatization rate.

effects of temperature on calcification rates and pH/Ω_A from the potentially subtler effects of these carbonate chemistry parameters on calcification (*9*). Also, time lags between determinant properties and response variables, such as light intensity and calcification, could muddle the predictive capacity of different variables.

The temperature-induced control and seasonal increase of *P. astreoides* and *D. labyrinthiformis* coral calcification rates observed here partly agree with previous laboratory experiments and field observations, which suggest that calcification has a parabolic response to increasing seawater temperature (*2*, *12*). In contrast, the present NEC and in situ calcification data appear to increase across the full range of seasonal temperatures, thereby suggesting that the thermal optima of the parabolic temperature–calcification response curves have not been exceeded during the 2-year study (*2*). Note that the in situ calcification responses to temperature may in part be affected by the coarse temporal resolution of calcification measurements (2- to 3-month skeletal growth intervals) relative to the time scales for summer seawater temperature maxima but that NEC measurements in this study reflect temperature responses over the much shorter multiday seawater residence times at Hog Reef (*19*). Irrespective of this, the temperature correlations in this study suggest that peak summer seawater temperatures are not limiting calcification via thermal stress and, instead, that calcification rates are more strongly limited by cooler winter seawater temperatures (*15*). This implies that Bermudan *P. astreoides* and *D. labyrinthiformis* coral calcification rates may increase with gradual ocean warming as has been suggested based on the analysis of interannual calcification rates from coral cores for other high-latitude coral reef environments (*2*). For example, a +0.1°C decade^{-1} rate of warming yielded a 23.7% increase in calcification rates for high-latitude (28°C) *Porites* corals in the Houtman Abrolhos Islands off the coast of Western Australia over a 110-year period (*26*). Conversely, the slopes of the calcification responses to temperature in this study suggest only a ~2 to 4% increase in coral calcification rates due to the +0.05°C decade^{-1} warming in Bermuda predicted for RCP 2.6. This potential increase is much lower than the +23.7% previously observed by Cooper *et al.* (*26*), suggesting that further research should be conducted to understand the mechanisms of coral calcification responses owing to gradual ocean warming (that is, ≤+0.1°C decade^{-1}) and to bridge the varying insights gained from conducting laboratory experiments, in situ growth experiments, and interannual coral coring studies.

However, the benefits of gradual future warming must be weighed against the reduced calcification and potential mortality owing to coral bleaching (*2*, *10*–*12*). For example, note that, following the coring study of Cooper *et al.* (*26*), an anomalous +5°C heat wave in 2010–2011 caused coral bleaching in the Houtman Abrolhos Islands, with 22 ± 2.7% (mean ± SE) of corals bleached and a corresponding 11.3 ± 6.9% (mean ± SE) decline in overall coral cover (*29*). In Bermuda, there are no recorded widespread bleaching-induced mortalities, reductions in coral cover, or changes in coral community composition, but there have been some observations of coral diseases and periodic mild coral bleaching since 1988 (≤20% of some coral species bleached) followed by subsequent post-bleaching recovery (*15*). It remains unclear whether the absence of extreme bleaching events in Bermuda is due to Bermudan reefs thus far escaping intense thermal stress events or resisting thermal stress through adaptation or acclimation [for example, see discussion of Great Barrier Reef bleaching patterns in the study of Hughes *et al.* (*30*)]. On the basis of the 1°C DHM static bleaching threshold (*27*) and the CMIP5 climate data for Bermuda, no frequent, severe bleaching is predicted for Bermudan *P. astreoides* and *D. labyrinthiformis* corals under RCP 2.6 (Fig. 4B). However, given the recent history of mild coral bleaching events (≤20% of some coral species bleached) in Bermuda (*15*), it is likely that mild bleaching may continue in the 21st century unless Bermudan corals adapt or acclimate to these mild thermal stress events. Nonetheless, the gradual warming and absence of predicted 21st-century frequent, severe coral bleaching under RCP 2.6 in this analysis support the hypothesis that Bermudan *P. astreoides* and *D. labyrinthiformis* calcification rates could increase under RCP 2.6 throughout the 21st century with continued adequate nutrition.

However, a recent integrated assessment model utilizing recent estimates for fossil fuel resources found a 100% likelihood of exceeding

warming provided by RCP 2.6, 92% for RCP 4.5, 42% for RCP 6.0, and 12% for RCP 8.5 (*31*). The Paris Agreement came into effect in November 2016 following this likelihood analysis, providing an alternative pathway for individual signatory countries to collectively reduce CO_2 emissions to limit global warming to well below 2°C above preindustrial levels. A 150% greater commitment to reduce CO_2 emissions by the current signatory countries before 2030 would yield a warming equivalent to RCP 4.5, resulting in drastically improved predicted global coral reef futures (*32*). Although it is less likely for Bermuda coral calcification to increase under the warming provided by RCP 4.5 (Fig. 4A), it could provide a pathway for Bermudan *P. astreoides* and *D. labyrinthiformis* corals to avoid regular severe bleaching until after 2070 (Fig. 4B), assuming no increases in coral acclimatization to future warming. Yet, there is uncertainty whether Bermudan corals can acclimatize to warming at rates faster, or slower, than the +0.1°C decade^{-1} rate from the study of Cooper *et al.* (*26*). However, a +0.1°C decade^{-1} increase in bleaching threshold could enable Bermudan corals to avoid regular severe bleaching in the 21st century under the RCP 2.6, 4.5, and 6.0 emissions pathways (Fig. 4B). In the absence of regular severe bleaching, the RCP 4.5 warming scenario therefore suggests that Bermudan *P. astreoides* and *D. labyrinthiformis* corals could maintain positive calcification at least until 2070 (Fig. 4B) with acclimatization rates of +0.1°C decade^{-1} extending this beyond the end of the 21st century (Fig. 4B). However, note that net reef calcification and the maintenance of coral reef structure additionally depend on $CaCO_3$ dissolution and bioerosion processes, which are predicted to increase under ocean acidification (*33*). The calcification projections for the 21st century in this study assume that available coral nutrition remains adequate to maintain the insensitivity of adult *P. astreoides* and *D. labyrinthiformis* colonies to ocean acidification [as observed in the present mesocosm experiment and in previous studies (*6*, *7*)] and that corals are able to successfully recruit despite the potential for negative effects of ocean acidification on scleractinian coral settlement and early life stages (*34*). This highlights the need for reducing CO_2 emissions to lessen ocean acidification impacts on Bermudan coral reef $CaCO_3$ dissolution to maintain net positive reef calcification over the coming century.

Every scleractinian species comprising the reef calcification budget for Hog Reef (*D. labyrinthiformis*, *P. astreoides*, *Pseudodiploria strigosa*, *Favia fragum*, *Madracis decactis*, *Montastrea cavernosa*, and *Orbicella franksi*) (*35*) is categorized as having either weedy, generalist, or stress-tolerant life histories; such species are hypothesized to be better adapted to ocean warming and acidification than faster-growing architecturally complex corals with competitive life histories (for example, *Acropora*) (*36*). The high natural variability of the Bermudan coral reef environment documented in this study (Crescent Reef annual Δ seawater temperature = 12.4°C) may provide elevated thermal tolerance to corals (*37*) and annually variable pH_{sw} (Hog Reef annual ΔpH_{sw} = 0.22) may explain the lack of sensitivity of coral calcification for adequately fed corals to predicted end-of-century ocean acidification observed in the mesocosm experiments of this study. High Bermudan coral genetic variability and population connectivity with the Caribbean may additionally increase the resilience of Bermudan coral populations during and after potential future ecological disturbances (*38*), with the deep reefs of Bermuda providing an additional refuge for select coral species (*39*). The combination of these factors and legislation protecting Bermudan coral reefs from local anthropogenic stressors (*40*) confer additional resiliency to this stress-tolerant coral community under current and predicted end-of-century warming and acidification. Bermudan coral reefs have maintained a relatively constant stress-tolerant, weedy, and generalist coral community composition (table S2) (*35*, *41*) and high coral cover (*40*) at least since 1980, further highlighting the resilience of Bermudan coral reefs and suggesting that reef calcification has also remained constant. That same time period in the Caribbean was characterized by declining coral cover and coral community shifts from competitive, structurally complex, and fast-growing *Acropora* corals to stress-tolerant, weedy, and generalist corals (*36*), driving basin-wide reductions in structural complexity (*42*) and net coral reef calcification (*43*).

These findings that Caribbean coral communities are shifting toward stress-tolerant life histories resembling the current community composition of Bermudan coral reefs suggest that a Bermuda-type coral reef system is one of many potential future stable states for coral reefs in the Caribbean and elsewhere. Characterized by anomalously high coral cover (*40*) and net positive reef calcification (*35*), coral reef systems resembling those of Bermuda may provide greater ecological resilience to 21st-century climate change and the maintenance of ecosystem services that these reef systems provide to humanity. This potentially brighter than previously predicted future for Bermudan and Caribbean coral reefs depends on mitigating other local-scale stressors (for example, overfishing and impacts of increasing human populations) (*40*) coupled with a continued global commitment to rapidly and drastically reducing CO_2 emissions to lessen the impacts of ocean warming and acidification.

MATERIALS AND METHODS

In situ coral calcification

Twenty-four colonies each of *P. astreoides* and *D. labyrinthiformis* were collected from Hog Reef and Crescent Reef, Bermuda, for a total of 96 coral colonies and mounted onto acrylic tiles using Z-SPAR A-788 epoxy. Twelve colonies of each species were deployed at two locations on both a rim reef site, Hog Reef, and an outer lagoon reef site, Crescent Reef, over a 2-year period (September 2010 to September 2012 at Hog Reef and August 2010 to September 2012 at Crescent Reef). Buoyant weights of each colony (*16*) were measured in triplicate and averaged at the end of each 2- to 3-month growth interval using a correction term for seawater density at the time of measurement and subtraction of the weight of both tile and epoxy to determine calcification as the change in weight during each growth interval. Mean initial weights (±SD) for *P. astreoides* were 433 ± 112 g and 372 ± 73 g at Hog Reef and Crescent Reef, respectively, and for *D. labyrinthiformis*, the corresponding values were 345 ± 109 g and 379 ± 83 g.

Carbonate chemistry

Carbonate chemistry samples for Hog Reef and Crescent Reef were collected monthly or more frequently using a 5-liter Niskin bottle at a depth of 0.5 to 1.0 m, according to best practices (*44*). Offshore samples were collected monthly as part of the BATS (*18*). Samples for DIC and TA were collected in 200-ml Kimax glass sample bottles, fixed using 100 μl of saturated solution of $HgCl_2$. Reef samples of TA were analyzed via closed-cell potentiometric titrations using a Versatile INstrument for the Determination of Titration Alkalinity 3S (VINDTA 3S) system, whereas BATS samples were analyzed on a VINDTA 2S (Marianda). DIC was analyzed using coulometric methods on a VINDTA 3C or infrared-based analysis on an Automated Infra Red Inorganic Carbon Analyzer (AIRICA) system (Marianda). The accuracy and precision of TA and DIC analyses were verified against certified reference material (CRM) provided by the laboratory of A. Dickson of the Scripps Institution of Oceanography. Analysis of replicate CRMs yielded a typical

accuracy and precision of ±1 to 2 μmol/kg for both TA and DIC. A YSI 556 Handheld Multiparameter Instrument was used to measure in situ temperature (accuracy, ±0.15°C) and salinity (accuracy, ±1%), and an Autosal Salinometer (accuracy, <0.002) was preferentially used when available to measure salinity for 66% of all bottle samples at Hog Reef and Crescent Reef. The complete carbonate system parameters (that is, pH_{sw}, P_{CO_2}, and Ω_A) were calculated using the program CO2SYS for Excel (*45*) and MATLAB (*46*) using the K_1 and K_2 dissociation constants from the study of Mehrbach *et al.* (*47*) refit by Dickson and Millero (*48*), K_{HSO4} from Dickson (*49*), and pH on the seawater scale. Estimated uncertainties for calculated carbonate system parameters from the study of Millero (*50*) were used. Seawater and atmospheric P_{CO_2}, temperature, salinity, and atmospheric pressure were measured autonomously every 3 hours by the National Oceanic and Atmospheric Administration Pacific Marine Environmental Laboratory (PMEL) $MAPCO_2$ (Moored Autonomous P_{CO_2}) moorings stationed at Hog Reef and Crescent Reef. Each mooring used a Batelle Memorial Institute CO_2 system to measure the mole fraction of CO_2 and a Sea-Bird 16plus v2 to measure temperature and salinity (*51*).

Net ecosystem calcification

TA for Hog Reef and BATS bottle samples was normalized to the mean measured Hog Reef salinity of 36.59 g kg^{-1}. BATS bottle samples were linearly interpolated to match the sampling times at Hog Reef for analysis of NEC in this study. NEC was calculated for Hog Reef during the 2-year study interval and represents the net balance between calcification and $CaCO_3$ dissolution for a well-mixed water column, as per the following equation (*52*)

$$\mathrm{NEC} = \frac{\rho z(\mathrm{TA}_{\mathrm{offshore}} - \mathrm{TA}_{\mathrm{reef}})}{2\tau} \quad (1)$$

where ρ is seawater density calculated from temperature, salinity, and pressure at the time of sampling using the TEOS-10 Gibbs Seawater oceanographic toolbox (*53*); z is the mean ± SD water column depth of 10.3 ± 3.3 m calculated for Hog Reef (*35*); $TA_{offshore}$ is the monthly interpolated BATS salinity normalized TA bottle sample data; TA_{reef} is the approximately monthly Hog Reef salinity normalized TA bottle sample; and τ is the mean ± SD seawater residence time (2.5 ± 0.4 days) calculated using a multitracer approach at the nearby North Rock rim reef site (*19*).

Environmental parameters

Daily averages of temperature (°C) and light (lux) for Hog Reef and Crescent Reef were obtained from averaging four onset HOBO Pendant data loggers deployed at each reef site. Hog Reef lux data were not available for the 15, 22, and 25 September 2010 and 19 October 2010 measurements of Hog Reef NEC. A linear model constructed in MATLAB between daily Hog Reef light data and fall 2010 Bermuda Weather Service hours of sunlight [lux ± SE = 146 ± 21 × (hours of sunlight) + 547 ± 137, $R^2 = 0.394$, $P < 0.001$, degrees of freedom (df) = 71, $F = 46.08$] was used to predict in situ Hog Reef lux data for the missing values. Monthly satellite chlorophyll *a* (mg $liter^{-1}$) for the reef sites was obtained by interpolating daily chlorophyll *a* measurements from the 4-km-resolution Moderate Resolution Imaging Spectroradiometer chlorophyll *a* product. Seawater nutrient samples were taken approximately monthly and according to best practices. Nutrient samples were filtered using a 0.4-μm filter and immediately frozen in opaque plastic bottles until processing at the Woods Hole Oceanographic Institution Nutrient Analytical Facility. All samples were analyzed on a SEAL AutoAnalyzer 3 four-channel segmented flow analyzer using approved U.S. Environmental Protection Agency methods for ammonium (method G-171-96; detection limit 0.034 μM), nitrite + nitrate (method G-172-96; detection limit 0.010 μM), silicate (method G-177-96; detection limit 0.016 μM), and phosphate (method G-297-03; detection limit 0.025 μM). Axis 1 of a principal components analysis (PCA) performed on the ammonium, nitrite + nitrate, silicate, and phosphate data was used as a bulk nutrient metric for parameterization of the SEM analysis.

Structural equation modeling

SEM was used to numerically solve the complex interactions between biotic and abiotic drivers of calcification to partition the direct and indirect effects of environmental drivers on calcification (*23*). All environmental data during the in situ coral growth monitoring at Hog Reef and Crescent Reef were monthly averaged to equally weight the data across the coral buoyant weight intervals. Coral growth was measured approximately every 2 to 3 months and was interpolated by a spline function with a cubic algorithm to link the data points and calculate monthly calcification rates so that it could be directly compared with the monthly averaged environmental data. Nutrients were synthesized by means of a standardized PCA. The first principal component was used as a proxy of nutrient variability and compared with the other environmental data. Because the Hog Reef NEC is based on a mean ± SD seawater residence time of 2.4 ± 0.4 days (*19*), environmental parameters that were as contemporaneous as possible to the NEC data were selected to yield the most accurate environmental parameters driving NEC. Parameters sampled at a lower resolution were interpolated to match NEC dates.

Thus, the SEM was performed on monthly averaged temperature, light, salinity, Ω_A, pH_{sw}, DIC, TA, P_{CO_2}, nutrients, and chlorophyll *a* drivers of *P. astreoides* and *D. labyrinthiformis* calcification rates, and approximately daily averages for Hog Reef NEC. The strength and sign of the links and quantification of the SEM were determined by simple and partial multivariate regression and Monte Carlo permutation tests (1000 replicates), whereas chi-square values were used to assess the fit of the overall path model (*54*). The individual path coefficients (that is, the partial regression coefficients) indicate the relationship between the causal and response variables. Significance levels for individual paths between variables were set at $\alpha = 0.05$. Structural equation models were run in Amos v.21 (IBM) (*55*).

Mesocosm seawater acidification experiment

The mesocosm experiments were conducted on *P. astreoides* and *D. labyrinthiformis* colonies (diameter, 12 to 16 cm) collected in July 2011 using a hammer and chisel from three Bermuda rim reef sites (near 32°26′N, 64°50′W; depth, 6 to 9 m) and exposed to three different seawater pH conditions (pH_{sw} = 8.0 ± 0.1, 7.8 ± 0.1, and 7.6 ± 0.1) in controlled mesocosms for 3 months. These experiments were conducted as part of a larger-scale yearlong mesocosm experiment, including a third coral species, *Madracis auretenra*, and testing for the additional effects of feeding on calcification responses to pH treatments.

After processing each colony with an initial weighing and cementing (Z-Spar A-788) onto a preweighed tagged acrylic tile, three colonies each of *P. astreoides* and *D. labyrinthiformis* were randomly assigned to each of nine experimental tanks (three replicate tanks per pH treatment). To account for possible tank effects, coral colonies were moved around within each tank once a week, and the tanks were scrubbed clean during this time. The buoyant weight technique (*16*) was applied approximately monthly to each coral to calculate the calcification rate for the duration of the experiment (fig. S2).

Seawater was pumped from a nearby inlet into header tanks that each fed into three replicated experimental tanks so that conditions could more closely mimic naturally fluctuating ambient reef conditions. The two reduced pH treatments were bubbled with additional CO_2 into the respective header tanks with P_{CO_2} controlled by rotameters (King Instrument) to simulate seawater acidification for those treatments. Each experimental tank had flow rates of 1.67 (±0.17) liter min^{-1}, yielding a ca. 42-min turnover time. Each tank was fed three times a week with a concentrated *Artemia* solution, resulting in approximate feeding concentrations of 1.8 mg $liter^{-1}$ for a 2-hour, no–flow-through period after sunset to allow corals to feed. Mesh light screens were used to protect the corals from the intense light of the shallow mesocosm tanks relative to the deeper in situ reef conditions. A YSI 556 multiparameter probe was calibrated according to standard protocols and used to monitor daily temperature, salinity, dissolved oxygen, and pH (fig. S2) with quantitative carbonate chemistry monitored by water samples analyzed for DIC, TA, and salinity. Carbonate chemistry samples were collected and analyzed, as described in the "Carbonate chemistry" section.

Before statistical analysis, all data were tested for equal variance and for normality (Kolmogorov-Smirnov test) in SigmaPlot v11 and were log-transformed (mg day^{-1} data) or arcsine square root–transformed (mg day^{-1} cm^{-2} data) if necessary. Mean calcification rates for each species per tank over each growth period were analyzed using two-way repeated measures analysis of variance (ANOVA) in SigmaPlot v11 with growth periods ($n = 4$) and tanks within treatment ($n = 3$) as fixed main effects. Significant interactions were further analyzed with multiple comparison procedures (Holm-Sidak method). Regression analysis was used to test for significant relationships between calcification rates and calculated carbon chemistry data, seawater temperature, and light.

Climate model predictions

The CMIP5 multimodel ensemble (*24*) was used in the analysis for 21st-century Bermuda SST predictions. Model output was generated by the NASA Goddard Institute for Space Studies model–run GISS-E2-H (2° latitude × 2.5° longitude 40-layer atmosphere coupled with HYbrid Coordinate Ocean Model 1° latitude × 1° longitude 26-layer ocean model) (*56*) using RCPs +2.6, +4.5, +6.0, and +8.5 W m^{-2} relative to preindustrial levels (*25*). Monthly SST data from the four closest points surrounding Bermuda were averaged to obtain mean changes in warming anticipated for Bermuda. Linear models were fit through the monthly SST data to determine a mean rate of SST increase for the 21st century under RCP 2.6 (+0.05°C $decade^{-1}$, $P = 0.059$, df = 1138, $F = 3.57$), RCP 4.5 (+0.13°C $decade^{-1}$, $P < 0.0001$, df = 1138, $F = 29.8$), RCP 6.0 (+0.15°C $decade^{-1}$, $P < 0.0001$, df = 1138, $F = 36$), and RCP 8.5 (+0.27°C $decade^{-1}$, $P < 0.0001$, df = 1138, $F = 120$). These rates were compared to the +0.1°C $decade^{-1}$ warming-induced calcification increases observed by Cooper *et al.* (*26*) for 20th-century massive *Porites* corals in the East Indian Ocean (28°S). Because the RCP 2.6 emissions scenario predicted a rate of warming less than the +0.1°C $decade^{-1}$ from the study of Cooper *et al.* (*26*), only that emissions scenario was used to predict potential increases in coral calcification rates in Bermuda. Single-variable linear calcification responses to temperature were constructed for *P. astreoides* (Hog Reef: slope = 0.0027% $day^{-1}°C^{-1}$, $P = 0.0003$, df = 23, $F = 17.8$; Crescent Reef: slope = 0.0035% $day^{-1}°C^{-1}$, $P = 0.0002$, df = 22, $F = 20.2$), *D. labyrinthiformis* (Hog Reef: slope = 0.0026% $day^{-1}°C^{-1}$, $P = 0.0006$, df = 23, $F = 15.9$; Crescent Reef: slope = 0.0023% $day^{-1}°C^{-1}$, $P = 0.02$, df = 22, $F = 6.1$), and Hog Reef NEC (slope = 0.42 kg m^{-2} $year^{-1}°C^{-1}$, $P < 0.001$, df = 44, $F = 50.4$). The slopes of these calcification responses per degree Celsius were multiplied by the +0.4°C predicted for end-of-21st-century Bermuda from mean RCP 2.6 warming rates to estimate potential warming-induced increases in calcification. The maximum monthly SST for each year was extracted from the output of each climate model to compare to coral bleaching thresholds. Coral bleaching is predicted to occur during a DHM in which monthly maximum summer SSTs are 1°C above mean maximum summer climatology, with an annual accumulation of two DHMs being a predictor of extreme coral bleaching and mortality (*27*). The first 10 years of CMIP5 maximum monthly summer SST model output (2006–2016) were averaged to approximate a mean maximum summer climatology used in calculating a relative DHM for the future warming. The difference between the summer model output and this mean maximum summer climatology was plotted to determine when maximum summer SSTs are expected to exceed the DHM of 1°C with and without a +0.1°C $decade^{-1}$ acclimatization rate, respectively, under RCPs 2.6, 4.5, 6.0, and 8.5.

SUPPLEMENTARY MATERIALS

Supplementary material for this article is available at http://advances.sciencemag.org/cgi/content/full/3/11/e1701356/DC1

fig. S1. Hog Reef and Crescent Reef environmental data for salinity, nutrients, and satellite chlorophyll *a*.

fig. S2. Mesocosm seawater acidification experiment data.

table S1. Model estimates from the structural ecosystem models.

table S2. Bermuda coral community composition.

table S3. Mesocosm seawater acidification experiment statistical summary.

REFERENCES AND NOTES

1. J. P. G. Spurgeon, The economic valuation of coral reefs. *Mar. Pollut. Bull.* **24**, 529–536 (1992).
2. M. S. Pratchett, K. D. Anderson, M. O. Hoogenboom, E. Widman, A. H. Baird, J. M. Pandolfi, P. J. Edmunds, J. M. Lough, Spatial, temporal and taxonomic variation in coral growth—Implications for the structure and function of coral reef ecosystems. *Oceanogr. Mar. Biol.* **53**, 215–296 (2015).
3. N. Knowlton, R. E. Brainard, R. Fisher, M. Moews, L. Plaisance, M. J. Caley, in *Life in the World's Oceans: Diversity, Distribution, and Abundance*, A. D. McIntyre, Ed. (Wiley-Blackwell, 2010), pp. 65–78.
4. G. D. Stanley Jr., Early history of scleractinian corals and its geological consequences. *Geology* **9**, 507–511 (1981).
5. B. G. Hatcher, Coral reef primary productivity: A beggar's banquet. *Trends Ecol. Evol.* **3**, 106–111 (1988).
6. K. D. Castillo, J. B. Ries, J. F. Bruno, I. T. Westfield, The reef-building coral Siderastrea siderea exhibits parabolic responses to ocean acidification and warming. *Proc. Biol. Sci.* **281**, 20141856 (2014).
7. E. K. Towle, I. C. Enochs, C. Langdon, Threatened Caribbean coral is able to mitigate the adverse effects of ocean acidification on calcification by increasing feeding rate. *PLOS ONE* **10**, e0123394 (2015).
8. A. McMahon, I. R. Santos, T. Cyronak, B. D. Eyre, Hysteresis between coral reef calcification and the seawater aragonite saturation state. *Geophys. Res. Lett.* **40**, 4675–4679 (2013).
9. A. Venti, A. Andersson, C. Langdon, Multiple driving factors explain spatial and temporal variability in coral calcification rates on the Bermuda platform. *Coral Reefs* **33**, 979–997 (2014).
10. J. M. Lough, N. E. Cantin, J. A. Benthuysen, T. F. Cooper, Environmental drivers of growth in massive *Porites* corals over 16 degrees of latitude along Australia's northwest shelf. *Limnol. Oceanogr.* **61**, 684–700 (2016).
11. J. M. Lough, N. E. Cantin, Perspectives on massive coral growth rates in a changing ocean. *Biol. Bull.* **226**, 187–202 (2014).
12. P. L. Jokiel, S. L. Coles, Effects of temperature on the mortality and growth of Hawaiian reef corals. *Mar. Biol.* **43**, 201–208 (1977).
13. K. Schneider, J. Erez, The effect of carbonate chemistry on calcification and photosynthesis in the hermatypic coral *Acropora eurystoma*. *Limnol. Oceanogr.* **51**, 1284–1293 (2006).
14. K. L. Yeakel, A. J. Andersson, N. R. Bates, T. J. Noyes, A. Collins, R. Garley, Shifts in coral reef biogeochemistry and resulting acidification linked to offshore productivity. *Proc. Natl. Acad. Sci. U.S.A.* **112**, 14512–14517 (2015).
15. S. R. Smith, S. Sarkis, T. J. T. Murdoch, E. Weil, A. Croquer, N. R. Bates, R. J. Johnson, S. de Putron, A. J. Andersson, Threats to coral reefs of Bermuda, in *Coral Reefs of the United*

Kingdom Overseas Territories, C. Sheppard, Ed. (Springer Science and Business Media, 2013), vol. 4, pp. 173–188.
16. P. L. Jokiel, J. E. Maragos, L. Franzisket, Coral growth: Buoyant weight technique, in *Coral Reefs: Research Methods*, D. R. Stoddardt, R. E. Johannes, Eds. (UNESCO,1978), pp. 529–541.
17. S. V. Smith, Carbon dioxide dynamics: A record of organic carbon production, respiration, and calcification in the Eniwetok reef flat community. *Limnol. Oceanogr.* **18**, 106–120 (1973).
18. N. R. Bates, M. H. P. Best, K. Neely, R. Garley, A. G. Dickson, R. J. Johnson, Detecting anthropogenic carbon dioxide uptake and ocean acidification in the North Atlantic Ocean. *Biogeosciences* **9**, 2509–2522 (2012).
19. A. Venti, D. Kadko, A. J. Andersson, C. Langdon, N. R. Bates, A multi-tracer model approach to estimate reef water residence times. *Limnol. Oceanogr. Methods* **10**, 1078–1095 (2012).
20. R. J. Jones, Bermuda Institute of Ocean Sciences (BIOS), Marine Environmental Program (MEP) Annual Report (2006–2007), submitted to the Bermuda Government Department of Environmental Protection, Ministry of the Environment (2006).
21. N. R. Bates, A. Amat, A. J. Andersson, Feedbacks and responses of coral calcification on the Bermuda reef system to seasonal changes in biological processes and ocean acidification. *Biogeosciences* **7**, 2509–2530 (2010).
22. H. C. Barkley, A. L. Cohen, D. C. McCorkle, Y. Golbuu, Mechanisms and thresholds for pH tolerance in Palau corals. *J. Exp. Mar. Biol. Ecol.* **489**, 7–14 (2017).
23. J. B. Grace, *Structural Equation Modeling and Natural Systems* (Cambridge Univ. Press, 2006).
24. K. E. Taylor, R. J. Stouffer, G. A. Meehl, An overview of CMIP5 and the experiment design. *Bull. Am. Meteorol. Soc.* **93**, 485–498 (2012).
25. R. H. Moss, J. A. Edmonds, K. A. Hibbard, M. R. Manning, S. K. Rose, D. P. van Vuuren, T. R. Carter, S. Emori, M. Kainuma, T. Kram, G. A. Meehl, J. F. B. Mitchell, N. Nakicenovic, K. Riahi, S. J. Smith, R. J. Stouffer, A. M. Thomson, J. P. Weyant, T. J. Wilbanks, The next generation of scenarios for climate change research and assessment. *Nature* **463**, 747–756 (2010).
26. T. Cooper, R. A. O'Leary, J. M. Lough, Growth of Western Australian corals in the anthropocene. *Science* **335**, 593–596 (2012).
27. S. D. Donner, W. J. Skirving, C. M. Little, M. Oppenheimer, O. Hoegh-Gulberg, Global assessment of coral bleaching and required rates of adaptation under climate change. *Glob. Chang. Biol.* **11**, 2251–2265 (2005).
28. S. V. Smith, F. Pesret, Processes of carbon dioxide flux in the Fanning Island lagoon. *Pac. Sci.* **28**, 225–245 (1974).
29. J. A. Y. Moore, L. M. Bellchambers, M. R. Depczynski, R. D. Evans, S. N. Evans, S. N. Field, K. J. Friedman, J. P. Gilmour, T. H. Holmes, R. Middlebrook, B. T. Radford, T. Ridgway, G. Shedrawi, H. Taylor, D. P. Thomson, S. K. Wilson, Unprecedented mass bleaching and loss of coral across 12° of latitude in Western Australia in 2010–11. *PLOS ONE* **7**, e51807 (2012).
30. T. P. Hughes, J. T. Kerry, M. Álvarez-Noriega, J. G. Álvarez-Romero, K. D. Anderson, A. H. Baird, R. C. Babcock, M. Beger, D. R. Bellwood, R. Berkelmans, T. C. Bridge, I. R. Butler, M. Byrne, N. E. Cantin, S. Comeau, S. R. Connolly, G. S. Cumming, S. J. Dalton, G. Diaz-Pulido, C. M. Eakin, W. F. Figueira, J. P. Gilmour, H. B. Harrison, S. F. Heron, A. S. Hoey, J.-P. A. Hobbs, M. O. Hoogenboom, E. V. Kennedy, C.-. Kuo, J. M. Lough, R. J. Lowe, G. Liu, M. T. McCulloch, H. A. Malcolm, M. J. McWilliam, J. M. Pandolfi, R. J. Pears, M. S. Pratchett, V. Schoepf, T. Simpson, W. J. Skirving, B. Sommer, G. Torda, D. R. Wachenfeld, B. L. Willis, S. K. Wilson, Global warming and recurrent mass bleaching of corals. *Nature* **543**, 373–377 (2017).
31. I. Capellán-Pérez, I. Arto, J. M. Polanco-Martínez, M. González-Eguino, M. B. Neumann, Likelihood of climate change pathways under uncertainty on fossil fuel resource availability. *Energy Environ. Sci.* **9**, 2482–2496 (2016).
32. R. van Hooidonk, J. Maynard, J. Tamelander, J. Gove, G. Ahmadia, L. Raymundo, G. Williams, S. F. Heron, S. Planes, Local-scale projections of coral reef futures and implications of the Paris Agreement. *Sci. Rep.* **6**, 39666 (2016).
33. B. D. Eyre, A. J. Andersson, T. Cyronak, Benthic coral reef calcium carbonate dissolution in an acidifying ocean. *Nat. Clim. Chang.* **4**, 969–976 (2014).
34. R. Albright, C. Langdon, Ocean acidification impacts multiple early life history processes of the Caribbean coral *Porites astreoides*. *Glob. Chang. Biol.* **17**, 2478–2487 (2011).
35. T. A. Courtney, A. J. Andersson, N. R. Bates, A. Collins, T. Cyronak, S. J. de Putron, B. D. Eyre, R. Garley, E. J. Hochberg, R. Johnson, S. Musielewicz, T. J. Noyes, C. L. Sabine, A. J. Sutton, J. Toncin, A. Tribollet, Comparing chemistry and census-based estimates of net ecosystem calcification on a rim reef in Bermuda. *Front. Mar. Sci.* **3**, 181 (2016).
36. E. S. Darling, L. Alvarez-Filip, T. A. Oliver, T. R. McClanahan, I. M. Côté, Evaluating life-history strategies of reef corals from species traits. *Ecol. Lett.* **15**, 1378–1386 (2012).
37. T. A. Oliver, S. R. Palumbi, Do fluctuating temperature environments elevate coral thermal tolerance? *Coral Reefs* **30**, 429–440 (2011).
38. J. M. Locke, K. A. Coates, J. P. Bilewitch, L. P. Holland, J. M. Pitt, S. R. Smith, H. G. Trapido-Rosenthal, Biogeography, biodiversity and connectivity of Bermuda's coral reefs, in *Coral Reefs of the United Kingdom Overseas Territories*, C. Sheppard, Ed. (Springer Science and Business Media, 2013), pp. 153–172.
39. Pim Bongaerts, Cynthia Riginos, Ramona Brunner, Norbert Englebert, Struan R. Smith, Ove Hoegh-Guldberg, Deep reefs are not universal refuges: Reseeding potential varies among coral species. *Sci. Adv.* **3**, e1602373 (2017).
40. J. B. C. Jackson, M. K. Donovan, K. L. Cramer, V. V. Lam, *Status and Trends of Caribbean Coral Reefs : 1970–2012* (Global Coral Reef Monitoring Network, IUCN, 2014).
41. R. E. Dodge, A. Logan, A. Antonius, Quantitative reef assessment studies in Bermuda: A comparison of methods and preliminary results. *Bull. Mar. Sci.* **32**, 745–760 (1982).
42. L. Alvarez-Filip, N. K. Dulvy, J. A. Gill, I. M. Côté, A. R. Watkinson, Flattening of Caribbean coral reefs: Region-wide declines in architectural complexity. *Proc. Biol. Sci.* **276**, 3019–3025 (2009).
43. C. T. Perry, G. N. Murphy, P. S. Kench, S. G. Smithers, E. N. Edinger, R. S. Steneck, P. J. Mumby, Caribbean-wide decline in carbonate production threatens coral reef growth. *Nat. Commun.* **4**, 1402 (2013).
44. A. G. Dickson, C. L. Sabine, J. R. Christian, *Guide to Best Practices for Ocean CO_2 Measurements* (PICES Special Publication, 2007), vol. 3, 191 pp.
45. E. Lewis, D. Wallace, *Program Developed for CO_2 System Calculations: Carbon Dioxide Information Analysis Center, Oak Ridge National Laboratory, ORNL/CDIAC-105* (US DOE, 1998).
46. S. Van Heuven, D. Pierrot, J. W. B. Rae, E. Lewis, D. W. R. Wallace, MATLAB program developed for CO_2 system calculations, ORNL/CDIAC-105b, Carbon Dioxide Inf. Anal. Cent., Oak Ridge Natl. Lab., US DOE, Oak Ridge, TN (2011).
47. C. Mehrbach, C. H. Culberson, J. E. Hawley, R. M. Pytkowicx, Measurement of the apparent dissociation constants of carbonic acid in seawater at atmospheric pressure. *Limnol. Oceanogr.* **18**, 897–907 (1973).
48. A. G. Dickson, F. J. Millero, A comparison of the equilibrium constants for the dissociation of carbonic acid in seawater media. *Deep Sea Res.* **34**, 1733–1743 (1987).
49. A. G. Dickson, Thermodynamics of the dissociation of boric acid in synthetic seawater from 273.15 to 318.15 K. *Deep Sea Res.* **37**, 755–766 (1990).
50. F. J. Millero, The marine inorganic carbon cycle. *Chem. Rev.* **107**, 308–341 (2007).
51. A. J. Sutton, C. L. Sabine, S. Maenner-Jones, N. Lawrence-Slavas, C. Meinig, R. A. Feely, J. T. Mathis, S. Musielewicz, R. Bott, P. D. McLain, H. J. Fought, A. Kozyr, A high-frequency atmospheric and seawater pCO_2 data set from 14 open-ocean sites using a moored autonomous system. *Earth Syst. Sci. Data.* **6**, 353–366 (2014).
52. C. Langdon, J.-P. Gattuso, A. Andersson, in *Guide to Best Practices for Ocean Acidification Research and Data Reporting*, U. Riebesell, V. Fabry, L. Hansson, J. Gattuso, Eds. (Office for Official Publications of the European Communities, 2010), pp. 213–232.
53. T. J. McDougall, P. M. Barker, *Getting Started with TEOS-10 and the Gibbs Seawater (GSW) Oceanographic Toolbox* (SCOR/IAPSO WG 127, 2011), 28 pp.
54. C. Alsterberg, J. S. Eklöf, L. Gamfeldt, J. N. Havenhand, K. Sundbäck, Consumers mediate the effects of experimental ocean acidification and warming on primary producers. *Proc. Natl. Acad. Sci. U.S.A.* **110**, 8603–8608 (2013).
55. J. L. Arbuckle. Amos (Version 21.0) [Computer Program]. Chicago: IBM SpSS (2014).
56. G. A. Schmidt, M. Kelley, L. Nazarenko, R. Ruedy, G. L. Russell, I. Aleinov, M. Bauer, S. E. Bauer, M. K. Bhat, R. Bleck, V. Canuto, Y.-H. Chen, Y. Cheng, T. L. Clune, A. Del Genio, R. de Fainchtein, G. Faluvegi, J. E. Hansen, R. J. Healy, N. Y. Kiang, D. Koch, A. A. Lacis, A. N. LeGrande, J. Lerner, K. K. Lo, E. E. Matthews, S. Menon, R. L. Miller, V. Oinas, A. O. Oloso, J. P. Perlwitz, M. J. Puma, W. M. Putman, D. Rind, A. Romanou, M. Sato, D. T. Shindell, S. Sun, R. A. Syed, N. Tausnev, K. Tsigaridis, N. Unger, A. Voulgarakis, M.-S. Yao, J. Zhang, Configuration and assessment of the GISS ModelE2 contributions to the CMIP5 archive. *J. Adv. Model. Earth Syst.* **6**, 141–184 (2014).

Acknowledgments: This project was made possible by the countless contributions by researchers, staff, volunteers, and interns at the Bermuda Institute of Ocean Sciences. We acknowledge the World Climate Research Programme's Working Group on Coupled Modelling for Coupled Model Intercomparison Project and thank the NASA Goddard Institute for Space Studies for producing and making their CMIP5 model output available. We thank F. Melin for extracting and providing the satellite chlorophyll *a* data. Additionally, we thank two anonymous reviewers for improving this manuscript with their constructive comments and feedback. This is PMEL contribution number 4705. **Funding:** This work was funded by National Science Foundation (NSF) OCE 09-28406 (to A.J.A., N.R.B., and S.J.d.P), NSF OCE 14-16518 (to A.J.A. and R.J.), and the NSF Graduate Research Fellowship Program (to T.A.C.). **Author contributions:** A.J.A., N.R.B., and S.J.d.P. designed the study. A.J.A., N.R.B., S.J.d.P., A.C., R.G., R.J., T.J.N., and C.L.S. conducted measurements and/or contributed data. T.A.C., A.J.A., M.L., and J.-C.M. analyzed the data and results. T.A.C. and A.J.A. wrote the manuscript with input from all coauthors. **Competing interests:** The authors declare that they have no competing interests. **Data availability:** All data needed to evaluate the conclusions in the paper are present in the paper and/or the Supplementary Materials. Additional data related to this paper may be requested from the authors. The data presented in this manuscript will be made available in the Biological and Chemical Oceanography Data Management Office database under the BEACON project (http://bco-dmo.org/project/2190).

Submitted 26 April 2017
Accepted 17 October 2017
Published 8 November 2017
10.1126/sciadv.1701356

Citation: T. A. Courtney, M. Lebrato, N. R. Bates, A. Collins, S. J. de Putron, R. Garley, R. Johnson, J.-C. Molinero, T. J. Noyes, C. L. Sabine, A. J. Andersson, Environmental controls on modern scleractinian coral and reef-scale calcification. *Sci. Adv.* **3**, e1701356 (2017).

Science Advances

AAAS

advances.sciencemag.org/cgi/content/full/3/11/e1701356/DC1

Supplementary Materials for

Environmental controls on modern scleractinian coral and reef-scale calcification

Travis A. Courtney, Mario Lebrato, Nicholas R. Bates, Andrew Collins, Samantha J. de Putron, Rebecca Garley, Rod Johnson, Juan-Carlos Molinero, Timothy J. Noyes, Christopher L. Sabine, Andreas J. Andersson

Published 8 November 2017, *Sci. Adv.* **3**, e1701356 (2017)
DOI: 10.1126/sciadv.1701356

This PDF file includes:

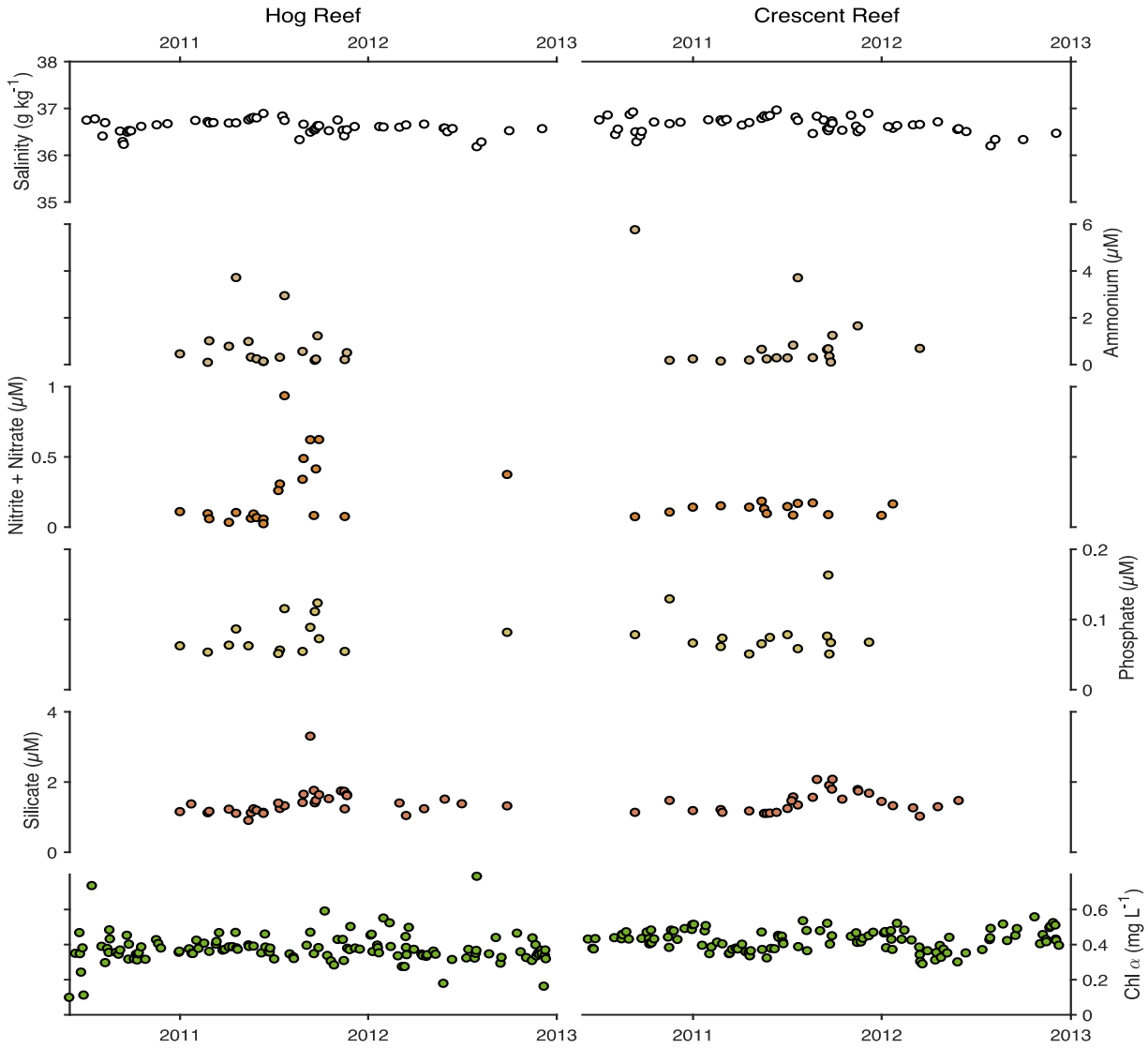

fig. S1. Hog Reef and Crescent Reef environmental data for salinity, nutrients, and satellite chlorophyll *a*. The data show stable salinity values, low-nutrients year-round, and a seasonal trend in Chl α in which Chl α is generally elevated year round and lowest in the summer months.

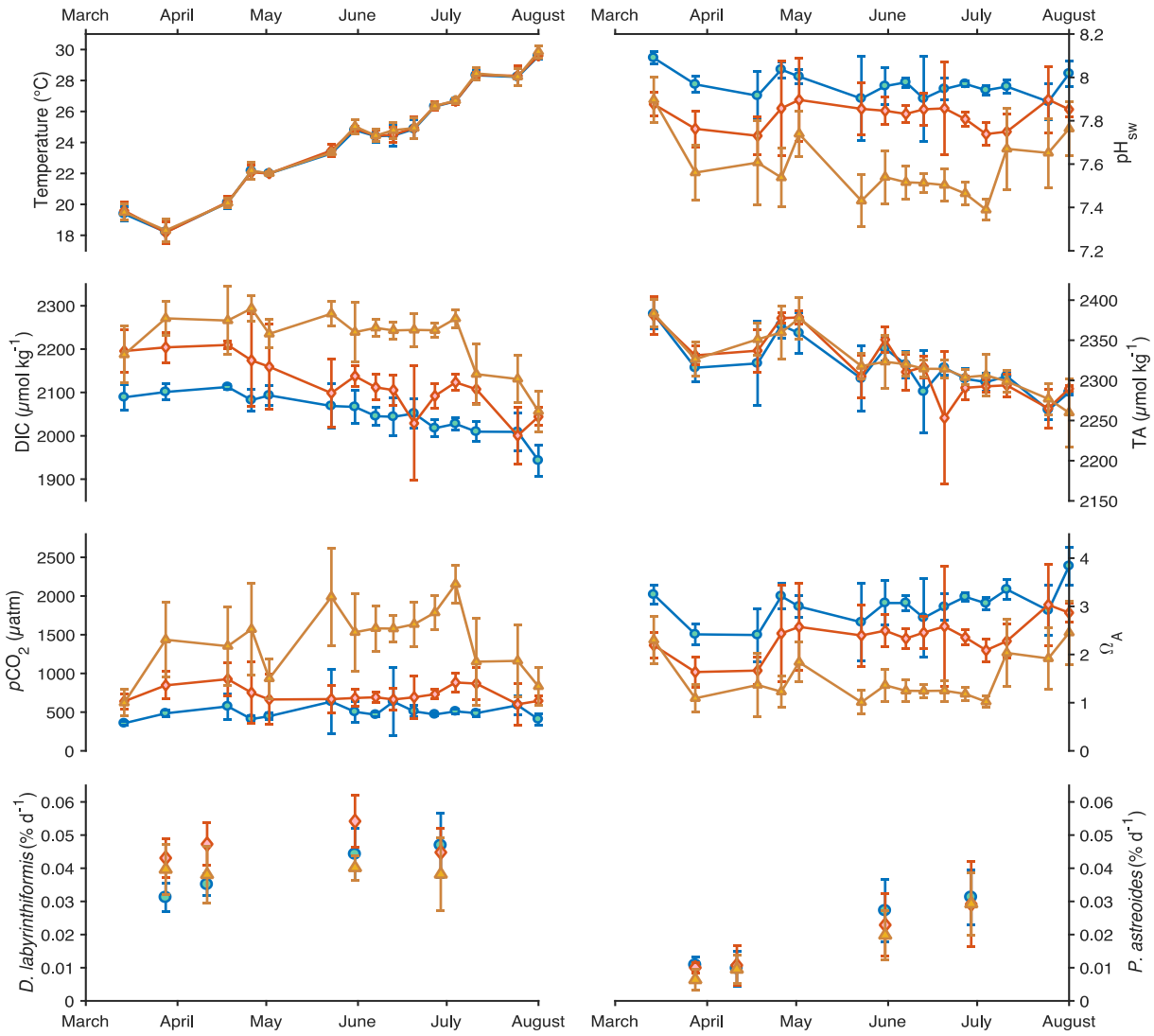

fig. S2. Mesocosm seawater acidification experiment data. Temperature, pH_{sw}, DIC, TA, pCO_2, Ω_A, *Diploria labyrinthiformis* calcification rates, and *Porites astreoides* calcification rates are plotted for the duration the three-month mesocosm seawater acidification experiment. For all plots, blue circles represent ambient 8.0±0.1 pH treatment, red diamonds represent 7.8±0.1 pH treatment, and yellow triangles represent 7.6±0.1 pH treatment. All points are means ± standard deviation for each treatment.

table S1. Model estimates from the structural ecosystem models. Model estimates are expressed for all the interactions between environmental parameters and drivers of calcification with standard error (S.E.) and p-values for Crescent Reef and Hog Reef *Porites astreoides* and *Diploria labyrinthiformis* and for Hog Reef Net Ecosystem Calcification. Each model estimate represents the standard deviation change in effect variable for a one standard deviation increase in driving variable. Below each set of model estimates are the results of the Chi-square test for fit of the SEM. All p-values significant at the $\alpha = 0.05$ level are in bold.

table S1 (A). Crescent Reef *Porites astreoides* SEM results.

Crescent Reef *Porites astreoides*

Variable	Link	Predictor	Estimate	S.E.	P
P. astreoides	←	Chl α	0.233	0.049	**<0.001**
P. astreoides	←	pCO_2	0.460	0.187	0.078
P. astreoides	←	Light	0.027	0.053	0.701
P. astreoides	←	Nutrients	-0.199	0.067	**0.009**
P. astreoides	←	Ω_A	0.399	0.122	**0.003**
P. astreoides	←	pH_{sw}	-1.100	0.268	**<0.001**
P. astreoides	←	Temperature	2.220	0.328	**<0.001**
Chl α	←	Light	-0.624	0.129	**<0.001**
Chl α	←	Nutrients	-0.233	0.277	0.405
Chl α	←	Temperature	0.275	0.173	0.067
pCO_2	←	DIC	0.034	0.134	0.732
pCO_2	←	Salinity	0.211	0.111	**0.049**
pCO_2	←	TA	-0.278	0.083	**0.003**
pCO_2	←	Temperature	0.753	0.132	**<0.001**
DIC	←	*P. astreoides*	-0.857	0.054	**<0.001**
DIC	←	Salinity	0.38	0.083	**<0.001**
Ω_A	←	DIC	-1.635	0.156	**<0.001**
Ω_A	←	Salinity	0.097	0.095	0.342
Ω_A	←	TA	1.596	0.078	**<0.001**
Ω_A	←	Temperature	0.128	0.123	0.111
pH_{sw}	←	DIC	-0.562	0.132	**<0.001**
pH_{sw}	←	Salinity	-0.092	0.083	0.298
pH_{sw}	←	TA	0.906	0.085	**<0.001**
pH_{sw}	←	Temperature	-0.622	0.144	**<0.001**
Salinity	←	Temperature	-0.024	0.177	0.933
TA	←	*P. astreoides*	-0.845	0.132	**<0.001**
TA	←	Salinity	0.678	0.183	**<0.001**
Temperature	←	Light	0.145	0.199	0.354

Minimum was achieved
Chi-square = 59.455
Degrees of freedom = 26
Probability level = **<0.001**

table S1 (B). Crescent Reef *Diploria labyrinthiformis* SEM results.

Crescent Reef *Diploria labyrinthiformis*

Variable	Link	Predictor	Estimate	S.E.	P
D. labyrinthiformis	←	Chl α	0.391	0.192	**0.044**
D. labyrinthiformis	←	pCO_2	0.800	0.456	0.078
D. labyrinthiformis	←	Light	0.116	0.187	0.344
D. labyrinthiformis	←	Nutrients	0.315	0.211	0.133
D. labyrinthiformis	←	Ω_A	0.334	0.385	0.432
D. labyrinthiformis	←	pH_{sw}	-0.620	0.622	0.222
D. labyrinthiformis	←	Temperature	2.830	1.054	**0.001**
Chl α	←	Light	-0.624	0.133	**<0.001**
Chl α	←	Nutrients	-0.233	0.256	0.388
Chl α	←	Temperature	0.275	0.144	0.087
pCO_2	←	DIC	0.330	0.533	0.077
pCO_2	←	Salinity	0.656	0.398	0.088
pCO_2	←	TA	-0.605	0.288	**0.050**
pCO_2	←	Temperature	0.368	0.520	0.565
DIC	←	*D. labyrinthiformis*	-1.134	0.183	**<0.001**
DIC	←	Salinity	0.334	0.155	**0.043**
Ω_A	←	DIC	-1.521	0.132	**<0.001**
Ω_A	←	Salinity	0.071	0.089	0.456
Ω_A	←	TA	1.632	0.050	**<0.001**
Ω_A	←	Temperature	0.223	0.134	0.192
pH_{sw}	←	DIC	-0.734	0.132	**<0,001**
pH_{sw}	←	Salinity	-0.040	0.098	0.899
pH_{sw}	←	TA	0.814	0.056	**<0.001**
pH_{sw}	←	Temperature	-0.832	0.135	**<0.001**
Salinity	←	Temperature	-0.024	0.165	0.887
TA	←	*D. labyrinthiformis*	-0.983	0.254	**<0.001**
TA	←	Salinity	0.648	0.255	**0.017**
Temperature	←	Light	0.145	0.204	0.387

Minimum was achieved
Chi-square = 77.265
Degrees of freedom = 26
Probability level = **<0.001**

table S1 (C). Hog Reef *Porites astreoides* SEM results.

Hog Reef *Porites astreoides*

Variable	Link	Predictor	Estimate	S.E.	P
P. astreoides	←	Chl α	-0.028	0.134	0.765
P. astreoides	←	pCO_2	0.390	0.267	0.088
P. astreoides	←	Light	0.270	0.102	**0.033**
P. astreoides	←	Nutrients	-0.118	0.130	0.245
P. astreoides	←	Ω_A	0.539	0.178	**<0.001**
P. astreoides	←	pH_{sw}	-1.330	0.267	**<0.001**
P. astreoides	←	Temperature	2.050	0.345	**<0.001**
Chl α	←	Light	-0.268	0.190	0.143
Chl α	←	Nutrients	0.016	0.192	0.944
Chl α	←	Temperature	-0.190	0.193	0.266
pCO_2	←	DIC	0.377	0.140	**0.014**
pCO_2	←	Salinity	0.267	0.220	0.145
pCO_2	←	TA	-0.863	0.435	**0.034**
pCO_2	←	Temperature	0.549	0.246	**0.044**
DIC	←	*P. astreoides*	-0.401	0.141	**0.006**
DIC	←	Salinity	0.593	0.119	**<0.001**
Ω_A	←	DIC	-0.345	0.267	0.433
Ω_A	←	Salinity	-0.414	0.177	0.277
Ω_A	←	TA	2.065	0.888	**0.004**
Ω_A	←	Temperature	1.105	0.456	**0.006**
pH_{sw}	←	DIC	-0.532	0.088	**<0.001**
pH_{sw}	←	Salinity	-0.056	0.065	0.456
pH_{sw}	←	TA	0.945	0.112	**<0.001**
pH_{sw}	←	Temperature	-0.576	0.098	**<0.001**
Salinity	←	Temperature	-0.555	0.016	**0.002**
TA	←	*P. astreoides*	-0.972	0.355	**0.006**
TA	←	Salinity	0.678	0.143	**<0.001**
Temperature	←	Light	0.163	0.198	0.456

Minimum was achieved
Chi-square = 63.875
Degrees of freedom = 26
Probability level = **<0.001**

table S1 (D). Hog Reef *Diploria labyrinthiformis* SEM results.

Hog Reef *Diploria labyrinthiformis*

Variable	Link	Predictor	Estimate	S.E.	P
D. labyrinthiformis	←	Chl α	-0.038	0.124	0.654
D. labyrinthiformis	←	pCO_2	0.670	0.261	**0.033**
D. labyrinthiformis	←	Light	0.132	0.134	0.322
D. labyrinthiformis	←	Nutrients	0.075	0.133	0.589
D. labyrinthiformis	←	Ω_A	0.550	0.162	**<0.001**
D. labyrinthiformis	←	pH_{sw}	-1.060	0.342	**0.005**
D. labyrinthiformis	←	Temperature	1.830	0.363	**<0.001**
Chl α	←	Light	-0.284	0.207	0.198
Chl α	←	Nutrients	0.016	0.204	0.873
Chl α	←	Temperature	-0.183	0.194	0.435
pCO_2	←	DIC	0.432	0.161	**0.005**
pCO_2	←	Salinity	0.319	0.197	0.111
pCO_2	←	TA	-1.007	0.378	**0.009**
pCO_2	←	Temperature	0.483	0.244	**0.049**
DIC	←	*D. labyrinthiformis*	-0.432	0.153	**0.035**
DIC	←	Salinity	0.624	0.134	**<0.001**
Ω_A	←	DIC	-0.567	0.293	0.435
Ω_A	←	Salinity	-0.403	0.369	0.288
Ω_A	←	TA	2.138	0.741	**0.003**
Ω_A	←	Temperature	0.830	0.467	**0.002**
pH_{sw}	←	DIC	0.567	0.057	**<0.001**
pH_{sw}	←	Salinity	-0.037	0.067	0.456
pH_{sw}	←	TA	0.975	0.120	**<0.001**
pH_{sw}	←	Temperature	-0.587	0.080	**<0.001**
Salinity	←	Temperature	-0.555	0.170	**0.002**
TA	←	*D. labyrinthiformis*	-1.010	0.412	**0.044**
TA	←	Salinity	0.623	0.207	**0.006**
Temperature	←	Light	0.163	0.201	0.455
Minimum was achieved					
Chi-square = 61.387					
Degrees of freedom = 26					
Probability level = **<0.001**					

table S1 (E). Hog Reef net ecosystem calcification SEM results.

Hog Reef Net Ecosystem Calcification (NEC)

Variable	Link	Predictor	Estimate	S.E.	P
NEC	←	Chl α	0.265	0.124	**0.044**
NEC	←	pCO_2	1.380	0.445	0.093
NEC	←	Light	0.040	0.133	0.528
NEC	←	Nutrients	-0.075	0.122	0.541
NEC	←	Ω_A	1.180	0.883	0.104
NEC	←	pH_{sw}	-2.820	0.984	**0.040**
NEC	←	Temperature	4.330	1.465	**0.020**
Chl α	←	Light	-0.366	0.250	0.149
Chl α	←	Nutrients	0.116	0.241	0.629
Chl α	←	Temperature	-0.242	0.198	0.222
pCO_2	←	DIC	0.748	0.042	**<0.001**
pCO_2	←	Salinity	0.022	0.018	0.210
pCO_2	←	TA	-0.771	0.032	**<0.001**
pCO_2	←	Temperature	0.865	0.048	**<0.001**
DIC	←	NEC	-1.165	0.226	**<0.001**
DIC	←	Salinity	0.200	0.156	0.199
Ω_A	←	DIC	-1.314	0.645	0.234
Ω_A	←	Salinity	-0.047	0.004	0.288
Ω_A	←	TA	1.706	0.605	**0.004**
Ω_A	←	Temperature	0.369	0.123	**0.001**
pH_{sw}	←	DIC	-0.656	0.040	**<0.001**
pH_{sw}	←	Salinity	-0.034	0.020	0.522
pH_{sw}	←	TA	0.716	0.300	**<0.001**
pH_{sw}	←	Temperature	-0.863	0.040	**<0.001**
Salinity	←	Temperature	-0.637	0.158	**0.001**
TA	←	NEC	-0.870	0.063	**0.012**
TA	←	Salinity	0.325	0.050	**0.004**
Temperature	←	Light	0.105	0.271	0.697
Minimum was achieved					
Chi-square = 64.551					
Degrees of freedom = 26					
Probability level = **<0.001**					

table S2. Bermuda coral community composition. Results of the ca. 1980 benthic survey data for nearby North Rock (*41*) are expressed alongside 2010 benthic survey data for Hog Reef (*35*). Table shows the analogous coral community composition and total coral cover between the ca. 30-year interval between benthic surveys.

	% of Total Coral Cover	
Species	North Rock ca. 1980	Hog Reef 2010
Diploria labyrinthiformis	25.8	32.6
Psuedodiploria strigosa	40.6	36.3
Favia fragum	0.5	0.1
Madracis decactis	0.0	0.1
Millepora alcicornis	2.9	6.5
Montastraea cavernosa	2.6	2.2
Montastraea annularis/ Orbicella franksi	16.6	18.1
Porites astreoides	9.5	4.0
Total Coral Cover	30.7%	27.6%

table S3. Mesocosm seawater acidification experiment statistical summary. The model summary data (R^2 and p-value) are presented for linear models testing for the effects of environmental driver (i.e. Ω_A, $[CO_3^{2-}]$, $[HCO_3^-]$, Temperature, Light) on calcification rate for *Diploria labyrinthiformis* and *Porites astreoides* over the three-month mesocosm seawater acidification experiment. All p-values significant at the $\alpha = 0.05$ level are in bold. Table shows that calcification rates do not significantly correlate with any of the carbonate chemistry parameters tested (i.e. Ω_A, $[CO_3^{2-}]$, $[HCO_3^-]$).

	Calcification Rates (mg day^{-1})			
	Diploria labyrinthiformis		*Porites astreoides*	
Parameter	R^2	p-value	R^2	p-value
Ω_A	0.252	0.096	0.077	0.384
$[CO_3^{2-}]$	0.237	0.109	0.064	0.426
$[HCO_3^-]$	0.241	0.105	0.133	0.245
Temperature	0.321	0.055	0.845	**< 0.001**
Light	0.408	**0.025**	0.039	0.539

Chapter 4, in full, is a reprint of the material as it appears in Courtney TA, Lebrato M, Bates NR, Collins A, de Putron SJ, Garley R, Johnson, R, Molinero JC, Noyes TJ, Sabine CL, Andersson AJ. Environmental controls on modern scleractinian coral and reef-scale calcification. *Science Advances*, 2017, 3(11), p.e1701356. The dissertation author was the primary investigator and author of this paper.

CHAPTER 5

Recovery of reef-scale calcification following a bleaching event in Kāne'ohe Bay, Hawai'i

Courtney TA, De Carlo EH, Page HN, Bahr KD, Barro A, Howins N, Tabata R, Terlouw G, Rodgers KS, Andersson AJ

LIMNOLOGY AND OCEANOGRAPHY
Letters

ASLO
Open Access

Limnology and Oceanography Letters 00, 2017, 00–00

doi: 10.1002/lol2.10056

LETTER

Recovery of reef-scale calcification following a bleaching event in Kāne'ohe Bay, Hawai'i

T. A. Courtney [1]* *E. H. De Carlo,*[2] *H. N. Page,*[1] *K. D. Bahr,*[3] *A. Barro,*[2] *N. Howins,*[2] *R. Tabata,*[2] *G. Terlouw,*[2] *K. S. Rodgers,*[3] *A. J. Andersson*[1]

[1]Scripps Institution of Oceanography, University of California, San Diego, La Jolla, California; [2]Department of Oceanography, School of Ocean and Earth Science and Technology, University of Hawai'i at Mānoa, Honolulu, Hawaii; [3]Hawai'i Institute of Marine Biology, University of Hawai'i at Mānoa, Honolulu, Hawai'i

Scientific Significance Statement

Although bleached coral reef states have been extensively studied, reef-scale net calcification during and after bleaching events has received less attention. As a result, it is unclear what the impacts of coral bleaching are on the ability for coral reefs to calcify and maintain reef structure following bleaching. Our study of reef-scale net calcification provides evidence for rapid recovery to positive reef-scale calcification if there is limited coral mortality and fast return of the coral's symbiotic algae. Our results raise questions on the limit of coral reef resilience to maintain positive calcification under future climate change.

Abstract

Increasing anthropogenic disturbances have driven declines of many coral-dominated reef states, threatening critical ecosystem functions such as reef-scale calcification and accretion. Few studies have investigated the effect of coral bleaching on reef-scale calcification. In this study, we monitored bay-wide alkalinity anomalies in Kāne'ohe Bay, Hawai'i along an inshore-offshore transect as a proxy for net calcification during the 2015 coral bleaching event and following recovery over a full seasonal cycle. We observed no net calcification in October 2015 during the bleaching event followed by a recovery to significant, positive net calcification rates in June 2016, November 2016, and February 2017 across a range of seawater temperatures and hydrodynamic conditions. Post-bleaching net calcification rates were not significantly different between survey dates and agreed with the range of pre-bleaching net calcification rates from a previous study suggesting that net calcification in Kāne'ohe Bay had fully recovered following the 2015 bleaching event.

Particular attention has been given to understanding how resilient coral reef systems are able to maintain the roles and functions that coral-dominated reef states provide during the current period of coral reef declines (Done 1992; Hughes et al. 2003). Of specific concern for the decline of less-resilient coral-dominated systems is the balance between the constructive (i.e., calcification and accretion) and destructive (i.e., $CaCO_3$ dissolution and erosion) processes and the resulting net impact on reef growth (Kleypas et al. 2001; Hughes et al. 2003; Perry et al. 2013; Muehllehner et al. 2016; Yates et al. 2017). Rates of constructive reef-scale calcification have decreased across the Caribbean in recent decades owing to declining coral cover and coral community shifts toward more slowly growing species

*Correspondence: traviscourtney@gmail.com

Author Contribution Statement: TAC and AJA conceptualized the study. TAC, AJA, KDB, AB, EHDC, NH, HNP, RT, and GT participated in field efforts and collected samples. TAC and HNP analyzed the samples. TAC and AJA analyzed the data and wrote the manuscript with input from all coauthors.

Data Availability Statement: Data are available in the *figshare* repository at https://doi.org/10.6084/m9.figshare.5425906.

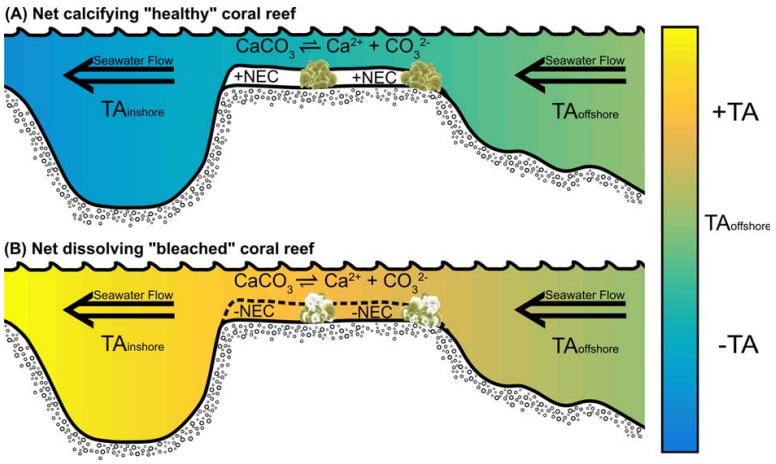

Fig. 1. Conceptual diagram of net coral reef calcification and seawater alkalinity anomalies. (**A**) In a net calcifying "healthy" coral reef system, total alkalinity is depleted (−TA) as seawater flows over the coral reef flat owing to the decrease in seawater Ca^{2+} and CO_3^{2-} ions. (**B**) For a net dissolving "bleached" coral reef system, TA increases (+TA) as seawater flows over the coral reef flat owing to the increase in seawater Ca^{2+} and CO_3^{2-} ions. Bleached and non-bleached *Porites lobata* coral animations are attributed to Joanna Woerner, Integration and Application Network, University of Maryland Center for Environmental Science (ian.umces.edu/imagelibrary).

(Perry et al. 2013). Meanwhile, rates of destructive $CaCO_3$ dissolution and bioerosion processes are anticipated to increase under anthropogenic ocean warming and acidification (Andersson and Gledhill 2013). These trends toward decreasing reef-scale calcification and increasing $CaCO_3$ erosion have already produced net erosional reefs in the Caribbean and Pacific thereby threatening the persistence of coral reef structure and the ecosystem services (e.g., food production, shoreline protection, and tourism; Moberg and Folke 1999) coral reefs provide to humanity (Perry et al. 2013; Muehllehner et al. 2016; Perry and Morgan 2017; Yates et al. 2017).

Coral bleaching events have increased in both frequency and intensity, further reducing the accretion capacity of many coral-dominated systems (Hughes et al. 2003). Global coral bleaching events occurred in 1997–1998, 2010, and 2015–2016 (Hughes et al. 2017). Thermal stress induced coral bleaching, the breakdown of symbiosis between host coral and symbiont zooxanthellae, can occur if sea surface temperatures exceed ~ 1°C above mean ambient summer temperatures with coral mortality correlated to the magnitude and duration of thermal stress (Jokiel and Coles 1977; Glynn 1993). Because corals are the dominant reef-calcifiers (Hart and Kench 2007) and bleached corals exhibit reduced calcification rates (Jokiel and Coles 1977; Glynn 1993; Hughes et al. 2003), coral bleaching events are expected to reduce coral reef net ecosystem calcification (NEC = calcification − $CaCO_3$ dissolution). In addition, NEC may also decrease owing to increased $CaCO_3$ dissolution fueled by increased heterotrophy resulting from decomposition of coral derived organic matter and decreased primary production. While coral bleaching events have been well documented (e.g., Glynn 1993; Hughes et al. 2003, 2017; Bahr et al. 2017), only a few studies known to the authors have explored coral bleaching impacts on NEC finding reduced NEC rates associated with bleaching for coral reefs in Palau and Taiwan (Kayanne et al. 2005; Watanabe et al. 2006; DeCarlo et al. 2017) and no change in NEC for a bleached coral reef in Japan (Kayanne et al. 2005). An additional study utilizing census-based carbonate production budgets observed a bleaching-induced shift from positive to negative carbonate production budgets in the Maldives (Perry and Morgan 2017). This previously observed variability in coral reef ΔNEC and net carbonate production budgets reflects differential responses to coral bleaching events and highlights the need to better understand these responses in light of projected increases in frequency and severity of coral bleaching events.

Because calcification reduces total alkalinity (TA) by two moles for each mole of $CaCO_3$ formed, reef-scale calcification can be measured by changes in salinity-normalized seawater TA, with the magnitude of TA depletion a function of benthic NEC rates and volumetric seawater flow rates over the benthos (Smith 1973; Chisholm and Gattuso 1991; Falter et al. 2013; Muehllehner et al. 2016). Here, we utilized alkalinity anomalies to test the hypothesis that NEC of the Kāneʻohe Bay, Hawaiʻi barrier reef flat would decrease in fall 2015 owing to the predicted reduction of coral calcification and or enhanced $CaCO_3$ dissolution during the coral bleaching event (Fig. 1). We then hypothesized that the barrier reef flat would return to positive NEC following the recovery of corals in Kāneʻohe Bay. These hypotheses were tested by surveying seawater TA and dissolved

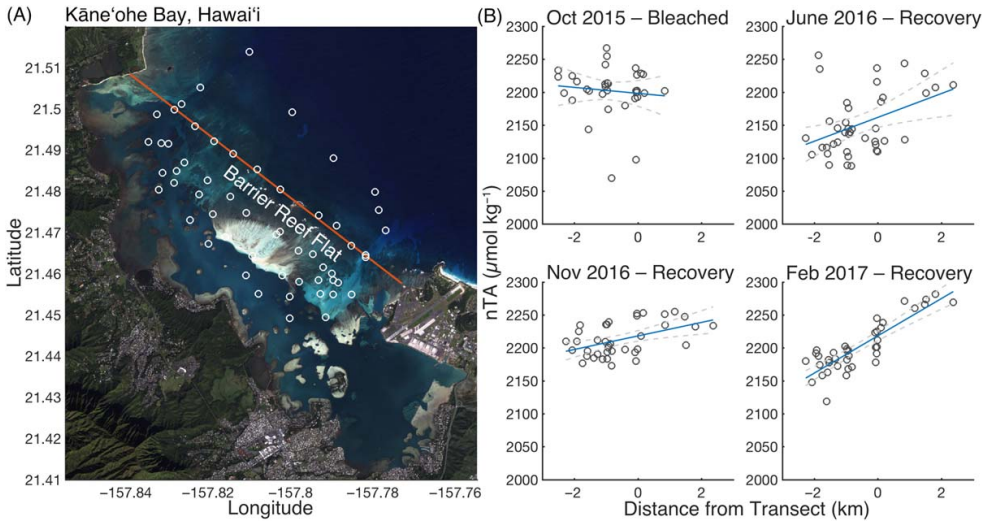

Fig. 2. Spatial map of sample locations and salinity normalized TA across the Kāne'ohe Bay barrier reef. (**A**) Sample locations (white circles) in Kāne'ohe Bay are plotted relative to the Kapapa Island reef flat transect (red line). (**B**) Salinity normalized total alkalinity (nTA) is plotted relative to the inshore-offshore distance (km) of each sample location relative to the Kapapa Island transect such that positive distances are offshore and negative distances are inshore from the red transect line. Regression lines of ΔnTA drawdown are plotted in blue with gray dashed confidence intervals (±SE) for each sample date.

inorganic carbon (DIC) across the entire Kāne'ohe Bay barrier reef flat during the bleaching event (fall 2015) and over a full seasonal cycle (summer 2016, fall 2016, winter 2017) of coral reef recovery. This study addresses bleaching impacts on truly ecosystem-scale calcification (~ 12.4 km^2 study area) at multiple time points during the bleaching event and a ~ 1.5 yr recovery period.

Methods

Site description

The Kāne'ohe Bay ecosystem on the northeast shore of O'ahu, Hawai'i represents a coral reef exhibiting elevated resilience to centuries of human perturbations (Bahr et al. 2015) with thermal stress driven coral bleaching events in 1996, 2014, and 2015 (Bahr et al. 2017). The system consists of an estuarine bay separated from the open ocean by a highly productive barrier reef flat consisting of 5–10% coral cover interspersed by coral rubble, algae, coarse sand, and volcanic rock (Smith et al. 1981; Jokiel 1991). Water circulation in Kāne'ohe Bay is predominately wave-driven with the additional effects of wind and tides driving a landward flow over the barrier reef flat and seaward flow out of the bay through channels in the north and south (Smith et al. 1981; Jokiel 1991; Lowe et al. 2009). Previous work using TA anomalies in Kāne'ohe Bay found that positive NEC is maintained year-round (Fagan and Mackenzie 2007; Shamberger et al. 2011) with no significant seasonal variability in rates (Shamberger et al. 2011).

Kāne'ohe Bay 2015 bleaching event

In this study, we examined the effects of the fall 2015 Kāne'ohe Bay bleaching event and subsequent recovery on NEC of the barrier reef flat. Notably, 46% ± 4% (mean ± SE) of corals in Kāne'ohe Bay were observed as pale or bleached in October 2015 with a resulting cumulative mortality of 22% ± 5% (mean ± SE) (Bahr et al. 2017). By November 2016, 99.96% ± 0.02% (mean ± SE) of corals showed no signs of paling or bleaching with a 5% ± 5% (mean ± SE) decline in overall coral cover relative to the October 2015 survey, highlighting the relatively rapid recovery of the Kāne'ohe Bay coral reef ecosystem to the 2015 coral bleaching event (Bahr et al. 2017).

Seawater TA and DIC spatial surveys

TA and DIC spatial surveys were conducted across the entire Kāne'ohe Bay barrier reef flat including samples offshore from the reef flat boundary (Fig. 2A) on 31 October 2015, 29 June 2016, 12 November 2016, and 26 February 2017. Surface seawater samples were collected by hand at ~ 0.25 m depth using 250 mL *Pyrex* glass bottles and immediately fixed with 100 μL $HgCl_2$ as per standard protocols (Dickson et al. 2007). Handheld *YSI* multiprobes (October 2015: *YSI 6600 V2*; June 2016, November 2016: *YSI Professional Plus*; February 2017: *YSI 556*) were calibrated and used to measure temperature (± 0.2°C) and salinity (± 0.3 g kg^{-1}) at the time of sampling. All seawater samples were transported to the Scripps Coastal and Open Ocean Biogeochemistry lab and analyzed for TA via an open-cell potentiometric acid titration system developed at Scripps

Table 1. Summary of measured and calculated environmental data. Measured and calculated environmental data during each survey are reported as the mean ± SD for the portion of each sampling day that samples were collected. Seawater height is measured with respect to Mean Lower Low Water. ΔnTA and ΔnDIC are the mean ± SE TA and DIC drawdowns (μmol kg^{-1} km^{-1}) multiplied by the 2-km width of the Kāne'ohe Bay barrier reef flat. ΔnTA and ΔnDIC were combined with seawater density (ρ_{sw}), depth (z), and residence time (τ) in Eqs. 1, 2, respectively, to calculate NEC and NEP with uncertainty estimated from Monte Carlo simulations.

Environmental parameters	31 Oct 15 Bleached	29 Jun 16 Recovery	12 Nov 16 Recovery	26 Feb 17 Recovery
Temperature (°C)	27.6 ± 0.3	27.6 ± 1.0	26.6 ± 0.3	23.2 ± 0.4
Wind (m s^{-1})	1.0 ± 0.4	3.3 ± 0.5	0.9 ± 0.3	0.6 ± 0.3
Wave H_s (m)	1.38 ± 0.08	1.18 ± 0.03	2.03 ± 0.10	1.22 ± 0.06
Measured tidal range (m)	0.8	0.5	0.6	0.9
Tidal cycle	Flood	Ebb	Flood-slack-ebb	Flood-slack-ebb
ρ_{sw} (kg m^{-3})	1021.5 ± 0.5	1022.5 ± 0.5	1022.7 ± 0.1	1023.4 ± 0.2
Depth (m)	5 ± 4	4 ± 4	4 ± 4	5 ± 4
τ (d)	6.0 ± 2.8	6.0 ± 2.8	3.4 ± 1.5	6.0 ± 2.8
NEC				
ΔnTA/km (μmol kg^{-1} km^{-1})	−5 ± 8	18 ± 6	10 ± 3	28 ± 3
ΔnTA (μmol kg^{-1})	−10 ± 16	36 ± 12	20 ± 6	56 ± 6
NEC (mmol $CaCO_3$ m^{-2} d^{-1})	−5 ± 6	15 ± 9	15 ± 9	26 ± 15
NEC (kg $CaCO_3$ m^{-2} yr^{-1})	−0.2 ± 0.2	0.5 ± 0.3	0.5 ± 0.3	0.9 ± 0.5
NEP				
ΔnDIC/km (μmol kg^{-1} km^{-1})	−6 ± 8	20 ± 7	15 ± 4	19 ± 4
ΔnDIC (μmol kg^{-1})	−12 ± 16	40 ± 14	30 ± 8	38 ± 8
NEP (mmol C m^{-2} d^{-1})	−7 ± 12	18 ± 14	36 ± 33	9 ± 7

Institution of Oceanography (SIO) by A. G. Dickson (Dickson et al. 2007) and DIC via an automated infrared inorganic carbon analyzer (AIRICA, *Marianda*). The mean accuracy (TA ± 1.3 μmol kg^{-1}, DIC ± 1.6 μmol kg^{-1}) and precision (TA ± 1.3 μmol kg^{-1}, DIC ± 1.4 μmol kg^{-1}) of TA and DIC measurements were evaluated using certified reference materials provided by the laboratory of A. G. Dickson at SIO. Seawater TA and DIC were normalized to a mean salinity across all bottle samples of 34.6 g kg^{-1} to directly compare nTA and nDIC between samples of variable salinity (e.g., as discussed in Shamberger et al. 2011).

Environmental data

Environmental data were aggregated for each spatial survey. Temperature and salinity were measured at each sample location as previously described. Mean significant wave height (H_s), the mean of the 1/3 highest waves measured over the 30 min averaging interval, was determined by the Coastal Data Information Program (CDIP) Kāne'ohe Buoy 198 (http://cdip.ucsd.edu). Wind speed and tidal range from recorded water levels were measured every 6 min at the Moku o Lo'e monitoring station in Kāne'ohe Bay (https://tidesandcurrents.noaa.gov). Each parameter was averaged over the respective sampling duration to determine the mean environmental conditions for each sample date (Table 1).

Statistical analysis

Salinity-normalized seawater TA was interpolated across the survey regions using the *MATLAB* "natural" three-dimensional triangulation-based nearest neighbor interpolation to visualize spatial heterogeneity in nTA (Fig. 3). The distance between each sampling location and a transect drawn parallel to the barrier reef along Kapapa Island (Fig. 2A) was calculated to analyze inshore-offshore changes in nTA and nDIC of seawater flowing across the barrier reef flat. The *fitlm()* and *anova()* functions of the *MATLAB Statistics and Machine Learning Toolbox* were used to generate and assess linear least-squares fits of nTA and nDIC as functions of distance from the Kapapa Island transect for each spatial survey. These responses are hereafter referred to as the ΔnTA and ΔnDIC drawdowns wherein positive ΔnTA slopes represent net coral reef calcification (i.e., reduction in seawater nTA flowing over the reef flat) and organic carbon negative ΔnTA slopes represent net $CaCO_3$ dissolution. ΔnDIC slopes represent the sum of net calcification and net organic carbon production.

NEC and NEP

NEC and net ecosystem production (NEP) for the entire ~ 12.4 km^2 barrier reef flat (i.e., Kapapa Island transect to 2 km inshore of transect) were calculated using the following modified equations based on the assumptions that (1) calcification and $CaCO_3$ dissolution are the dominant processes affecting

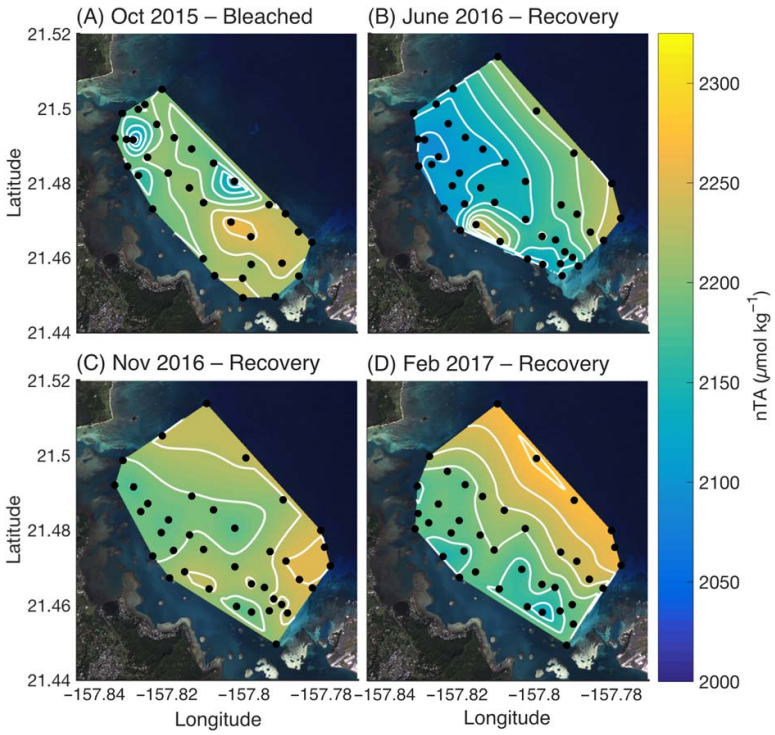

Fig. 3. Seasonal contour plots of salinity normalized total alkalinity. Discrete salinity normalized total alkalinity (nTA) samples from survey stations (black dots) were spatially interpolated to visualize spatial nTA gradients of ΔnTA drawdown occurring during the October 2015 coral bleaching event (A) and during a year of recovery (June 2016 (B), November 2016 (C), February 2016 (D)) following the bleaching event.

the TA balance and (2) that changes in DIC owing to CO_2 air–sea exchange are negligible relative to the influence of NEC and NEP (Langdon et al. 2010; Page et al. 2017):

$$\mathrm{NEC} = \frac{\rho z(\Delta \mathrm{nTA})}{2\tau} \quad (1)$$

$$\mathrm{NEP} = \frac{\rho z\left(\Delta \mathrm{nDIC} - \frac{\Delta \mathrm{nTA}}{2}\right)}{\tau} \quad (2)$$

wherein ρ is mean ± SD seawater density calculated from measured temperature, salinity, and pressure using the *Gibbs Seawater (GSW) Oceanographic Toolbox* (McDougall and Barker 2011), and z is the mean ± SD seawater depth for the sample sites calculated from a 4-m bathymetric grid of Kāne'ohe Bay (www.soest.hawaii.edu/pibhmc). ΔnTA and ΔnDIC are the nTA and nDIC drawdowns (μmol kg^{-1} km^{-1}) × 2 km width of the barrier reef flat. τ is the mean ± SE seawater residence time derived for the barrier reef flat by Lowe et al. (2009) for the following forcing conditions: tidal range of 0.7 m; mean wind velocity of 5 m s^{-1}; and mean significant wave height (H_s) of 1.0 m (October 2015, June 2016, February 2017) or 2.0 m (November 2016) (for details, see zones 1–3 as described in Lowe et al. 2009). A Monte Carlo approach was used to estimate uncertainty in NEC and NEP using random numbers ($n = 10^7$) generated within the range of SD or SE for each NEC and NEP equation parameter (Table 1) using the *MATLAB rand()* function. The mean ± SD of the Monte Carlo output for each NEC and NEP survey was used to estimate mean NEC and NEP rates ± uncertainty.

Results

No net reduction in seawater nTA in the dominating shoreward seawater flow direction was observed in the nTA gradients across the Kāne'ohe Bay reef flat during the October 2015 bleaching event suggesting NEC ~ 0 at this time (Fig. 3). This finding was quantified with linear models for the October 2015 data, which showed no statistically significant drawdown in nTA (slope ± SE = −5 ± 8 μmol kg^{-1} km^{-1}, $R^2 = 0.011$, $n = 33$, $F = 0.333$, $p = 0.568$) or nDIC (slope ± SE = −6 ± 8 μmol kg^{-1} km^{-1}, $R^2 = 0.019$, $n = 33$, $F = 0.612$, $p = 0.44$) across the reef (Figs. 2B, 4A). In contrast, significant reductions in seawater nTA and nDIC were observed across the reef and along the predominant flow direction in June 2016, November 2016, and February 2017 (Figs. 2B, 4A). The strongest nTA drawdown was

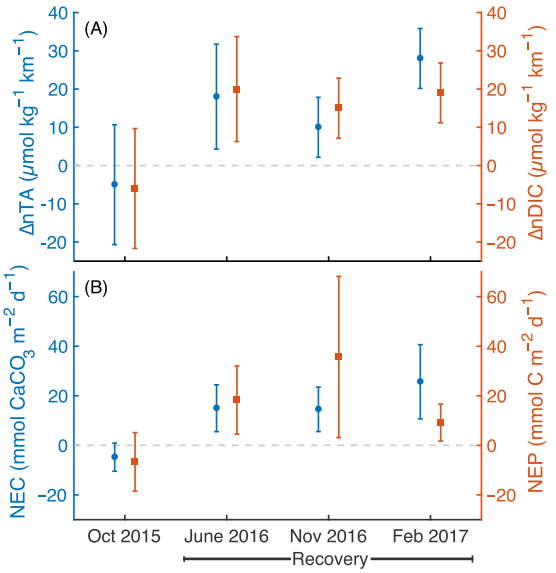

Fig. 4. NEC and NEP in Kāne'ohe Bay. (**A**) Slopes (± 95% confidence intervals) of salinity normalized total alkalinity (ΔnTA km^{-1}, in blue) and DIC (ΔnDIC km^{-1}, in red) drawdown of seawater flowing over the reef flat. Positive values signify a net drawdown of nTA or nDIC whereas negative values signify production of nTA or nDIC. If the confidence intervals overlap the dashed zero line, ΔnTA or ΔnDIC drawdown is not significantly different from zero. (**B**) Calculated mean (± uncertainty) NEC (in blue) and NEP (in red). Values with estimated uncertainty above zero indicate positive reef NEC or NEP whereas values with estimated uncertainty overlapping zero indicate zero NEC or NEP.

observed in February of 2017 (slope ± SE = 28 ± 3 μmol kg^{-1} km^{-1}, $R^2 = 0.737$, $n = 39$, $F = 103.9$, $p < 0.001$) followed by June 2016 (slope ± SE = 18 ± 6 μmol kg^{-1} km^{-1}, $R^2 = 0.174$, $n = 41$, $F = 8.222$, $p = 0.007$) and November 2016 (slope ± SE = 10 ± 3 μmol kg^{-1} km^{-1}, $R^2 = 0.227$, $n = 38$, $F = 10.598$, $p = 0.002$). The strongest nDIC drawdown was observed in June 2016 (slope ± SE = 20 ± 7 μmol kg^{-1} km^{-1}, $R^2 = 0.166$, $n = 41$, $F = 7.78$, $p = 0.008$) followed by February 2017 (slope ± SE = 19 ± 4 μmol kg^{-1} km^{-1}, $R^2 = 0.383$, $n = 39$, $F = 23$, $p < 0.001$) and November 2016 (slope ± SE = 15 ± 4 μmol kg^{-1} km^{-1}, $R^2 = 0.274$, $n = 38$, $F = 13.6$, $p < 0.001$). Calculations of NEC and NEP showed values close to zero (−5 ± 6 mmol $CaCO_3$ m^{-2} d^{-1}and −7 ± 12 mmol C m^{-2} d^{-1}, respectively) during the October 2015 bleaching event while positive NEC (15–26 mmol $CaCO_3$ m^{-2} d^{-1}) and NEP (9–36 mmol C m^{-2} d^{-1}) rates were calculated for June 2016, November 2016, and February 2017 with overlapping uncertainties implying that NEC and NEP rates were not statistically different between post-bleaching surveys (Fig. 4B; Table 1).

Discussion

Our results show that ecosystem-scale NEC and NEP were essentially zero during the October 2015 coral bleaching event in Kāne'ohe Bay, but exhibited rapid recovery as evidenced by positive NEC and NEP in the year following the bleaching event (June 2016, November 2016, February 2017). These observations support the hypotheses of reduced NEC during the coral bleaching event with a subsequent return to positive NEC as the corals recovered (Figs. 2B, 4B; Table 1). While no measurements of NEC were conducted before the bleaching event as part of this study, previous work (2003–2004; 2008–2010) has quantified year-round positive NEC occurring on the Kāne'ohe Bay barrier reef (Fagan and Mackenzie 2007; Shamberger et al. 2011) suggesting the cessation of NEC observed in this study was a direct consequence of the bleaching event.

Our findings of positive NEC with overlapping uncertainties (Fig. 4B; Table 1) for each of the spatial surveys conducted following the bleaching event (June 2016, November 2016, February 2017) suggest that Kāne'ohe Bay NEC recovered at a rate faster than the temporal resolution of the first spatial sampling events (i.e., October 2015 to June 2016). This is partially supported by visual observations of the recovery of coral coloration. For example, peak bleaching was observed in October 2015 with 46% ± 4% (mean ± SE) corals recorded as either pale or bleached with just 9% ± 2% of corals observed as pale or bleached and 8% ± 2% recorded as dead at ~ 2 months post-bleaching in December 2015 (Bahr et al. 2017). However, gradual and sequential increases in NEC during the post-bleaching period that are less than the uncertainty measured in this study may also be possible, but are not quantifiable given the limits of our uncertainty (Fig. 4B; Table 1).

Additionally, the findings that 99.96% ± 0.02% (mean ± SE) of corals observed in November 2016 were neither bleached nor pale and total coral cover did not decrease relative to October 2015 suggest a post-bleaching recovery of corals in Kāne'ohe Bay (Bahr et al. 2017) and that a similar recovery in NEC is probable. The finding that post-recovery NEC in this study (February 2017 NEC = 26 ± 15 mmol $CaCO_3$ m^{-2} d^{-1}) agrees with Kāne'ohe Bay mesocosm NEC rates linearly scaled to 10% coral cover (27 ± 11 mmol $CaCO_3$ m^{-2} d^{-1} *sensu* Page et al. 2017) suggests NEC has recovered for this ~ 5–10% coral cover ecosystem (Jokiel 1991). While previous estimates of Kāne'ohe Bay barrier reef flat NEC before the bleaching event are much higher (range = 174–331 mmol $CaCO_3$ m^{-2} d^{-1}, Shamberger et al. 2011), this discrepancy is primarily due to differences in estimating seawater residence times (i.e., numerical residence time models in this study compared to current flow velocities across the reef flat in Shamberger et al. 2011) and differing spatial scales between the two studies. Nonetheless, if the post-recovery NEC rates from this study are recalculated utilizing the average depth ($z = 2$ m) and range of residence times ($\tau = 4.5$–13.6 h) from Shamberger et al. (2011), the much higher recalculated February 2017 post-recovery NEC rates (range = 101–306 mmol $CaCO_3$ m^{-2} d^{-1}) from this

study agree with the range of rates (174–331 mmol $CaCO_3$ m^{-2} d^{-1}) from Shamberger et al. (2011). This lends strong support that NEC indeed has recovered for Kāne'ohe Bay and reconciles the divergent rates presented here and in Shamberger et al. (2011).

Differences in environmental parameters between survey dates may also explain variations in measured ΔnTA and calculated NEC in this study via changes in coral reef metabolism and/or seawater residence time (Falter et al. 2013). Mean residence times of ~ 3–6 d (Table 1) show that NEC rates represent integrations over multiple days and are therefore less influenced by anomalous daily phenomena. Environmental conditions were similar across sample dates with the exception that H_s was ~ 1 m higher in November 2016 relative to the other surveys and the February 2017 survey was ~ 3–4°C cooler than previous surveys (Table 1). Lowe et al. (2009) have shown that the barrier reef flat seawater residence time is directly related to the wave height. Consequently, significantly lower ΔnTA drawdown was observed in November 2016 compared to February 2017 (nonoverlapping 95% confidence intervals in Fig. 4A, Table 1), but NEC was not significantly different between those dates (overlapping uncertainties in Fig. 4B, Table 1) due to the reduced seawater residence time in November 2016. Neither ΔnTA drawdown nor NEC was significantly different between February 2017 and June 2016, suggesting reductions in temperature did not affect net reef-scale calcification. This finding agrees with previous work showing no significant seasonal variability in Kāne'ohe Bay NEC (Shamberger et al. 2011).

The observation of zero NEC during the fall 2015 coral bleaching event in Kāne'ohe Bay agrees with decreased calcification rates observed in bleached coral colonies (Jokiel and Coles 1977; Glynn 1993; Hughes et al. 2003) and with reductions in total coral cover (Page et al. 2017; Perry and Morgan 2017). For example, a 75% reduction in coral cover (i.e., from 25.6% to 6.3%) following the 2016 coral bleaching event in the Maldives was the primary driver of a shift from net positive (mean 5.92 kg m^{-2} yr^{-1}) to net negative (mean −2.96 kg m^{-2} yr^{-1}) carbonate production budgets (Perry and Morgan 2017). However, observed reductions in NEC may also be due to enhanced metabolically driven $CaCO_3$ dissolution associated with coral bleaching events. For example, the zero NEP observed during the bleaching event (Table 1; Fig. 4B) suggests a shift toward net heterotrophy that could have fueled an increase in $CaCO_3$ dissolution rates (Andersson and Gledhill 2013). Irrespective of this, the cessation of NEC in this study is unique among results from previous hydrochemical field observations wherein positive NEC was maintained during bleaching events at similar or reduced rates compared to non-bleaching conditions (Kayanne et al. 2005; Watanabe et al. 2006; DeCarlo et al. 2017). In Palau, reef flat NEC was found to decrease ~ 43% between surveys conducted before (July 1994) and after (September 2000) the 1998 coral bleaching event, coinciding with a reduction in pre-bleaching coral cover of 8.1 to 1.4% after bleaching (Kayanne et al. 2005), while lagoon NEC decreased 60–70% over that same interval (Watanabe et al. 2006). During a widespread bleaching event in June 2014 at Dongsha Atoll, Taiwan, a 40% reduction in NEC rates was observed for a reef flat with 25% total coral cover (DeCarlo et al. 2017). In contrast, measurements of NEC at Shiraho Reef, Japan did not change during the September 1998 bleaching event, where 51% of the total 7.1% total coral cover was bleached compared to a recovery survey conducted in September 1999 with 6.7% total coral cover and no bleaching observed (Kayanne et al. 2005). Kayanne et al. (2005) hypothesized that calcification by living bleached corals, calcifying algae, and benthic foraminifera may have compensated for bleaching-induced losses in NEC at Shiraho Reef. Indeed, the dominant calcifiers of coral reefs include corals, red coralline algae, molluscs, green calcifying algae, and benthic foraminifera (Montaggioni and Braithwaite 2009), but their relative contributions to coral reef $CaCO_3$ budgets and how these change under different reef states are uncertain. This raises the question and need to further quantify the relative importance of contributions by other calcifiers to coral reef NEC especially for low coral cover (< 10%) and bleached coral reefs.

In summation, the results of this study suggest that a temporary reduction in coral reef NEC can be expected during a coral bleaching event while rapid post-bleaching recovery of positive NEC is possible given limited coral mortality and rapid regain of symbiotic algae. As coral bleaching events are expected to increase in both frequency and magnitude (Hughes et al. 2003), the resilience capacity of coral reef systems such as Kāne'ohe Bay will continue to be tested (Done 1992; Hughes et al. 2003; Bahr et al. 2017), with bleached coral reefs that recover quickly likely experiencing ephemeral reductions in reef NEC while systems shifting to alternative non coral-dominated states are likely to face lasting decreases in NEC. Although the Kāne'ohe Bay coral reef system appears to have recovered to a net calcifying system following the recent global mass bleaching event, other reefs around the world including parts of the Great Barrier Reef in Australia that experienced > 80% bleaching (Hughes et al. 2017) may be faced with a different outcome. It is prudent that future investigations of reef-scale NEC target these sites to evaluate the impact and time to recover to guide future management. In either case, the increasing frequency of time during which an intermittently bleached coral reef is predicted to calcify at reduced rates during the 21st century threatens the ability for contemporary coral reef structures to maintain ecological form and function. The question thus remains, for how long can we depend on coral reef resiliency to maintain calcifying reef states and the ecosystem services they provide?

References

Andersson, A. J., and D. Gledhill. 2013. Ocean acidification and coral reefs: Effects on breakdown, dissolution, and net ecosystem calcification. Ann. Rev. Mar. Sci. **5**: 321–348. doi:10.1146/annurev-marine-121211-172241

Bahr, K. D., K. S. Rodgers, and P. L. Jokiel. 2017. Impact of Three Bleaching Events on the Reef Resiliency of Kāne'ohe Bay, Hawai'i. Front. Mar. Sci. **4**: 398. doi:10.3389.fmars.2017.00398

Bahr, K. D., P. L. Jokiel, and R. J. Toonen. 2015. The unnatural history of Kāne'ohe Bay: Coral reef resilience in the face of centuries of anthropogenic impacts. PeerJ **3**: e950. doi:10.7717/peerj.950

Chisholm, J. R. M., and J.-P. Gattuso. 1991. Validation of the alkalinity anomaly technique for investigating calcification and photosynthesis in coral reef communities. Limnol. Oceanogr. **36**: 1232–1239. doi:10.4319/lo.1991.36.6.1232

DeCarlo, T. M., A. L. Cohen, G. T. F. Wong, F. Shiah, S. J. Lentz, K. A. Davis, K. E. F. Shamberger, and P. Lohmann. 2017. Community production modulates coral reef pH and the sensitivity of ecosystem calcification to ocean acidification. J. Geophys. Res. Oceans **122**: 745–761. doi:10.1002/2016JC012326

Dickson, A. G., C. L. Sabine, and J. R. Christian [eds.]. 2007. Guide to best practices for ocean CO_2 measurements, p. 191. PICES special publication 3. North Pacific Marine Science Organization.

Done, T. J. 1992. Phase shifts in coral reef communities and their ecological significance. Hydrobiologia **247**: 121–132. doi:10.1007/BF00008211

Fagan, K. E., and F. T. Mackenzie. 2007. Air-sea CO_2 exchange in a subtropical estuarine-coral reef system, Kaneohe Bay, Oahu, Hawaii. Mar. Chem. **106**: 174–191. doi:10.1016/j.marchem.2007.01.016

Falter, J. L., R. J. Lowe, Z. Zhang, and M. McCulloch. 2013. Physical and biological controls on the carbonate chemistry of coral reef waters: Effects of metabolism, wave forcing, sea level, and geomorphology. PLoS One **8**: e53303. doi:10.1371/journal.pone.0053303

Glynn, P. W. 1993. Coral reef bleaching: Ecological perspectives. Coral Reefs **12**: 1–17. doi:10.1007/BF00303779

Hart, D. E., and P. S. Kench. 2007. Carbonate production of an emergent reef platform, Warraber Island, Torres Strait, Australia. Coral Reefs **26**: 53–68. doi:10.1007/s00338-006-0168-8

Hughes, T. P., and others. 2003. Climate change, human impacts, and the resilience of coral reefs. Science **301**: 929–933. doi:10.1126/science.1085046

Hughes, T. P., and others. 2017. Global warming and recurrent mass bleaching of corals. Nature **543**: 373–377. doi:10.1038/nature21707

Jokiel, P. L. 1991. Jokiel's illustrated scientific guide to Kane'ohe Bay, O'ahu, p. 1–65. Hawai'ian Coral Reef Assessment and Monitoring Program.

Jokiel, P. L., and S. L. Coles. 1977. Effects of temperature on the mortality and growth of Hawaiian reef corals. Mar. Biol. **43**: 201–208. doi:10.1007/BF00402312

Kayanne, H., and others. 2005. Seasonal and bleaching-induced changes in coral reef metabolism and CO_2 flux. Global Biogeochem. Cycles **19**: 1–11. doi:10.1029/2004GB002400

Kleypas, J. A., R. W. Buddemeier, and J. P. Gattuso. 2001. The future of coral reefs in an age of global change. Int. J. Earth Sci. **90**: 426–437. doi:10.1007/s005310000125

Langdon, C., J.-P. Gattuso, and A. Andersson. 2010. Measurements of calcification and dissolution of benthic organisms and communities, p. 213–232. *In* U. Riebesell, V. Fabry, L. Hansson, and J. Gattuso [eds.], Guide to best practices for ocean acidification research and data reporting. Office for Official Publications of the European Communities.

Lowe, R. J., J. L. Falter, S. G. Monismith, and M. J. Atkinson. 2009. A numerical study of circulation in a coastal reef-lagoon system. J. Geophys. Res. Oceans **114**: 1–18. doi:10.1029/2008JC005081

McDougall, T. J., and P. M. Barker. 2011. Getting started with TEOS-10 and the Gibbs Seawater (GSW) oceanographic toolbox, p. 1–28. SCOR/IAPSO WG 127.

Moberg, F., and C. Folke. 1999. Ecological goods and services of coral reef ecosystems. Ecol. Econ. **29**: 215–233. doi:10.1016/S0921-8009(99)00009-9

Montaggioni, L., and C. Braithwaite. 2009. Quaternary coral reef systems: History, development processes and controlling factors. Elsevier B.V.

Muehllehner, N., C. Langdon, A. Venti, and D. Kadko. 2016. Dynamics of carbonate chemistry, production, and calcification of the Florida Reef Tract (2009–2010): Evidence for seasonal dissolution. Global Biogeochem. Cycles **30**: 661–688. doi:10.1002/2015GB005327

Page, H. N., T. A. Courtney, A. Collins, E. H. De Carlo, and A. J. Andreas. 2017. Net community metabolism and seawater carbonate chemistry scale non-intuitively with coral cover. Front. Mar. Sci. **4**:161. doi:10.3389/fmars.2017.00161

Perry, C. T., G. N. Murphy, P. S. Kench, S. G. Smithers, E. N. Edinger, R. S. Steneck, and P. J. Mumby. 2013. Caribbean-wide decline in carbonate production threatens coral reef growth. Nat. Commun. **4**: 1402. doi:10.1038/ncomms2409

Perry, C. T., and K. M. Morgan. 2017. Bleaching drives collapse in reef carbonate budgets and reef growth potential on southern Maldives Reefs. Nat. Sci. Rep. **7**: 40581. doi:10.1038/srep40581

Shamberger, K. E. F., R. A. Feely, C. L. Sabine, M. J. Atkinson, E. H. DeCarlo, F. T. Mackenzie, P. S. Drupp, and D. A. Butterfield. 2011. Calcification and organic production on a Hawaiian coral reef. Mar. Chem. **127**: 64–75. doi:10.1016/j.marchem.2011.08.003

Smith, S. V. 1973. Carbon dioxide dynamics: A record of organic carbon production, respiration, and calcification

in the Eniwetok reef flat community. Limnol. Oceanogr. **18**: 106–120. doi:10.4319/lo.1973.18.1.0106

Smith, S. V., W. J. Kimmerer, E. A. Laws, R. E. Brock, and T. W. Walsh. 1981. Kaneohe Bay sewage diversion experiment: Perspectives on ecosystem responses to nutritional perturbation. Pac. Sci. **35**: 279–395. doi:hdl.handle.net/10125/616

Watanabe, A., and others. 2006. Analysis of the seawater CO_2 system in the barrier reef-lagoon system of Palau using total alkalinity-dissolved inorganic carbon diagrams. Limnol. Oceanogr. **51**: 1614–1628. doi:10.4319/lo.2006.51.4.1614

Yates, K. K., D. G. Zawada, N. A. Smiley, and G. Tiling-Range. 2017. Divergence of seafloor elevation and sea level rise in coral reef regions. Biogeosciences **14**: 1739–1772. doi:10.5194/bg-14-1739-2017

Acknowledgments

We thank Tyler Cyronak for processing high-resolution satellite imagery of Kāne'ohe Bay, HI that was graciously provided by an imagery grant from the DigitalGlobe Foundation. Two anonymous reviewers are also thanked for improving this manuscript with their helpful comments and suggestions. The authors gratefully acknowledge financial support from the Shepard Foundation (TAC, AJA), National Science Foundation (NSF) Graduate Research Fellowship Program (TAC, HNP), NSF OCE 1255042 (AJA), and a grant/cooperative agreement from the National Oceanic and Atmospheric Administration (NOAA), Project R/IR-27 (EHDC), which is sponsored by the University of Hawai'i Sea Grant College Program, SOEST, under Institutional Grant NA14OAR4170071 from NOAA Office of Sea Grant, Department of Commerce. This is Hawaii Sea Grant contribution number JC-16-08 and SOEST contribution number 10223.

Submitted 24 June 2017
Revised 20 September 2017
Accepted 12 November 2017

Chapter 5, in full, is a reprint of the material as it appears in Courtney TA, De Carlo EH, Page HN, Bahr KD, Barro A, Howins N, Tabata R, Terlouw G, Rodgers KS, Andersson AJ. Recovery of reef-scale calcification following a bleaching event in Kāne'ohe Bay, Hawai'i. *Limnology & Oceanography Letters* 2018, 3:1–9. The dissertation author was the primary investigator and author of this paper.

CHAPTER 6

Disturbances drive changes in coral community assemblages and coral calcification capacity

Courtney TA, Barnes BB, Chollett I, Elahi R, Gross K, Guest JR, Kuffner IB, Lenz EA, Nelson HR, Rogers CS, Toth LT, Andersson AJ

Abstract

Anthropogenic environmental change has increased coral reef disturbance regimes in recent decades, altering the structure and function of many coral reefs globally. In this study, we used survey data collected from 1996 to 2015 to evaluate coral calcification capacity (CCC) dynamics for 121 reef sites in the main Hawaiian Islands, Florida Keys reef tract, Mo'orea (French Polynesia), and St. John (U.S. Virgin Islands). CCC remained relatively high at Hawaiian sites in the absence of recorded widespread disturbances; decreased and remained low following coral bleaching in the Florida Keys reef tract; declined and subsequently recovered in Mo'orea following a crown-of-thorns sea star outbreak, coral bleaching, and major cyclone; and decreased following coral bleaching and disease in St. John. We also observed high variability in CCC vs. coral cover that was in part explained by coral life history strategies, with increased 'weedy' and decreased 'competitive' coral contributions to CCC over time. Global change is therefore predicted to affect the maintenance and stability of CCC through time as the increasing frequency and intensity of disturbances continue to alter coral community composition.

6.1 Introduction

The growth of calcium carbonate ($CaCO_3$) structures is one of the most important functions of a coral reef as these structures provide the foundation for the ecosystem services that reefs provide to humanity (Courtney *et al.* 2017; Cyronak *et al.* 2018; Edmunds *et al.* 2016; Kleypas *et al.* 2001; Perry *et al.* 2018). Scleractinian corals typically account for the majority of $CaCO_3$ production on coral reefs (Montaggioni & Braithwaite 2009) and are therefore critical to the provisioning of shoreline protection, fisheries habitat, and tourism revenue services that coral reefs provide (Moberg & Folke 1999). However, the maintenance of these services is threatened by global and local environmental change that have led to pantropical declines in coral cover

(Bruno & Selig 2007; Gardner *et al.* 2003; Jackson *et al.* 2014) and shifts in coral community composition (Alvarez-Filip *et al.* 2013; Hughes *et al.* 2018; Perry *et al.* 2015), which will likely prevent some coral reefs around the world from keeping up with 21st century sea-level rise (Perry *et al.* 2018).

The frequency and intensity of disturbances shape coral community structure (Connell 1978) with enhanced disturbance regimes typically driving a sustained loss of fast-growing, architecturally complex corals in favor of slow-growing, massive stress-tolerant and/or fast-growing, weedy early-successional colonizers (e.g., Darling *et al.* 2013; Grottoli *et al.* 2014; Hughes *et al.* 2018; Fabricius *et al.* 2011; Loya *et al.* 2001; McClanahan & Maina 2003; McClanahan *et al.* 2008; Van Woesik *et al.* 2011). These differences in coral traits have been further analyzed in the context of hypothesized coral life history strategies, which differentiate 'competitive' (i.e., fast-growing, broadcast spawning corals with branching/plating morphologies) from 'stress-tolerant' (i.e., slow-growing, long-lived, highly fecund, broadcast spawning corals with large corallites, thick tissue, and massive/encrusting morphologies) and 'weedy' (i.e., small-colony, brooding, corals with higher rates of sexual and asexual reproduction) corals with a notable fourth category of 'generalists' representing a mixture of traits found in the previous three groups (Darling *et al.* 2012). Shifts from reefs dominanated by 'competitive' to 'stress-tolerant' and 'weedy' corals can drive declines in reef-scale calcification as evidenced by modeled (Alvarez-Filip *et al.* 2013) and observed (Kuffner & Toth 2016; Lange & Perry 2019; Perry *et al.* 2015; Toth *et al.* 2019) decreases in net coral reef $CaCO_3$ production budgets; however, the impacts of the shifting coral life history strategies on reef-scale calcification through time and across broad geographic spatial scales remains to be rigorously characterized.

In this study, we quantified coral calcification capacity (CCC) across a variety of disturbance regimes using a life history strategies perspective for 121 reef sites surveyed from ~1996 to 2015 across four focal regions in the Pacific (main Hawaiian Islands and Mo'orea) and Western Atlantic (Florida Keys and St. John). We hypothesized that the contribution to CCC by competitive corals would decrease throughout the time series and, in contrast, the contribution to CCC by stress-tolerant and weedy corals would increase owing to alterations of coral communities by disturbances throughout the time series of this study. Our results reveal how disturbance-driven shifts in the species composition of coral communities and overall coral cover drove reef CCC trajectories at our sites in the Pacific and Western Atlantic and how these changes may impact the critical reef-building function of coral reefs now and in the future.

6.2 Materials and methods

6.2.1 *Introduction to focal region surveys and disturbance histories*

The four focal regions analyzed in this study were selected because of publicly available datasets (Guest et al. 2018b) of coral reef benthic surveys (i.e., total and taxon-specific percent coral cover) that were conducted on a range of reef types (e.g., patch, spur and groove, fringing, barrier, forereef, etc.) across a range in depth from 1 to 22 m. The surveys were conducted using standardized protocols at a total of 121 sites surveyed a minimum of three times over at least ten years from ~1996 to 2015 (see Guest *et al.* [2018a] for a complete discussion of sites and survey methods). The data from the focal regions overlap from 2005–2014, but the total length of the time series varied slightly with the main Hawaiian Islands survey data ranging from 1999–2014, Florida Keys reef tract from 1996–2015, Mo'orea from 2005–2015, and St. John from 1999–2015.

In addition to data availability, the focal regions were chosen to include a broad range of disturbance histories during the survey period (see Guest *et al.* (2018a); Fig. 6.1). All focal regions experienced coral bleaching events during the study periods. Bleaching was recorded in 2002, 2004, and 2014 in the main Hawaiian Islands (Bahr *et al.* 2017; Jokiel & Brown 2004; Rodgers *et al.* 2017); 1997, 1998, 2005, 2011, 2014, and 2015 in the Florida Keys (Manzello *et al.* 2007, 2018; Ruzicka *et al.* 2013; Wagner *et al.* 2010); in 2007 in Mo'orea (Adjeroud *et al.* 2018); and in 2005 in St. John (Edmunds 2013; Miller *et al.* 2006, 2009). While the before and after effects of hurricanes were not directly quantified for each site in this study, we considered hurricanes to potentially impact the focal regions if a Category 1–5 storm passed within 100 nautical miles of the following locations during the respective time series of the focal regions in this study: Hilo Harbor, Kahului Harbor, Honolulu Harbor, or Kalaheo (Main Hawaiian Islands); Big Pine Key or Dry Tortugas (Florida Keys reef tract); Virgin Islands National Park (St. John); and Paopao (Mo'orea). Based on these search criteria in the NOAA hurricanes database (https://coast.noaa.gov/hurricanes/), there were two recorded hurricanes in the Main Hawaiian Islands, seven recorded hurricanes in the Florida Keys reef tract, no recorded cyclones in the search region for Mo'orea but waves from Cyclone Oli impacted some reefs in 2010 (Adjeroud *et al.* 2018; Han *et al.* 2016), and seven recorded hurricanes in St. John (Fig. 6.1). The Florida Keys also experienced a cold-water coral mortality event due to anomalously cold winter temperatures in 2010 (Kemp *et al.* 2011; Lirman *et al.* 2011; Ruzicka *et al.* 2013). Mo'orea additionally experienced a crown-of-thorns sea star (COTS), *Acanthaster planci*, outbreak from 2006–2010 (Adam *et al.* 2011; Adjeroud *et al.* 2018; Han *et al.* 2016; Pratchett *et al.* 2011). In St. John, a prolonged period of coral disease occurred from 2005–2007 following the 2005 coral bleaching event (Edmunds 2013; Miller *et al.* 2006, 2009). As a result of these extensive, yet

variable, disturbance histories and dissimilar initial coral community compositions across sites, there is a large variation in coral cover and community compositions over time across the focal regions, which allowed us to evaluate the community-level drivers of CCC for a range of coral reefs across ocean basins between ~1996 and 2015.

6.2.2 *Coral calcification capacity*

We define CCC as an estimate of the annual calcification rate (kg $CaCO_3$ m^{-2} y^{-1}) of the coral community on a reef. Although CCC as defined here is similar to the gross carbonate production terms calculated as part of complete $CaCO_3$ budgets (e.g., Chave *et al.* 1972; Hubbard *et al.* 1990; Perry *et al.* 2012; Stearn *et al.* 1977), our analysis does not include non-coral $CaCO_3$ producers, $CaCO_3$ export/loss terms (Kleypas *et al.* 2001), or local variability in calcification rates through space and time owing to genetic variability and the environmental drivers of coral calcification (e.g., Pratchett *et al.* 2015). Because data on the percent cover of coral taxa are more commonly collected than the complete community census required for traditional $CaCO_3$ budget calculations (see Perry *et al.* 2012), the CCC method should allow for retrospective analysis of mean capacity for annual coral community calcification in most historical time series studies. The usage of CCC as an ecologically meaningful metric is supported by previous studies showing that corals are typically the dominant coral reef $CaCO_3$ producers (Montaggioni & Braithwaite 2009) and by the high degree of agreement between coral colony and reef-scale calcification (Courtney *et al.* 2016, 2017).

To calculate temporal trends in CCC for our focal regions, we first estimated annual calcification rates of individual scleractinian coral and hydrozoan *Millepora* taxa (hereafter collectively referred to as "corals") as the product of published taxon-specific linear extension rates (cm y^{-1}), skeletal density (g $CaCO_3$ cm^{-3}), and a growth form adjustment factor that

estimates the void space between topographic features generated by complex (i.e., branching, plating, corymbose, digitate, columnar, foliose, sub-massive) morphologies following established methods (Morgan & Kench 2012). We additionally tested for differences in calcification capacity based solely on the taxa present in each of the focal regions by calculating mean calcification rates for all taxa surveyed in each focal region. The contribution of each species to annual, reef-wide calcification was then determined by multiplying taxon-specific calcification rates (kg $CaCO_3$ m^{-2} y^{-1}) by their respective planar benthic cover (%) after Perry *et al.* (2012) and Guest *et al.* (2018a). Reef-wide calcification rates were calculated for each species where species-level benthic cover data were available (main Hawaiian Islands, Florida Keys reef tract, St. John) and by genus for Mo'orea, where benthic cover was surveyed at the genus level. Annual reef CCC (kg $CaCO_3$ m^{-2} y^{-1}) was then determined by summing the calcification (kg $CaCO_3$ m^{-2} y^{-1}) by all coral taxa. The average of CCC across all surveyed sites within a focal region for each given year was calculated to visualize the changes in mean annual CCC through time.

6.2.3 *Dominant calcifying corals and life history strategies*

We parsed the contribution of each taxon to mean annual CCC in each focal region to identify the dominant calcifying taxa, which were defined in this study as taxa that contributed at least an average of 5% to the total CCC across all sites in each focal region for the duration of the time series. It is important to note, however, that surveys of the Main Hawaiian Islands reef sites in this study were non-uniformly distributed across space and time, which preclude any robust conclusions about the changes in mean annual CCC through time for this focal region. Because there is a substantial amount of variation between the relationship of CCC and percent coral cover (Guest *et al.* 2018a), hypothetical scaling of calcification rates for each of the

dominant calcifying corals from 0–100% cover were superimposed on plots relating percent coral cover and CCC to graphically visualize the effects of coral community composition on CCC (Fig. 6.2) Points with higher CCC for a given level of coral cover therefore have a greater dominance by faster calcifying (i.e., ≥ 20 kg $CaCO_3$ m^{-2} yr^{-1}) corals and conversely sites with a lower CCC for a given level of coral cover have a greater dominance by slower calcifying (i.e., ≤ 10 kg $CaCO_3$ m^{-2} yr^{-1}) corals. The dominant calcifying corals were then characterized as competitive, stress-tolerant, weedy, or generalist *sensu* Darling *et al.* (2012) to evaluate whether life history strategy classifications predict shifts in contribution to CCC throughout the time series in each of the focal regions of this study.

6.2.4 *Statistical analyses*

Statistical models were developed in *R* (R Core Team 2017) to test whether contributions by the dominant calcifying taxa to CCC shifted during the time series in each of the focal regions and whether these changes match classifications and expectations for the respective coral life history strategies following disturbances (Darling *et al.* 2012, 2013). To accomplish this task of evaluating long-term changes in the percent contribution of calcifying taxa to CCC, linear mixed effects models were constructed to test whether year was a significant ($p < 0.05$) predictor of percent contribution to CCC by each of the dominant calcifying taxa. Significant slopes indicate whether there were statistically significant mean increases (positive slope), statistically significant mean decreases (negative slope), or non-significant changes (zero slope) in the contribution of the dominant calcifying corals to CCC for the duration of the time series for each of the focal regions. Statistical models used the percentage of annual site-level CCC by each dominant calcifying genus as the response and included fixed effects for year and a random intercept and slope for each site. Random intercepts and slopes for each site were included to

account for the fact that each site had a different initial percent contributions of dominant calcifying coral to CCC (random intercepts) and that each site had difference disturbance histories resulting in variable responses in dominant calcifying coral contributions to CCC over time (random slopes). Models were fit using the *R* package *nlme* (Pinheiro *et al.* 2017), and parameters were estimated by maximum likelihood. Because sites were repeatedly surveyed through time, a continuous autocorrelation correlation structure (*corCAR1* in package *nlme*) was included in each model to account for temporal autocorrelation (Pinheiro *et al.* 2017).

6.3 Results

Mean of focal region CCC (mean ± 95% confidence intervals) through time was generally higher for the Pacific focal regions than Western Atlantic focal regions (Fig. 6.1). Additionally, mean (±95% confidence intervals) calcification rates for all surveyed taxa in the Pacific focal regions were slightly greater (Main Hawaiian Islands = 14.1±3.6 kg $CaCO_3$ m^{-2} yr^{-1} and Mo'orea = 14.1±2.1 kg $CaCO_3$ m^{-2} yr^{-1}) than the Western Atlantic focal regions (Florida Keys reef tract =10.1±3.0 kg $CaCO_3$ m^{-2} yr^{-1} and St. John = 10.0±2.2 kg $CaCO_3$ m^{-2} yr^{-1}). CCC for the main Hawaiian Islands was consistently the highest of the four focal regions although the large interannual variability resulting from non-uniform sampling efforts (i.e., not all sites were surveyed in all years) and relatively larger, overlapping confidence intervals preclude any formal conclusions about changes in CCC through time. In the Florida Keys CCC (mean ±95% confidence intervals) decreased following the 1997/1998 coral bleaching events from 1.7±0.4 kg $CaCO_3$ m^{-2} yr^{-1} in 1996 to 1.0±0.3 kg $CaCO_3$ m^{-2} yr^{-1} in 2000 and remained approximately stable afterwards (Fig. 6.1). In Mo'orea CCC declined following a combination of a crown-of-thorns outbreak (2006–2010), coral bleaching (2007), and Cyclone Oli (2010) from 4.8±0.5 kg $CaCO_3$ m^{-2} yr^{-1} in 2006 to a minimum of 1.5±0.8 kg $CaCO_3$ m^{-2} yr^{-1} in 2012 and then increased to

2.5±0.8 kg $CaCO_3$ m^{-2} yr^{-1} in 2015 (Fig. 6.1). CCC in St. John increased slightly from 0.6±0.5 kg $CaCO_3$ m^{-2} yr^{-1} in 1999 to 1.1±0.6 kg $CaCO_3$ m^{-2} yr^{-1} in 2005 and then decreased with the 2005 coral bleaching event and associated 2005–2007 disease outbreak to 0.5±0.3 kg $CaCO_3$ m^{-2} yr^{-1} and remained approximately stable thereafter (Fig. 6.1).

Twelve species representing nine genera of corals out of the 84 species and 50 genera surveyed in this study were identified as the dominant calcifying taxa (i.e., calcified mean ≥ 5% of total CCC across all sites and all years for the respective time series) across the four focal regions with *Acropora*, *Montipora*, *Pavona*, *Pocillopora*, and *Porites* spp. contributing the most to CCC in the Pacific and *Acropora*, *Millepora*, *Montastraea*, *Orbicella*, *Porites*, and *Siderastrea* spp. in the Western Atlantic (Fig. 6.1, Table 6.1). The dominant calcifying species were further characterized by life history strategies *sensu* Darling *et al.* (2012) to evaluate the respective changes of the dominant calcifying corals with respect to life history strategies (Table 6.1). Although CCC generally increases with increasing coral cover (Guest et al. 2018a) there is high variability in that relationship as a result of spatial variability in coral community composition (Fig. 6.2; Guest *et al.* [2018]). In the Main Hawaiian Islands, which have sites with the highest coral cover out of any of the focal regions, CCC vs. coral cover generally falls along the trajectories predicted for *Montipora* spp. or *Porites lobata* corals (Fig. 6.2). In the Florida Keys reef tract, where most reef sites have comparatively lower coral cover trajectories, the data follow the trajectories predicted for the *Orbicella annularis* complex/*Montastraea cavernosa* or *Acropora palmata* (Fig. 6.2). Coral cover in Mo'orea was greater for many sites than the Western Atlantic and whereas the data for some sites appear to follow the trajectory predicted for a mixed *Montipora*/*Acropora* community, most sites appear to follow the *Porites* calcification trajectory (Fig. 6.2). Lastly, in St. John the CCC vs. coral cover data suggests that nearly every

site survey follows the trajectory predicted for the *Orbicella annularis* complex/*Montastraea cavernosa* (Fig. 6.2) owing to the dominance of *Orbicella annularis* complex calcification for this focal region (Fig. 6.1D).

To assess whether calcification by each of the dominant calcifying taxa was consistent with life history strategy expectations of shifting coral cover following disturbances (Darling *et al.* 2012, 2013), long-term changes of percent contribution by each of the dominant calcifying corals to total CCC across all sites for the duration of the time series were assessed using linear mixed effects models. In this analysis, positive slopes indicate mean increases in the percent contribution of the respective coral to CCC within the focal region over the time series whereas the opposite is true for corals with negative slopes and non-significant slopes indicate no change in coral contribution to CCC (Fig. 6.3, Table 6.1). In the main Hawaiian Islands, percent of CCC by *Montipora capitata* (competitive) increased, *Porites compressa* (competitive) decreased, and the other dominant calcifiers did not change significantly (Fig. 6.3A, Table 6.1). Conversely, in the Florida Keys, all dominant calcifying corals shifted their relative contributions to CCC wherein percent of CCC by *Millepora alcicornis* (weedy), *Porites astreoides* (weedy), and *Siderastrea siderea* (stress-tolerant) increased, and *Acropora palmata* (competitive), *Montastraea cavernosa* (stress-tolerant), and *Orbicella annularis* complex (generalist/stress-tolerant) decreased (Fig. 6.3B, Table 6.1). In Mo'orea, percent calcification by *Montipora* spp. (competitive/intermediate/stress-tolerant) increased, *Acropora* spp. (competitive) decreased, and the other dominant calcifiers exhibited no significant change (Fig. 6.3C, Table 6.1). In St. John, percent of CCC by *Porites porites* (weedy) increased, *Orbicella annularis* complex (generalist/stress-tolerant) decreased, and the other dominant calcifiers exhibited no change (Fig. 6.3D, Table 6.1).

6.4 Discussion

Here we have used CCC to retroactively estimate ecologically meaningful $CaCO_3$ production by corals in historical datasets (Guest *et al.* 2018a) to explore the ecological drivers of CCC across the Pacific and Western Atlantic over an approximately 20 year interval. Our results suggest that coral bleaching (Florida Keys, St. John, Mo'orea), coral disease (St. John), and a crown-of-thorns outbreak (Mo'orea) were the dominant drivers of reductions in CCC across the time series of this study and that the declines in CCC were caused by a combination of reduced coral cover and shifting coral community compositions (Figs. 6.1, 6.2, 6.3). This finding agrees with the growing $CaCO_3$ budget and chemistry-based net ecosystem calcification literature showing that coral bleaching events and other disturbances can reduce reef-scale calcification rates (Courtney *et al.* 2018; DeCarlo *et al.* 2017; Kayanne *et al.* 2005; ; Lange & Perry 2019; Perry & Morgan 2017; Perry *et al.* 2008). It is important to note that reduced CCC rates for many of the lower percent coral cover reefs in this study (Fig. 6.2) may be exceeded by rates of $CaCO_3$ bioerosion and dissolution, which highlights the growing need for monitoring these destructive processes on coral reefs to better predict the future of coral reef $CaCO_3$ structures under anthropogenic and climatic change (Andersson & Gledhill 2013; Eyre *et al.* 2018; Kleypas *et al.* 2001; Kuffner *et al.* 2019; Perry *et al.* 2008, 2012, 2018; Van Woesik & Cacciapaglia 2018;). Indeed, recent work has already documented net dissolution across the Florida Keys reef tract (Muehllehner *et al.* 2016) and loss of seafloor elevation occurring for reef ecosystems in the Pacific and Western Atlantic (Yates *et al.* 2017).

Nonetheless, there were some sites with relatively high CCC and high variance in CCC vs. percent coral cover across sites and over time within each focal region (Fig. 6.2), which is consistent with observations from $CaCO_3$ budget assessments for reefs across the Western

Atlantic by Perry *et al.* (2013). Most importantly, some reef sites within the main Hawaiian Islands, Florida Keys, and Mo'orea focal regions have growth trajectories reflecting dominance by faster growing competitive corals (i.e., higher CCC per coral cover reefs along the *Acropora* and *Montipora* growth trajectories with ≥ 20 kg $CaCO_3$ m^{-2} yr^{-1}, Fig. 2 ABC) suggesting those sites may have been "oases" that either experienced fewer disturbances than neighboring sites, locally resisted them, or recovered following disturbances (Guest *et al.* 2018a). Although the hypothesis that some reefs have enhanced abilities to escape, resist, and/or recover from disturbances remains to be empirically tested, the use of CCC presented here serves as a potential means of quantifying the reef-growth potential of coral communities to improve our understanding and projections of future coral reef calcification trajectories.

We further explored changes in CCC by investigating the dominant calcifying corals that contributed at least 5% of the total CCC across the time series in this study (Fig. 6.1) and are potentially useful targets for management and restoration that will be most successful in maintaining reef-scale calcification in the future. However, many of these individual taxa shifted in relative contributions to CCC over the time series in this study. For example, the dominant calcifying taxa *Montipora capitata*, *Millepora alcicornis*, *Porites astreoides*, *Siderastrea siderea*, and *Porites porites* increased in relative contributions to CCC across the Main Hawaiian Islands, Florida Keys, and St. John (*Montipora* spp. also increased in Mo'orea; Fig. 6.3, Table 6.1) suggesting they are becoming increasingly important reef builders in the 21st century. Conversely, *Porites compressa*, *Acropora palmata, Montastraea cavernosa*, and *Orbicella annularis* complex (*Acropora* spp. decreased in Mo'orea; Fig. 6.3, Table 6.1) decreased in mean contributions to CCC across the focal regions over the time series in this study and are likely to make diminishing contributions to future reef building.

Dominant calcifying corals were classified by life history strategies to test whether hypothesized expected decreases in competitive corals and increases in weedy, stress-tolerant, and generalist corals following disturbances (Darling *et al.* 2012, 2013) could explain the changes in CCC observed in this study (Fig. 6.2, Table 6.1). Following the major coral bleaching, crown-of-thorns, and disease disturbance events across the focal regions in this study, all of the competitive *Acropora* spp. corals decreased and the weedy *Millepora alcicornis*, *Porites astreoides*, and *Porites porites* corals increased in all locations except for St. John (*Porites astreoides* CCC increased 0.29±0.15 % CCC yr^{-1} in St. John, but this change was marginally statistically significant at p=0.054), which is congruent with Darling *et al.* (2012) expectations for competitive and weedy corals under elevated thermal stress. The generalist/stress-tolerant *Orbicella annularis* complex corals decreased in mean CCC contributions throughout the time series across both the Florida Keys and St. John focal regions, which would agree with potential outcomes for generalist but not for stress-tolerant life history strategies under thermal stress. It is important to note however that *O. annularis* complex was disproportionally affected by white plague disease in St. John (Miller *et al.* 2009), highlighting the importance of considering disease susceptibility in the framework of shifting coral communities and life history strategies. Lastly, mean CCC by stress-tolerant *Montastraea cavernosa* decreased and *Siderastrea siderea* increased across the Florida Keys (*Siderastrea siderea* CCC decreased –0.18 ±0.16 albeit not significantly at p = 0.269 in St. John), which respectively contradicts and agrees with hypothesized stress-tolerant life history expectations under thermal stress for these corals (Darling *et al.* 2012). Thus, while the changes in competitive and weedy corals in this study appear to agree well with hypothesized life history expectations for thermal stress, the responses of generalist and stress-tolerant corals to CCC are

somewhat less consistent. Some of these discrepancies could in part be due to the widespread coral disease in St. John and/or other more localized drivers of coral community shifts and warrants further investigation to improve future projections of coral reef community structures and CCC.

The declines in contributions to CCC by competitive corals following disturbances in this study imply future projected decreases in overall CCC under predicted increasing coral bleaching and disease disturbance frequencies and intensities (Donner *et al.* 2005; Randall & van Woesik 2015, 2017; Van Hooidonk *et al.* 2016). These findings agree with previously observed declines in *Acropora* corals owing to coral bleaching and disease in recent decades (e.g., Aronson & Precht 2001; Hughes *et al.* 2018; Loya *et al.* 2001; Perry & Morgan 2017). The relative contribution to CCC by weedy corals may continue to increase as has been observed by the current dominance of non-framework building coral calcification in the Western Atlantic (Perry *et al.* 2015). However, observed fluctuations in weedy coral cover following disturbance events (Brown & Edmunds 2013; Darling *et al.* 2013) could drive corresponding interannual fluctuations in CCC. This suggests reefs with increased weedy CCC may therefore maintain less stable CCC through time (Alvarez-Filip *et al.* 2013), but, nevertheless, reefs with a veneer of weedy corals can reduce physical loss of $CaCO_3$ by rendering the reef framework less accessible to destructive grazing (Kuffner & Toth 2016; Toth *et al.* 2018). Additionally, the observed increase in contributions of some of the stress-tolerant corals in this study to CCC will likely decrease CCC for a given coral cover due to their generally slower calcification rates, but the greater bleaching resistance hypothesized for many of these stress-tolerant corals (e.g., Darling *et al.* 2013; Loya *et al.* 2001; McClanahan & Maina 2003; McClanahan *et al.* 2008; Van Woesik *et al.* 2011) may act to stabilize CCC under increased thermal stress (e.g., Ryan *et al.* 2019).

Further research should therefore also be conducted to rigorously quantify coral and reef-scale bleaching/disease resistance and recovery rates to better predict future bleaching-induced changes in CCC and coral reef $CaCO_3$ structures (e.g., Courtney *et al.* 2018; Gouezo *et al.* 2019; Mizerek *et al.* 2018, Ortiz *et al.* 2018; Swain *et al.* 2016; van woesik *et al.* 2018).

The observations of higher overall mean CCC and slightly greater mean calcification rates for surveyed taxa in the Pacific focal regions relative to the Western Atlantic focal regions (Figs. 6.1, 6.2) are congruent with the suggestion of greater functional redundancy of competitive coral life history traits in the Pacific relative to the Western Atlantic (Kuffner & Toth 2016; McWilliam *et al.* 2018). Fast-growing corals *Acropora cervicornis* and *Acropora palmata* were once widespread, dominant calcifiers in the Western Atlantic, but declined in the late 1970s and 1980s primarily due to white band disease and hurricanes (Aronson & Precht 2001; Kuffner & Toth 2016; Toth *et al.* 2019) and are no longer major $CaCO_3$ producers in this region (Perry *et al.* 2015). Thus, coral bleaching and disease appear to be the widespread drivers of declining CCC across the time series for the Western Atlantic focal regions, whereas coral bleaching and crown-of-thorns appeared to be the dominant drivers of declines in CCC in the Pacific focal region of Mo'orea. However, mean CCC in Mo'orea showed signs of recovery following these disturbance-induced CCC declines (Fig. 6.1C). The absence of significant and widespread recorded pulse disturbances (e.g., the 2002 and 2004 bleaching events were minor and the reefs recovered [Bahr *et al.* 2017]) and the large interannual CCC variability with overlapping 95% confidence intervals preclude any similar conclusions about CCC and disturbance events in the main Hawaiian Islands; however, widespread bleaching in Hawai'i was recorded in 2014 and 2015 at the conclusion of the time series in this study (Bahr *et al.* 2017;

Rodgers *et al.* 2017), with reduced reef-scale calcification observed for at least one reef system in the main Hawaiian Islands (Courtney *et al.* 2018).

As many coral reefs around the world continue to decline in coral cover and shift in coral species compositions under increasing frequencies of coral bleaching and other disturbances (Bruno & Selig 2007; Donner *et al.* 2005; Gardner *et al.* 2003; Hughes *et al.* 2018; Jackson *et al.* 2014; Van Hooidonk *et al.* 2016), metrics that evaluate historical reef condition from coral community data such as CCC may prove useful for understanding previous changes and projecting future coral reef $CaCO_3$ structures and functions. Likewise, evaluation of the ecological drivers of CCC in the context of coral life-history strategies and coral-reef disturbances could easily expand reef monitoring programs to include estimates and projections of $CaCO_3$ production. Nonetheless, the future of CCC for any given reef site relies on the reduction of the magnitude and frequency of coral reef disturbances through both global (i.e., reduction of greenhouse gas emissions that drive ocean warming and acidification) and local (e.g., reduction of land-based pollution, overfishing, and habitat destruction) efforts.

6.5 Acknowledgments

This paper is dedicated to Ruth D. Gates and was, in part, a product of the U.S. Geological Survey (USGS) John Wesley Powell Center for Analysis and Synthesis working group "Local-scale ecosystem resilience amid global-scale ocean change: the coral reef example" supported by funding awarded to P. J. Edmunds, R. D. Gates, and I. B. Kuffner with a Powell Fellowship to J. R. Guest. TAC and AJA additionally received funding from the National Science Foundation. We thank P. J. Edmunds and J. Miller for improving this manuscript with their helpful comments and the Powell Center for their support of the working group. We thank

K. Rodgers, E. Brown, R. Ruzicka, M. Colella, J. Miller, A. Atkinson, and M. Feely for providing the raw data used in this study that are now published in a USGS data release https://doi.org/10.5066/F78W3C7W. All *R* code with associated data files used in this analysis will be made publicly available on GitHub at https://github.com/traviscourtney/PowellCCC. Any use of trade, firm, or product names is for descriptive purposes only and does not imply endorsement by the U.S. Government. The authors declare no conflict of interest.

6.6 References

Adam, T.C., Schmitt, R.J., Holbrook, S.J., Brooks, A.J., Edmunds, P.J., Carpenter, R.C., Bernardi, G. (2011). Herbivory, connectivity, and ecosystem resilience: Response of a coral reef to a large-scale perturbation. *PLoS One*, 6, e23717.

Adjeroud, M., Michonneau, F., Edmunds, P.J., Chancerelle, Y., de Loma, T.L., Penin, L., Thibaut, L., Vidal-Dupiol, J., Salvat, B., Galzin, R. (2018). Recurrent disturbances, recovery trajectories, and resilience of coral assemblages on a South Central Pacific reef. *Sci. Rep.*, 8, 1–8.

Alvarez-Filip, L., Carricart-Ganivet, J.P., Horta-Puga, G., Iglesias-Prieto, R. (2013). Shifts in coral-assemblage composition do not ensure persistence of reef functionality. *Sci. Rep.*, 3, 3486.

Andersson, A.J. & Gledhill, D. (2013). Ocean Acidification and Coral Reefs: Effects on Breakdown, Dissolution, and Net Ecosystem Calcification. *Ann. Rev. Mar. Sci.*, 5, 321–348.

Aronson, R.B. & Precht, W.F. (2001). White band diseases and the changing face of Caribbean coral reefs. *Hydrobiologia*, 460, 25–38.

Bahr, K.D., Rodgers, K.S., Jokiel, P.L. (2017). Impact of Three Bleaching Events on the Reef Resiliency of Kāneʻohe Bay, Hawaiʻi. *Front. Mar. Sci.*, 4.

Brown, D. & Edmunds, P.J. (2013). Long-term changes in the population dynamics of the Caribbean hydrocoral *Millepora* spp. *J. Exp. Mar. Bio. Ecol.*, 441, 62–70.

Bruno, J.F. & Selig, E.R. (2007). Regional decline of coral cover in the Indo-Pacific: Timing, extent, and subregional comparisons. *PLoS One*, 2, e711.

Chave, K.E., Smith, S. V., Roy, K.J. (1972). Carbonate production by coral reefs. *Mar. Geol.*, 12, 123–140.

Connell, J.H. (1978). Diversity in Tropical Rain Forests and Coral Reefs. *Science*, 199, 1302–1310.

Courtney, T.A., Andersson, A.J., Bates, N.R., Collins, A., Cyronak, T., de Putron, S.J., Eyre, B.D., Garley, R., Hochberg, E.J., Johnson, R., Musielewicz, S., Noyes, T.J., Sabine, C.L., Sutton, A.J., Toncin, J., Tribollet, A. (2016). Comparing Chemistry and Census-Based Estimates of Net Ecosystem Calcification on a Rim Reef in Bermuda. *Front. Mar. Sci.*, 3, 181.

Courtney, T.A., De Carlo, E.H., Page, H.N., Bahr, K.D., Barro, A., Howins, N., Tabata, R., Terlouw, G., Rodgers, K.S., Andersson, A.J. (2018). Recovery of reef-scale calcification following a bleaching event in Kāne'ohe Bay, Hawai'i. *Limnol. Oceanogr. Lett.*, 3, 1–9.

Courtney, T.A., Lebrato, M., Bates, N.R., Collins, A., de Putron, S.J., Garley, R., Johnson, R., Molinero, J.C., Noyes, T.J., Sabine, C.L., Andersson, A.J. (2017). Environmental controls on modern scleractinian coral and reef-scale calcification. *Sci. Adv.*, 3, e1701356.

Cyronak, T., Andersson, A.J., Langdon, C., Albright, R., Bates, N.R., Caldeira, K., Carlton, R., Corredor, J.E., Dunbar, R.B., Enochs, I., Erez, J., Eyre, B.D., Gattuso, J.P., Gledhill, D., Kayanne, H., Kline, D.I., Koweek, D.A., Lantz, C., Lazar, B., Manzello, D., McMahon, A., Meléndez, M., Page, H.N., Santos, I.R., Schulz, K.G., Shaw, E., Silverman, J., Suzuki, A., Teneva, L., Watanabe, A., Yamamoto, S. (2018). Taking the metabolic pulse of the world's coral reefs. *PLoS One*, 13, 1–17.

Darling, E.S., Alvarez-Filip, L., Oliver, T.A., Mcclanahan, T.R., Cote, I.M. (2012). Evaluating life-history strategies of reef corals from species traits. *Ecol. Lett.*, 15, 1378–1386.

Darling, E.S., McClanahan, T.R., Côté, I.M. (2013). Life histories predict coral community disassembly under multiple stressors. *Glob. Chang. Biol.*, 19, 1930–1940.

DeCarlo, T.M., Cohen, A.L., Wong, G.T.F., Shiah, F., Lentz, S.J., Davis, K.A., Shamberger, K.E.F., Lohmann, P. (2017). Community production modulates coral reef pH and the sensitivity of ecosystem calcification to ocean acidification. *J. Geophys. Res. Ocean.*, 122, 745–761.

Donner, S.D., Skirving, W.J., Little, C.M., Oppenheimer, M., Hoegh-Gulberg, O. (2005). Global assessment of coral bleaching and required rates of adaptation under climate change. *Glob. Chang. Biol.*, 11, 2251–2265.

Edmunds, P.J. (2013). Decadal-scale changes in the community structure of coral reefs of St. John, US Virgin Islands. *Mar. Ecol. Prog. Ser.*, 489, 107–123.

Edmunds, P.J., Comeau, S., Lantz, C., Andersson, A., Briggs, C., Cohen, A., Gattuso, J.P., Grady, J.M., Gross, K., Johnson, M., Muller, E.B., Ries, J.B., Tambutté, S, Tambutté, E., Venn, A., Carpenter, R.C. (2016). Integrating the Effects of Ocean Acidification across Functional Scales on Tropical Coral Reefs. *Bioscience*, 66, 350–362.

Eyre, B.D., Cyronak, T., Drupp, P., Carlo, E.H. De, Sachs, J.P., Andersson, A.J. (2018). Coral reefs will transition to net dissolving before end of century. *Science*, 359, 908–911.

Fabricius, K.E., Langdon, C., Uthicke, S., Humphrey, C., Noonan, S., De 'ath, G., Okazaki, R., Muehllehner, N., Glas, M.S., Lough, J.M. (2011). Losers and winners in coral reefs acclimatized to elevated carbon dioxide concentrations. *Nat. Clim. Chang.*, 1, 165–169.

Gardner, T.A., Cote, I.M., Gill, J.A., Grant, A., Watkinson, A.R. (2003). Long-Term Region-Wide Declines in Caribbean Corals. *Science*, 301, 958–960.

Gouezo, M., Golbuu, Y., Fabricius, K., Olsudong, D., Mereb, G., Nestor, V., Wolanski, E., Harrison, P., Doropoulos, C. (2019). Drivers of recovery and reassembly of coral reef communities. *Proceedings of the Royal Society B*, 286, 20182908.

Grottoli, A.G., Warner, M.E., Levas, S.J., Aschaffenburg, M.D., Schoepf, V., Mcginley, M., Baumann, J., Matsui, Y. (2014). The cumulative impact of annual coral bleaching can turn some coral species winners into losers. *Glob. Chang. Biol.*, 20, 3823–3833.

Guest, J.R., Edmunds, P.J., Gates, R.D., Kuffner, I.B., Andersson, A.J., Barnes, B.B., Chollett, I., Courtney, T.A., Elahi, R., Gross, K., Lenz, E.A., Mitarai, S., Mumby, P.J., Nelson, H.R., Parker, B.A., Putnam, H.M., Rogers, C.S., Toth, L.T. (2018a). A framework for identifying and characterising coral reef "oases" against a backdrop of degradation. *J. Appl. Ecol.*, 55, 2867–2875.

Guest, J.R., Edmunds, P.J., Gates, R.D., Kuffner, I.B., Brown, E.K., Rodgers, K.S., Jokiel, P.L., Ruzicka, R.R., Colella, M.A., Miller, J., Atkinson, A., Feeley, M.W., Rogers, C.S. (2018b). Time-series coral-cover data from Hawaii, Florida, Moorea, and the Virgin Islands. *United States Geol. Surv. data release*.

Han, X., Adam, T.C., Schmitt, R.J., Brooks, A.J., Holbrook, S.J. (2016). Response of herbivore functional groups to sequential perturbations in Moorea , French Polynesia. *Coral Reefs*, 35, 997–1007.

Van Hooidonk, R., Maynard, J., Tamelander, J., Gove, J., Ahmadia, G., Raymundo, L., Williams, G., Heron, S.F., Planes, S. (2016). Local-scale projections of coral reef futures and implications of the Paris Agreement. *Sci. Rep.*, 6, 39666.

Hubbard, D.K., Miller, A.I., Scaturo, D. (1990). Production and cycling of calcium carbonate in a shelf-edge reef system (St. Croix, U.S. Virgin Islands): Applications to the nature of reef systems in the fossil record. *J. Sediment. Petrol.*, 3, 335–360.

Hughes, T.P., Kerry, J.T., Baird, A.H., Connolly, S.R., Dietzel, A., Eakin, C.M., Heron, S.F., Hoey, A.S., Hoogenboom, M.O., Liu, G., McWilliam, M.J., Pears, R.J., Pratchett, M.S., Skirving, W.J., Stella, J.S., Torda, G. (2018). Global warming transforms coral reef assemblages. *Nature*, 556, 492.

Jackson, J.B.C., Donovan, M.K., Cramer, K.L., Lam, V. (2014). *Status and Trends of Caribbean Coral Reefs : 1970-2012*. *Glob. Coral Reef Monit. Netw.* Global Coral Reef Monitoring Network, IUCN, Gland.

Jokiel, P.L. & Brown, E.K. (2004). Global warming, regional trends and inshore environmental conditions influence coral bleaching in Hawaii. *Glob. Chang. Biol.*, 10, 1627–1641.

Kayanne, H., Hata, H., Kudo, S., Yamano, H., Watanabe, A., Ikeda, Y., Nozaki, K., Kato, K., Negishi, A., Saito, H. (2005). Seasonal and bleaching-induced changes in coral reef metabolism and CO_2 flux. *Global Biogeochem. Cycles*, 19, 1–11.

Kemp, D.W., Oakley, C.A., Thornhill, D.J., Newcomb, L.A., Schmidt, G.W., Fitt, W.K. (2011). Catastrophic mortality on inshore coral reefs of the Florida Keys due to severe low-temperature stress. *Glob. Chang. Biol.*, 17, 3468–3477.

Kleypas, J.A., Buddemeier, R.W., Gattuso, J.P. (2001). The future of coral reefs in an age of global change. *Int. J. Earth Sci.*, 90, 426–437.

Knowlton, N., Brainard, R.E., Fisher, R., Moews, M., Plaisance, L., Caley, M.J. (2010). Coral Reef Biodiversity. In: *Life in the World's Oceans: Diversity, Distribution, and Abundance* (ed. McIntyre, A.D.). Wiley-Blackwell, Oxford, pp. 65–77.

Kuffner, I.B. & Toth, L.T. (2016). A geological perspective on the degradation and conservation of western Atlantic coral reefs. *Conserv. Biol.*, 30, 706–715.

Kuffner, I. B., Toth, L. T., Hudson, J. H., Goodwin, W. B., Stathakopoulos, A., Bartlett, L. A., Whitcher, E. M. (2019). Improving estimates of coral reef construction and erosion with in situ measurements. *Limnology and Oceanography*.

Lange, I.D. & Perry, C.T. (2019). Bleaching impacts on carbonate production in the Chagos Archipelago: influence of functional coral groups on carbonate budget trajectories. *Coral Reefs*, 1–6.

Lirman, D., Schopmeyer, S., Manzello, D., Gramer, L.J., Precht, W.F., Muller-Karger, F., Banks, K., Barnes, B., Bartels, E., Bourque, A., Byrne, J., Donahue, S., Duquesnel, J., Fisher, L., Gilliam, D., Hendee, J., Johnson, M., Maxwell, K., McDevitt, E., Monty, J., Rueda, D., Ruzicka, R., Thanner, S. (2011). Severe 2010 cold-water event caused unprecedented mortality to corals of the Florida reef tract and reversed previous survivorship patterns. *PLoS One*, 6, e23047.

Loya, Y., Sakai, K., Yamazato, K., Nakano, Y., Sambali, H., Van Woesik, R. (2001). Coral bleaching: The winners and the losers. *Ecol. Lett.*, 4, 122–131.

Manzello, D.P., Berkelmans, R., Hendee, J.C. (2007). Coral bleaching indices and thresholds for the Florida Reef Tract, Bahamas, and St. Croix, US Virgin Islands. *Mar. Pollut. Bull.*, 54, 1923–1931.

Manzello, D.P., Enochs, I.C., Kolodziej, G., Carlton, R., Valentino, L. (2018). Resilience in carbonate production despite three coral bleaching events in 5 years on an inshore patch reef in the Florida Keys. *Mar. Biol.*, 165.

McClanahan, T. R. & Maina, J. (2003). Response of coral assemblages to the interaction between natural temperature variation and rare warm-water events. Ecosystems, 6, 551-563.

McClanahan, T. R., Weil, E., Cortés, J., Baird, A. H., Ateweberhan, M. (2009). Consequences of coral bleaching for sessile reef organisms. In *Coral bleaching* (pp. 121-138). Springer, Berlin, Heidelberg.

McWilliam, M., Hoogenboom, M.O., Baird, A.H., Kuo, C., Madin, J.S., Hughes, T.P. (2018). Biogeographical disparity in the functional diversity and redundancy of corals. *Proc. Natl. Acad. Sci.*, 115, 3084–3089.

Miller, J., Muller, E., Rogers, C., Waara, R., Atkinson, A., Whelan, K.R.T., Patterson, M., Witcher, B. (2009). Coral disease following massive bleaching in 2005 causes 60% decline in coral cover on reefs in the US Virgin Islands. *Coral Reefs*, 28, 925–937.

Miller, J., Waara, R., Muller, E., Rogers, C. (2006). Coral bleaching and disease combine to cause extensive mortality on reefs in US Virgin Islands. *Coral Reefs*, 25, 418.

Mizerek, T.L., Baird, A.H., Madin, J.S. (2018). Species traits as indicators of coral bleaching. *Coral Reefs*, 37, 791–800.

Moberg, F. & Folke, C. (1999). Ecological goods and services of coral reef ecosystems. *Ecol. Econ.*, 29, 215–233.

Montaggioni, L.F. & Braithwaite, C.J.R. (2009). *Quaternary coral reef systems: history, development processes and controlling factors*. Elsevier.

Morgan, K.M. & Kench, P.S. (2012). Skeletal extension and calcification of reef-building corals in the central Indian Ocean. *Mar. Environ. Res.*, 81, 78–82.

Muehllehner, N., Langdon, C., Venti, A., Kadko, D. (2016). Dynamics of carbonate chemistry, production, and calcification of the Florida Reef Tract (2009–2010): Evidence for seasonal dissolution. *Global Biogeochem. Cycles*, 30, 661–688.

Ortiz, J.C., Wolff, N.H., Anthony, K.R., Devlin, M., Lewis, S., Mumby, P.J. (2018). Impaired recovery of the Great Barrier Reef under cumulative stress. *Science advances*, 4, eaar6127.

Perry, C.T., Alvarez-Filip, L., Graham, N.A.J., Mumby, P.J., Wilson, S.K., Kench, P.S., Manzello, D.P, Morgan, K.M., Slangen, A.B.A., Thomson, D.P., Januchowski-Hartley, F., Smithers, S.G., Steneck, R.S., Carlton, R., Edinger, E.N., Enochs, I.C., Estrada-Saldívar, N., Haywood, M.D.E., Kolodziej, G., Murphy, G.N., Pérez-Cervantes, E.,

Suchley, A., Valentino, L., Boenish., Wilson,. M., Macdonald, C. (2018). Loss of coral reef growth capacity to track future increases in sea level. *Nature*, 558, 396.

Perry, C.T., Edinger, E.N., Kench, P.S., Murphy, G.N., Smithers, S.G., Steneck, R.S., Mumby, P.J. (2012). Estimating rates of biologically driven coral reef framework production and erosion: A new census-based carbonate budget methodology and applications to the reefs of Bonaire. *Coral Reefs*, 31, 853–868.

Perry, C.T. & Morgan, K.M. (2017). Bleaching drives collapse in reef carbonate budgets and reef growth potential on southern Maldives reefs. *Sci. Rep.*, 7, 40581.

Perry, C.T., Murphy, G.N., Kench, P.S., Smithers, S.G., Edinger, E.N., Steneck, R.S., Mumby, P.J. (2013). Caribbean-wide decline in carbonate production threatens coral reef growth. *Nat. Commun.*, 4, 1402.

Perry, C.T., Spencer, T., Kench, P.S. (2008). Carbonate budgets and reef production states: A geomorphic perspective on the ecological phase-shift concept. *Coral Reefs*, 27, 853–866.

Perry, C.T., Steneck, R.S., Murphy, G.N., Kench, P.S., Edinger, E.N., Smithers, S.G., Mumby, P.J. (2015). Regional-scale dominance of non-framework building corals on Caribbean reefs affects carbonate production and future reef growth. *Glob. Chang. Biol.*, 21, 1153–1164.

Pinheiro, J., Bates, D., DebRoy, S., Sarkar, D., R Core Team. (2017). nlme: Linear and Nonlinear Mixed Effects Models. *R Packag. version 3.1-131, https//CRAN.R-project.org/package=nlme*.

Pratchett, M.S., Anderson, K.D., Hoogenboom, M.O., Widman, E., Baird, A.H., Pandolfi, J.M., Edmunds, P.J., Lough, J.M. (2015). Spatial, temporal and taxonomic variation in coral growth - implications for the structure and function of coral reef ecosystems. *Oceanogr. Mar. Biol. An Annu. Rev.*, 53, 215–296.

Pratchett, M.S., Trapon, M., Berumen, M.L., Chong-Seng, K. (2011). Recent disturbances augment community shifts in coral assemblages in Moorea, French Polynesia. *Coral Reefs*, 30, 183–193.

R Core Team. (2017). R: A language and environment for statistical computing. *R Found. Stat. Comput. Vienna, Austria. URL http//www.R-project.org/.*, R Foundation for Statistical Computing.

Randall, C. J., & van Woesik, R. (2015). Contemporary white-band disease in Caribbean corals driven by climate change. *Nature Climate Change*, *5*, 375.

Randall, C. J., & Van Woesik, R. (2017). Some coral diseases track climate oscillations in the Caribbean. *Scientific reports*, *7*, 5719.

Rodgers, K.S., Bahr, K.D., Jokiel, P.L., Richards Donà, A. (2017). Patterns of bleaching and mortality following widespread warming events in 2014 and 2015 at the Hanauma Bay Nature Preserve, Hawai‘i. *PeerJ*, 5, e3355.

Ruzicka, R.R., Colella, M.A., Porter, J.W., Morrison, J.M., Kidney, J.A., Brinkhuis, V., Lunz, K.S., Macaulay, K.A., Bartlett, L.A., Meyeres, M.K., Colee, J. (2013). Temporal changes in benthic assemblages on Florida Keys reefs 11 years after the 1997/1998 El Niño. *Mar. Ecol. Prog. Ser.*, 489, 125–141.

Ryan, E.J., Hanmer, K., Kench, P.S. (2019). Massive corals maintain a positive carbonate budget of a Maldivian upper reef platform despite major bleaching event. *Scientific reports*, *9*, 6515.

Stearn, W., Scoffin, T.P., Martindale, W. (1977). Calcium carbonate budget of a fringing reef on the west coast of Barbados. *Bull. Mar. Sci.*, 27, 479–510.

Swain, T.D., Vega-Perkins, J.B., Oestreich, W.K., Triebold, C., DuBois, E., Henss, J., Baird, A., Siple, M., Backman, V., Marcelino, L. (2016). Coral bleaching response index: a new tool to standardize and compare susceptibility to thermal bleaching. *Glob. Chang. Biol.*, 22, 2475–2488.

Toth, L.T., Kuffner, I.B., Stathakopoulos, A., Shinn, E.A. (2018). A 3,000-year lag between the geological and ecological shutdown of Florida’s coral reefs. *Glob. Chang. Biol.*, 24, 5471–5483.

Toth, L.T., Stahakopoulos, A., Kuffner, I.B., Ruzicka, R.R., Colella, M.A., Shinn, E.A. (2019) The unprecedented loss of Florida's reef-building corals and the emergence of a novel coral-reef assemblage. *Ecology*.

Veron, J. (1995). *Corals in space and time: the biogeography and evolution of the Scleractinia*. *Univ. New South Wales Press. Sydney, p 321*.

Wagner, D.E., Kramer, P. & Woesik, R. Van. (2010). Species composition, habitat, and water quality influence coral bleaching in southern Florida. *Mar. Ecol. Prog. Ser.*, 408, 65–78.

Van Woesik, R. & Cacciapaglia, C.W. (2018). Keeping up with sea-level rise: Carbonate production rates in Palau and Yap, Western Pacific Ocean. *PLoS One*, 13, 1–17.

Van Woesik, R., Köksal, S., Ünal, A., Cacciapaglia, C.W., Randall, C.J. (2018). Predicting coral dynamics through climate change. *Scientific Reports*, 8, 17997.

Van Woesik, R., Sakai, K., Ganase, A., Loya, Y. (2011). Revisiting the winners and the losers a decade after coral bleaching. *Mar. Ecol. Prog. Ser.*, 434, 67–76.

Yates, K.K., Zawada, D.G., Smiley, N.A., Tiling-Range, G. (2017). Divergence of seafloor elevation and sea level rise in coral reef regions. *Biogeosciences*, 14, 1739–1772.

Table 6.1: Life History Strategies (LHS) classifications from Darling *et al.* (2012) and linear mixed effects model results (Slope ± SE, p-value) of the percent contribution by the dominant calcifying corals vs. year are reported for the Main Hawaiian Islands (df = 358), Florida Keys reef tract (df = 709), Mo'orea (df = 179), and St. John (df = 206). Corals with *p*-values < 0.05 are denoted in **bold** text.

Focal Region	Coral	Life History Strategy	Slope ± SE	*p*-value
Main Hawaiian Islands	***Montipora capitata***	**competitive**	**0.27 ± 0.11**	**0.014**
	Montipora patula	competitive/intermediate/stress-tolerant[1]	0.08 ± 0.12	0.511
	Porites compressa	**competitive**	**–0.15 ± 0.08**	**0.046**
	Porites lobata	stress-tolerant	0.04 ± 0.17	0.798
Florida Keys Reef Tract	***Acropora palmata***	**competitive**	**–0.38 ± 0.11**	**< 0.001**
	Millepora alcicornis	**weedy[2]**	**0.96 ± 0.10**	**< 0.001**
	Montastraea cavernosa	**stress-tolerant**	**–0.15 ± 0.04**	**< 0.001**
	Orbicella annularis complex	**generalist/stress-tolerant[3]**	**–0.55 ± 0.16**	**< 0.001**
	Porites astreoides	**weedy**	**0.30 ± 0.08**	**< 0.001**
	Siderastrea siderea	**stress-tolerant**	**0.46 ± 0.07**	**< 0.001**
Mo'orea	***Acropora spp.***	**competitive[4]**	**–1.61 ± 0.44**	**< 0.001**
	Montipora spp.	**competitive/intermediate/stress-tolerant[4]**	**0.63 ± 0.29**	**0.029**
	Pavona spp.	stress-tolerant/generalist[4]	–0.07 ± 0.27	0.808
	Pocillipora spp.	competitive/weedy[4]	0.41 ± 0.36	0.258
	Porites spp.	weedy/stress-tolerant/competitive[4]	0.47 ± 0.52	0.363
St. John	*Montastrea cavernosa*	stress-tolerant	–0.04 ± 0.11	0.691
	Orbicella annularis complex	**generalist/stress-tolerant[3]**	**–0.56 ± 0.21**	**0.008**
	Porites astreoides	weedy	0.29 ± 0.15	0.054
	Porites porites	**weedy**	**0.20 ± 0.06**	**0.001**
	Siderastrea siderea	stress-tolerant	–0.18 ± 0.16	0.269

[1] LHS for all *Montipora spp.* from Darling et al. (2012)

[2] LHS inferred from Brown and Edmunds (2013)

[3] LHS for all species of *Orbicella annularis* complex described in Darling et al. (2012)

[4] LHS for species from the respective genera described in Darling et al. (2012)

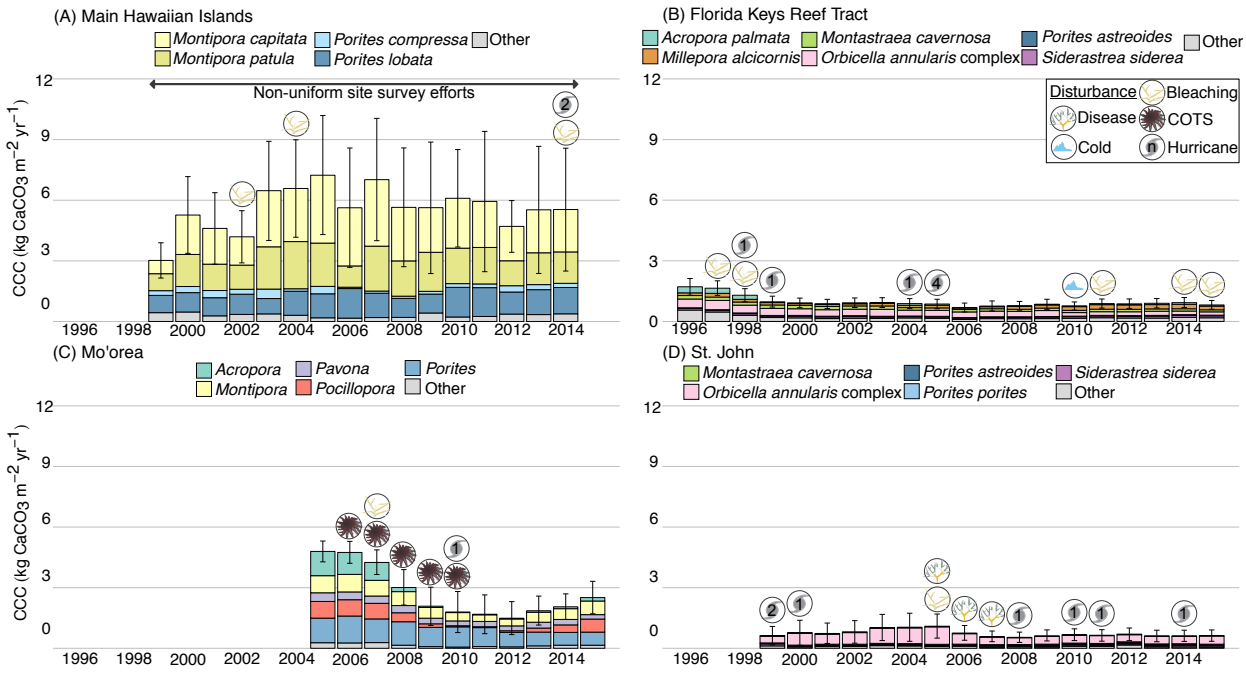

Figure 6.1: Mean annual coral calcification capacity (CCC) over time partitioned by the dominant calcifiers relative to recorded disturbance events. Mean (±95% confidence interval) annual CCC (kg $CaCO_3$ m^{-2} yr^{-1}) is reported for scleractinian coral and hydrozoan species contributing ≥5% CCC across all reef sites within a focal region for at least one year of the time series with all remaining species pooled into the "Other" category. Disturbances and icons in the legend refer to Bleaching = Severe coral bleaching event, Disease = Coral disease event, COTS = Crown-of-thorns sea star outbreak, Cold = Coldwater mortality event, and Hurricane = *n* number of recorded hurricanes/cyclones for the given year. Icons are courtesy of the Integration and Application Network, University of Maryland Center for Environmental Science (ian.umces.edu/symbols/).

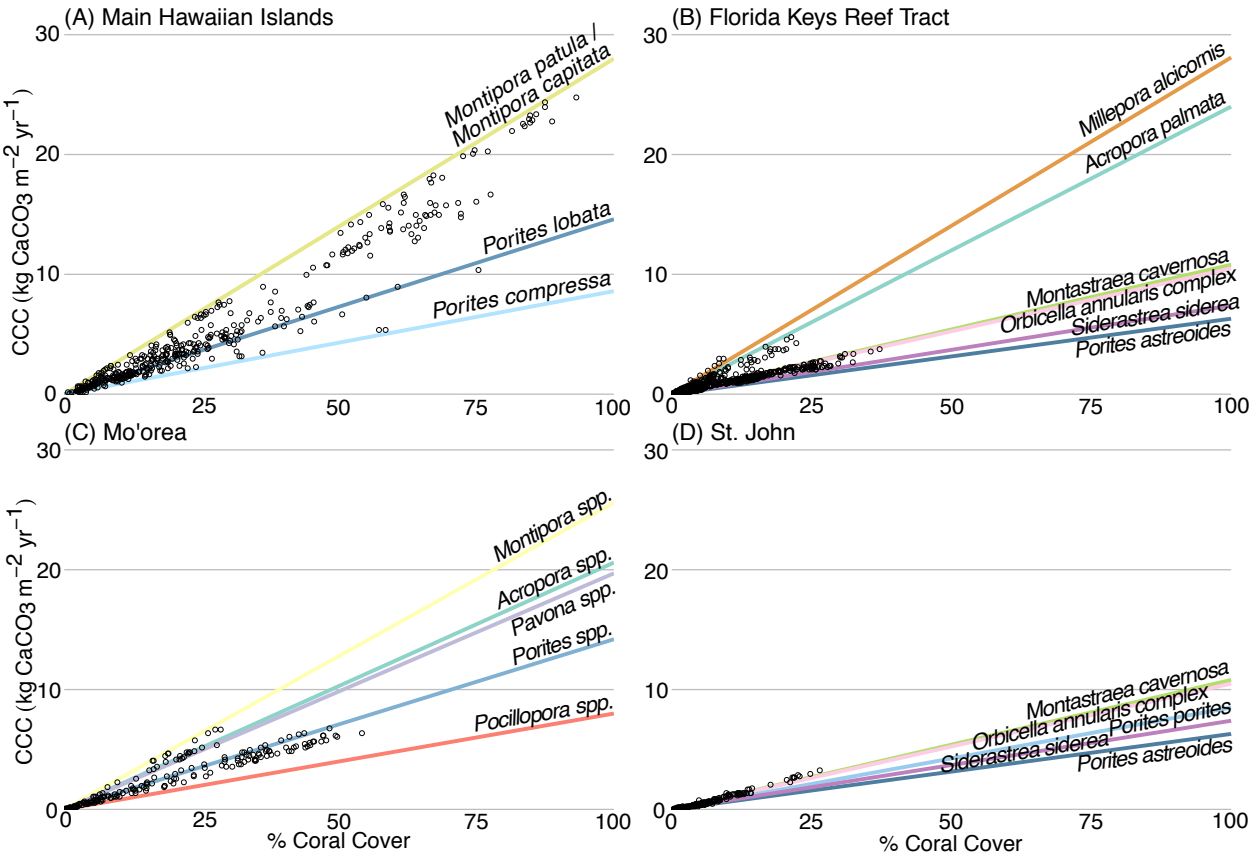

Figure 6.2: Coral calcification capacity (CCC) vs. percent coral cover for the Pacific and Western Atlantic focal regions. Panels show CCC versus percent coral cover for each year surveyed for all sites within each of the four focal regions. Colored lines represent the slope of calcification owing to coral cover ranging from 0–100% for each dominant coral genus within the focal region.

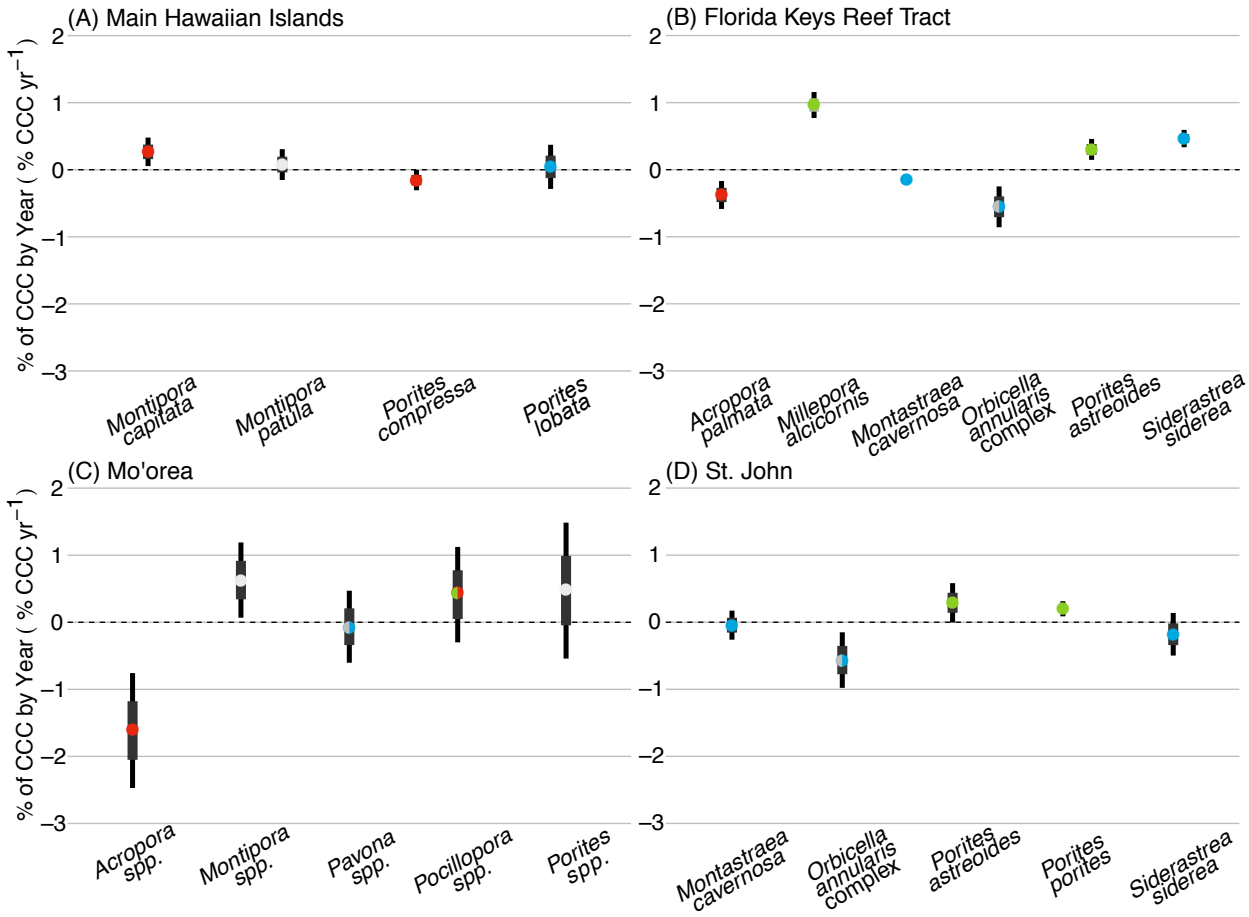

Figure 6.3: Mean percent change in CCC by dominant calcifying corals in each focal region. Each data point describes the coral-specific change in % contribution to CCC over time (by year) as derived from linear mixed effects models within each focal region, indicating the slope (colored by life history strategy from Table 1: red = competitive, green = weedy, blue = stress-tolerant, gray = generalist, white = more than two life history strategies), standard error (wide gray lines), and 95% confidence intervals (narrow black lines). Positive slopes ±95% above the dashed zero line indicate increases in % of CCC vs. year for the respective genus, slopes ±95% overlapping the dashed zero line indicate no change in % of CCC vs. year for the respective genus, and negative slopes ±95% below the dashed zero line indicate decreases in % of CCC vs. year for the respective coral.

Chapter 6, in full, is currently in review as Courtney TA, Barnes BB, Chollett I, Elahi R, Gross K, Guest JR, Kuffner IB, Lenz EA, Nelson HR, Rogers CS, Toth LT, Andersson AJ. Disturbances drive changes in coral community assemblages and coral calcification capacity. The dissertation author was the primary investigator and author of this paper.

CHAPTER 7

Conclusion

Travis A. Courtney

7.1 Summary of dissertation

Monitoring the impacts of local and global environmental change on the capacity for coral reefs to build and maintain their calcium carbonate structures is essential for understanding potential changes to the ecosystem services coral reefs provide to humanity in the Anthropocene. Because coral and reef-scale calcification depend on a combination of ecological and environmental controls, accurate assessments of these key processes require an interdisciplinary research perspective aided by relatively recent advancements in methodologies and instrumentation. This dissertation leverages these advancements through a combination of ecological, physiological, and biogeochemical perspectives to elucidate how the rates of coral reef calcification and the mechanisms driving these rates vary across space and time. The findings summarized here contribute directly to the growing need for effective evidence-based management of coral reef structures to assist in the resilience and capacity-building of human populations dependent on these rapidly changing ecosystems in the Anthropocene.

In Chapter 2 of this dissertation, a literature review of previous chemistry-based NEC studies showed that NEC positively correlated with percent calcifier cover in mesocosms, but not for studies conducted in the field (Courtney and Andersson 2019). Accurately constraining seawater hydrodynamics concurrently with alkalinity anomalies is a challenging task and here a biogeochemical modeling approach was utilized to show that uncertainties in constraining seawater depth and residence time have the capacity to mask any potential real correlation between NEC and calcifier cover in the field (Courtney and Andersson 2019). Further insights were gained from leveraging *in situ* coral growth literature and census-based reef growth methods to show that in addition to constraining seawater physics, coral reef structural complexity may similarly be masking any potential correlation between NEC and calcifier cover

in the field by increasing the amount of reef substrate available to calcifiers (Courtney and Andersson 2019).

These chemistry and census-based NEC methods were more formally compared at Hog Reef, Bermuda in Chapter 3 finding that the two methods agreed within relatively large but nonetheless overlapping uncertainties (Courtney et al. 2016). Chemistry-based methods provided greater confidence in capturing the net sum of all calcification and $CaCO_3$ dissolution occurring on a reef environment and the sub-annual variability and environmental drivers of NEC through space and time, but were limited by the aforementioned challenges in quantifying seawater depth and residence time discussed in Chapter 2 (Courtney et al. 2016). The environmental drivers of chemistry-based NEC were explored in Chapter 4 of this dissertation (see subsequent section). Conversely, the census-based approaches rapidly estimated a reef-scale net calcification budget from benthic cover data, but were primarily limited by the availability and applicability of literature-derived calcification/dissolution rates (Courtney et al. 2016). Census-based NEC nonetheless revealed that the majority of $CaCO_3$ dissolution at Hog Reef was likely due to microborers and the majority of calcification at Hog Reef was likely due to just four taxa: *Diploria labyrinthiformis, Pseudodiploria strigosa*, *Orbicella franksi*, and *Millepora alcicornis* (Courtney et al. 2016). These first two chapters suggest that either chemistry or census-based methods can be used to estimate reef-scale calcification, but that ideally multiple perspectives can be used to increase confidence in measured reef-scale calcification rates (Courtney et al. 2016; Courtney and Andersson 2019).

Chapter 4 built upon the rates of coral and reef-scale calcification at Hog Reef with additional coral calcification rates for a mid-platform reef site, Crescent Reef, and environmental drivers for both reef sites including seawater temperature, carbonate chemistry (i.e., seawater

pH_{sw}, saturation state with respect to aragonite Ω_A, pCO_2, TA, DIC), light, nutrients, chlorophyll–α (i.e., as a proxy for food availability), and salinity (Courtney et al. 2017). Over the two-year study period, the environmental drivers of coral and reef-scale calcification were assessed using a structural equation modeling approach (Courtney et al. 2017). This analysis showed that temperature yielded the greatest changes in calcification rates out of any of the other environmental parameters and was the only statistically significant environmental driver for reef-scale calcification and both coral species at both reef sites (Courtney et al. 2017). Furthermore, a manipulative mesocosm experiment conducted alongside the field-based calcification measurements showed that coral calcification was not significantly altered by reduced seawater pH conditions when food was present (Courtney et al. 2017). As a result, future calcification rates of *D. labyrinthiformis* and *P. astreoides* in Bermuda are likely to be primarily controlled by changes in temperature and have the potential to be maintained under the warming provided by the Paris Agreement, but are likely to be inhibited by regular, intense coral bleaching under business-as-usual climate scenarios (Courtney et al. 2017).

Coral bleaching events can also affect reef-scale calcification as explored in Chapter 5, where reef-scale calcification measurements were conducted using chemistry-based NEC methods in the Kāne'ohe Bay reef flat during and after the 2015 coral bleaching event (Courtney et al. 2018). Zero NEC was observed during the coral bleaching event and rapidly recovered along with the recovery of the bleached corals by the subsequent summer to pre-bleaching NEC rates (Courtney et al. 2018). However, the question remains as to how much the resilience of reef-scale calcification can be depended on as coral reef bleaching events are predicted to increase in frequency and magnitude in the coming decades (Courtney et al. 2018).

Chapter 6 further explored the effects of coral bleaching and other disturbance events on reef-scale calcification through analyses of 20 years of coral calcification capacity (CCC) time series data from 1996 to 2015 for Mo'orea, St. John, Florida Keys Reef Tract, and the main Hawaiian Islands (Courtney et al. in review). This study revealed a multi-year recovery of Mo'orea coral calcification capacity following a crown-of-thorns outbreak, coral bleaching event, and cyclone (Courtney et al. in review). Conversely, prolonged reduced CCC was observed in St. John and across the Florida Keys Reef Tract under continued disturbance events while no major reductions in CCC were observed in the absence of major disturbances for the main Hawaiian Islands (Courtney et al. in review). CCC across Mo'orea, St. John, Florida Keys Reef Tract, and the main Hawaiian Islands was further accompanied by disturbance-driven increases in the contributions of non-framework building 'weedy' corals at the expense of framework building 'competitive' corals over the time series (Courtney et al. in review). The integration of CCC with expectations for coral life history strategies can therefore provide useful tools for retroactive analysis of historical coral community data to improve projections for how coral bleaching and other disturbance events are likely to alter reef-scale calcification in the future (Courtney et al. in review).

In summation, the key findings were:

- Uncertainties in chemistry-based NEC measurements can be large enough to prevent a more functional understanding of the rates and drivers of coral reef calcification, but may be improved by leveraging multiple methods to calculate NEC
- Chemistry and census-based NEC measurements agreed within uncertainties suggesting that either method, but ideally both methods, can be useful for monitoring the growth and maintenance of coral reef structures

- Coral and reef-scale calcification in Bermuda were primarily driven by increases in temperature and were relatively insensitive to decreases in seawater pH suggesting future calcification can be maintained under reduced carbon dioxide emissions pathways
- NEC was reduced to zero in Kāne'ohe Bay, Hawai'i during a coral bleaching event, but recovered to pre-bleaching NEC rates less than a year later showing that reef-scale calcification can exhibit a high degree of resilience to coral bleaching events
- Pantropical coral taxa shuffled their relative contributions to CCC over time suggesting that shifting coral communities may increase the capacity for reef-scale calcification to adapt to the environmental change of the Anthropocene

Collectively, this dissertation discusses the strengths and weaknesses of various methods for measuring or approximating reef-scale calcification through chemistry and census-based NEC methods. By leveraging multiple approaches and insights, the chapters herein highlight the benefits of using interdisciplinary perspectives to reduce uncertainties and better constrain reef-scale calcification measurements. Furthermore, the capacity for environmental conditions and coral reef disturbances has been shown to drive reef-scale calcification rates directly through modification of coral and reef-scale calcification rates and indirectly through shifts in benthic communities. The magnitude and frequency of disturbances further affect the capacity for coral reefs to either recover to pre-disturbance reef-scale calcification rates or potentially remain at reduced rates of reef-scale calcification. Complete reef-scale calcification estimates or even simplified approaches such as CCC therefore have the capacity to improve our understanding of coral reef growth processes and will likely prove to be valuable assets for understanding how coral reef structures and the ecosystem services they provide may be affected by the current interval of local and global environmental change.

7.2 References cited

Courtney TA, Andersson AJ (2019) Evaluating measurements of coral reef net ecosystem calcification rates. Coral Reefs

Courtney TA, Andersson AJ, Bates NR, Collins A, Cyronak T, de Putron SJ, Eyre BD, Garley R, Hochberg EJ, Johnson R, Musielewicz S, Noyes TJ, Sabine CL, Sutton AJ, Toncin J, Tribollet A (2016) Comparing Chemistry and Census-Based Estimates of Net Ecosystem Calcification on a Rim Reef in Bermuda. Front Mar Sci 3:181

Courtney TA, Barnes B, Chollett I, Elahi R, Gross K, Guest J, Kuffner I, Lenz E, Nelson H, Rogers C, Toth L, Andersson A (in review) Disturbances drive changes in coral community assemblages and coral calcification capacity.

Courtney TA, De Carlo EH, Page HN, Bahr KD, Barro A, Howins N, Tabata R, Terlouw G, Rodgers KS, Andersson AJ (2018) Recovery of reef-scale calcification following a bleaching event in Kāne'ohe Bay, Hawai'i. Limnol Oceanogr Lett 3:1–9

Courtney TA, Lebrato M, Bates NR, Collins A, de Putron SJ, Garley R, Johnson R, Molinero J-C, Noyes TJ, Sabine CL, Andersson AJ (2017) Environmental controls on modern scleractinian coral and reef-scale calcification. Sci Adv 3:e1701356